Reading and Problem Assignments for Physics 243A
Surface Physics of Materials: Spectroscopy, Fall, 2016
(In order of coverage in lecture)

Reading:

- **Woodruff and Delchar, "Modern Techniques of Surface Science", 2nd Edition--**
  - **Chapter 1**
  - **Chapter 2: Sections 2.1, pp.22 (bottom)-23(top) on Wood notation for surface structures, 2.4, and 2.5 (pp. 31-37), 2.9.6 on standing waves**
  - **Chapter 6: 6.9, 6.10, 6.11**
  - **Chapter 3: Sections 3.1, 3.2, 3.3, 3.5**

- **Zangwill, "Physics at Surfaces", downloadable Chapters 1-5 (see course website)--**
  - **Chapter 1: Everything except "The roughening transition"**
  - **Chapter 3: pp. 28-34, pp. 49-52 on STM**
  - **Pages 85-86, 192-196, 204-212**
  - **Chapter 2: All**
  - **Chapter 4: Introduction, with lighter reading of *The jellium model*, *One-dimensional band theory, and Three-dimensional band theory*, and detailed reading of *Photoelectron spectroscopy, Metals, and Alloys***

- **Ibach, "Physics of Surfaces and Interfaces", downloadable book (see course website)—**
  - **Chapter 2: 2.1, 2.2**
  - **Chapter 8: 8.2**

- **Desjonqueres and Spanjaard, "Concepts of Surface Physics", excerpts downloadable from Course website: On STM current calculation, equilibrium shapes of surfaces, thermodynamics, kinetics and adsorption isotherms. No need to follow every step, but this fills in the line of arguments in Zangwill and lecture**

- **Fadley, "Basic Concepts of XPS", to be handed out, but also downloadeable—Sections I, II, and III. A-C, with remaining sections by the end of the course**

- **Attwood, Downloadeable excerpt on synchrotron radiation from the book "Soft X-Rays and Extreme Ultraviolet Radiation" (see course website)**

Reading coverage for midterm

Next reading in blue: Rest of "Basic Concepts" +Molecular Orbital Basics &Tight-Binding Basics (from website)

Problem assignments:

Problem Asst. 1-all of PS 1. Due Thursday, October 13th
Problem Asst. 2—all of PS 2, plus 3.1 and 3.2. Due Thursday, October 27th
Problem Asst. 3—finish PS 3, plus 4.1-4.4.4.6. Due Monday, November 21st
Problem Asst. 4—4.5, 4.7(a) only, 5.1, 5.2, 5.3. 5.4, 5.7, 5.8, 5.9, 5.10, due Friday, December 2nd

The Soft X-Ray Spectroscopies

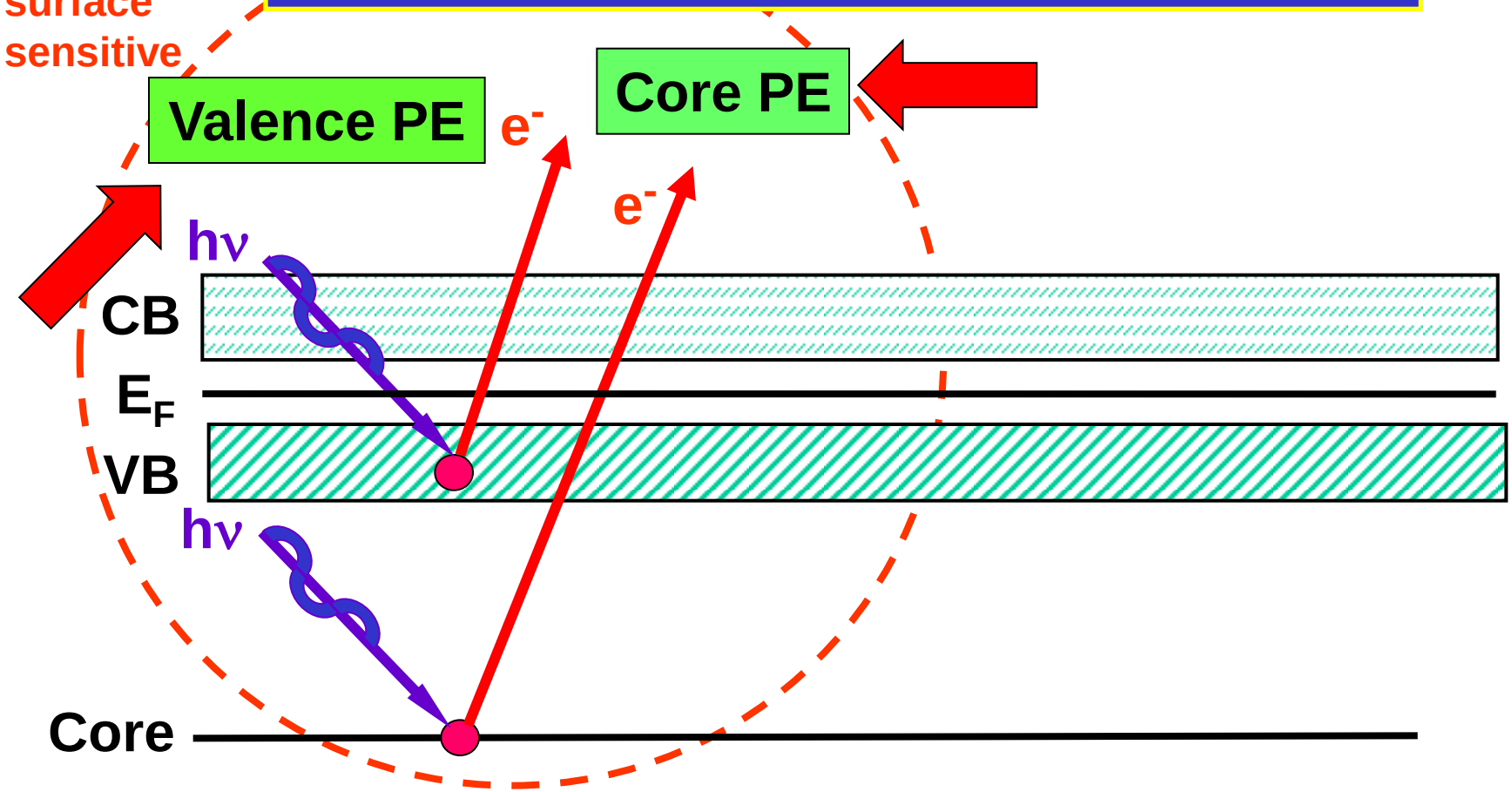

PE = photoemission = photoelectron spectroscopy

XAS = x-ray absorption spectroscopy

AES = Auger electron spectroscopy

XES = x-ray emission spectroscopy

REXS/RIXS = resonant elastic/inelastic x-ray scattering

MATRIX ELEMENTS IN THE SOFT X-RAY SPECTROSCOPIES: DIPOLE LIMIT

- ***<u>Photoelectron spectroscopy/photoemission:</u>***

$$I \propto \left| \hat{e} \bullet \langle \varphi_f(1) | \vec{r} | \varphi_i(1) \rangle \right|^2$$

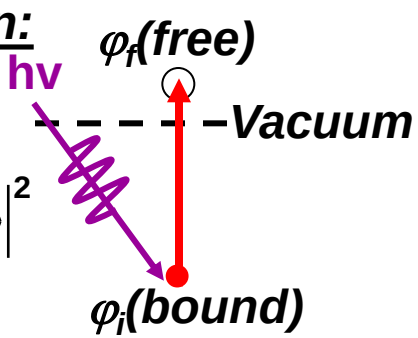

PHOTOELECTRON SPECTROSCOPY

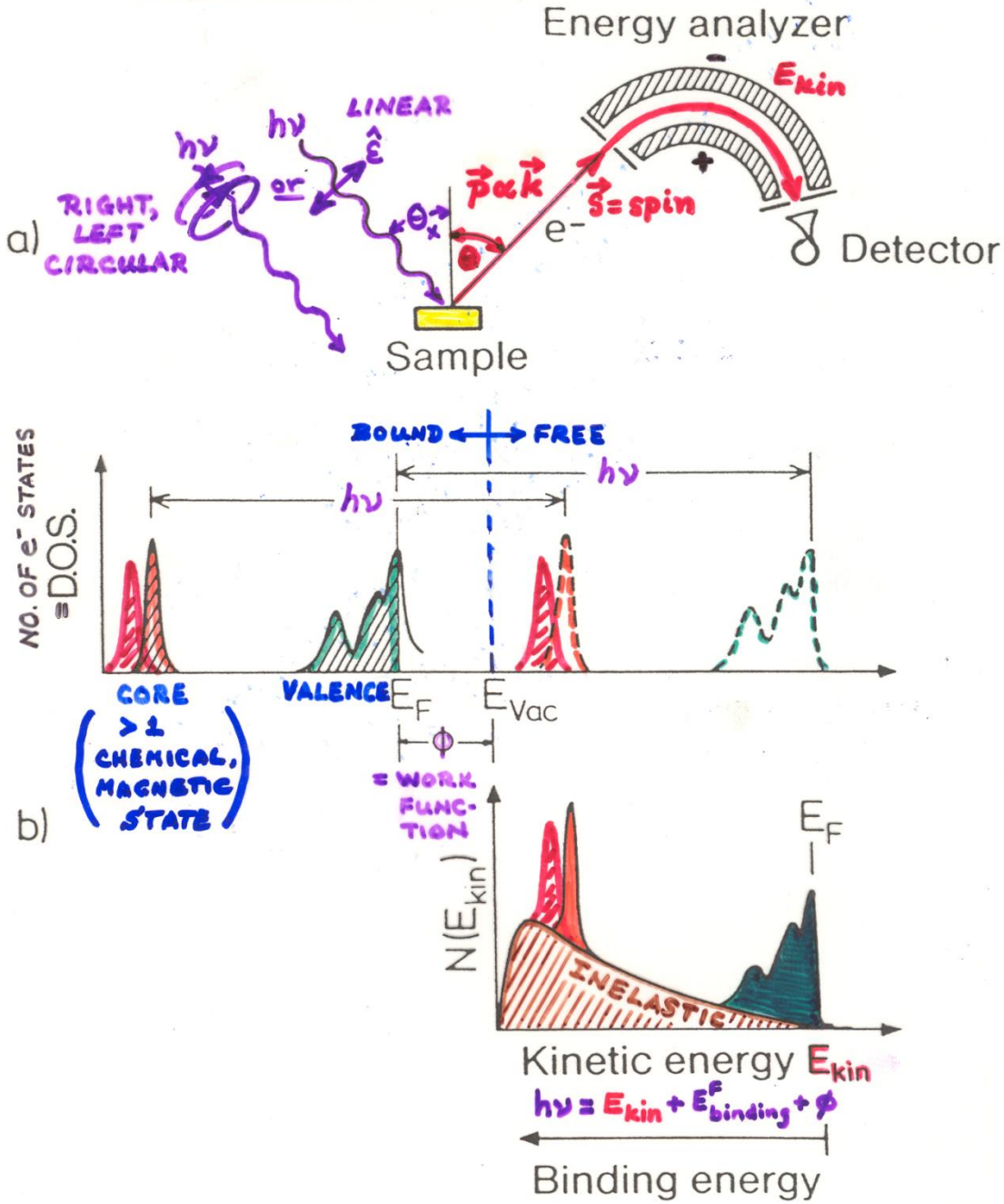

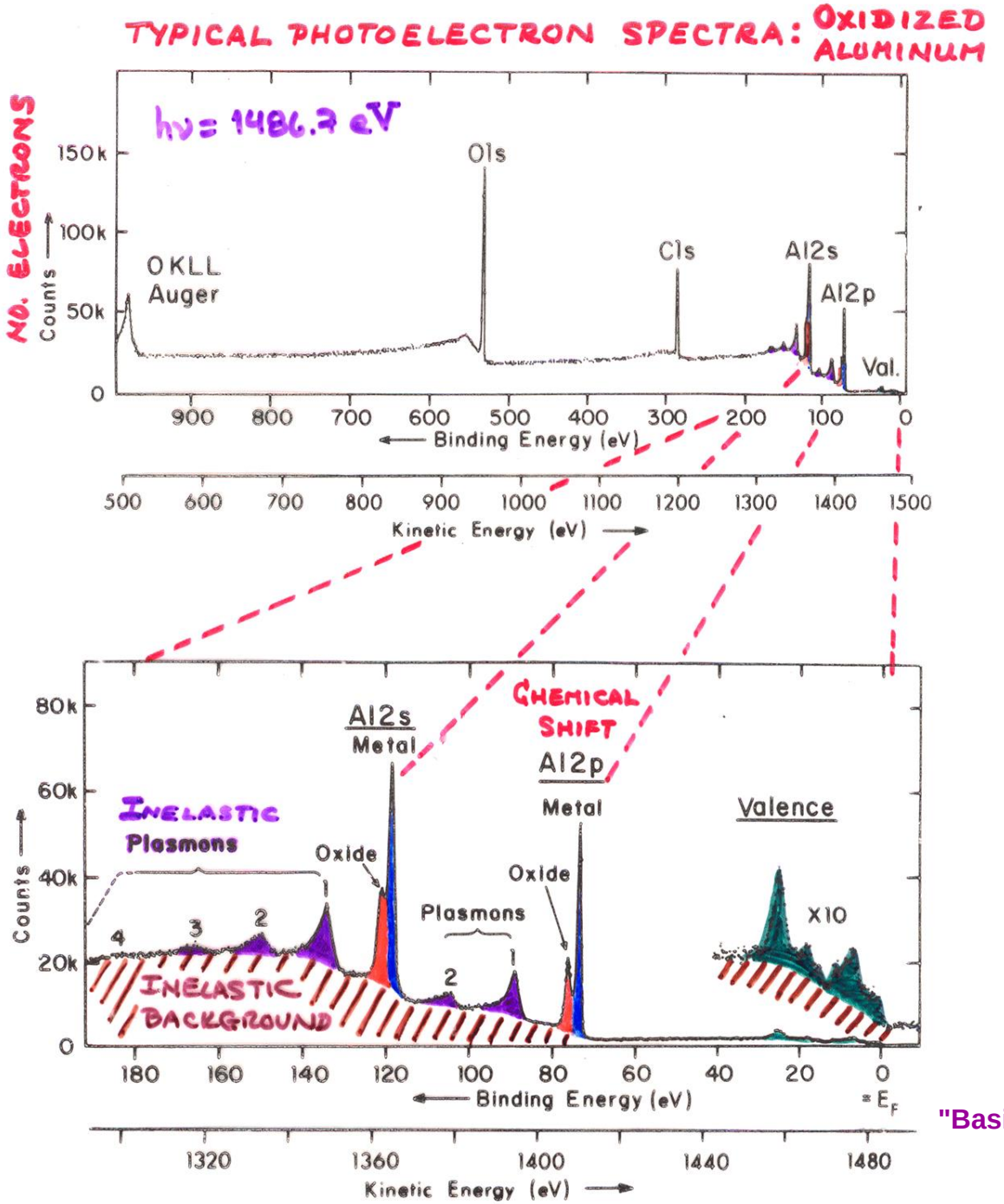

"Basic Concepts of XPS"
Figure 1

PHOTOELECTRON SPECTROSCOPY

THE PHOTOELECTRIC EFFECT (EINSTEIN, 1905):

(PHOTON ENERGY) = (e^- BINDING ENERGY IN SYSTEM) + (PHOTOELECTRON KINETIC ENERGY)

(ABSORBED) (EMITTED)

= B.E. + K.E.

EXAMPLE – CO MOLECULE:

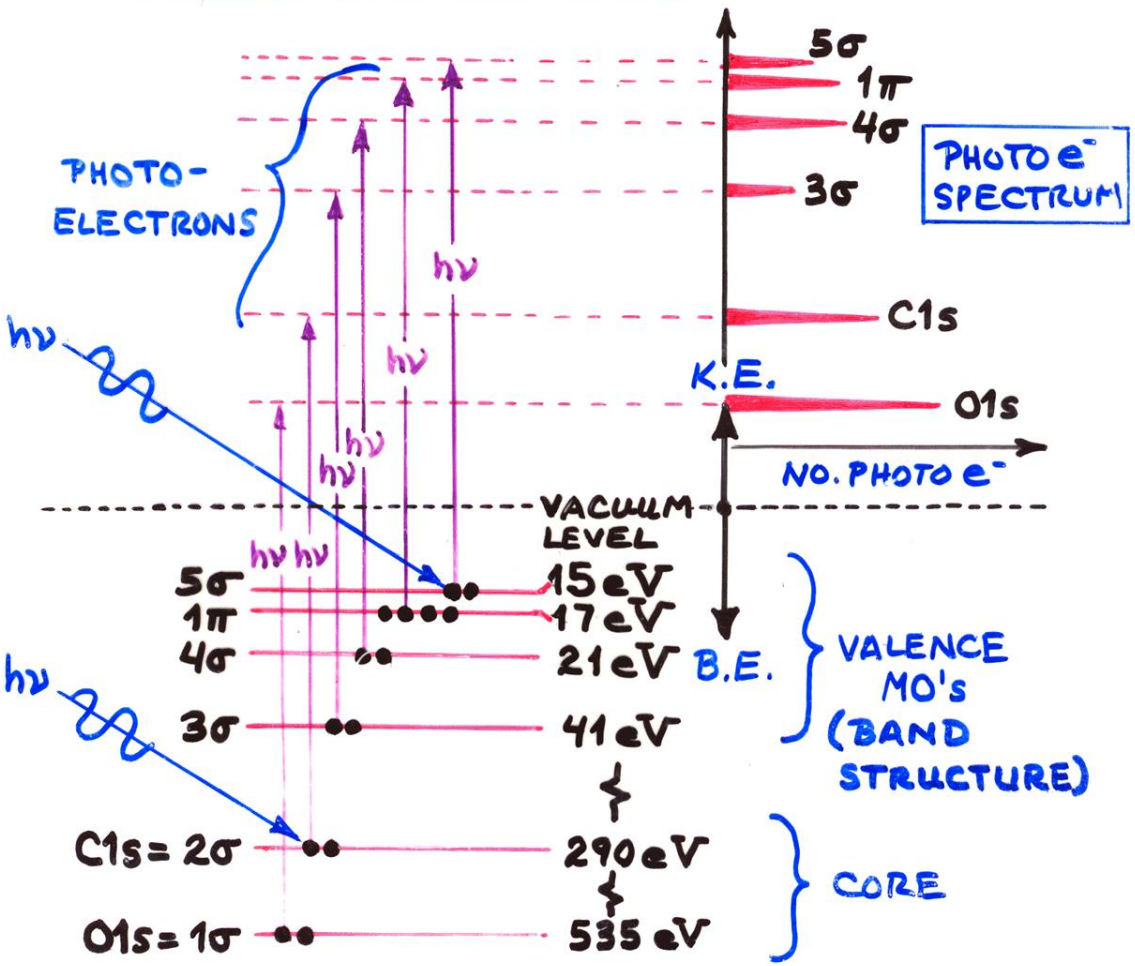

X-RAY PHOTOELECTRON SPECTRUM OF CO

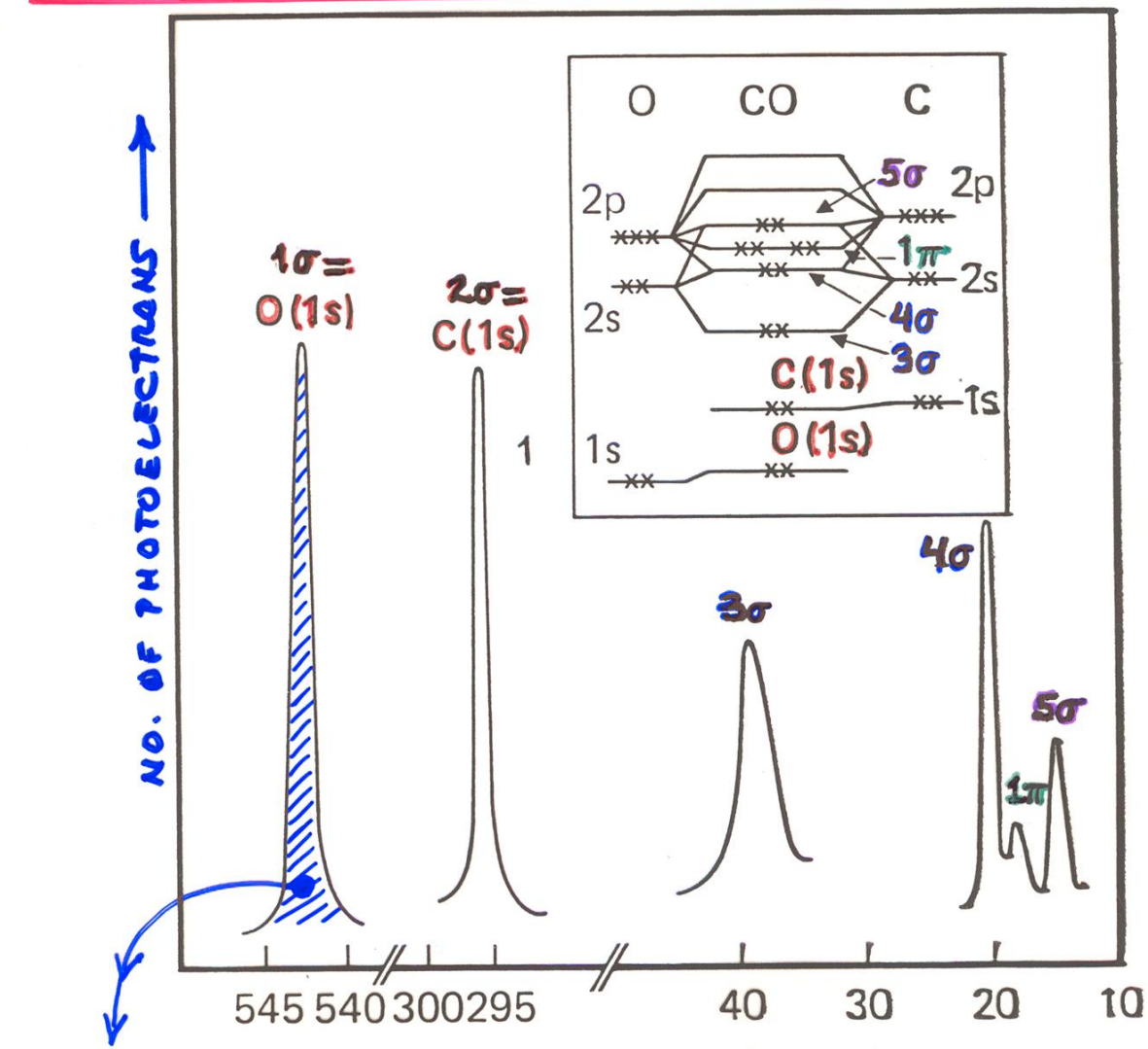

INTENSITY

∝ AREA

∝ PHOTOELECTRIC CROSS SECTION × NO. ATOMS → QUANTITATIVE SURFACE ANALYSIS

← BINDING ENERGY (ELECTRON-VOLTS)

The LCAO or tight-binding picture for CO:

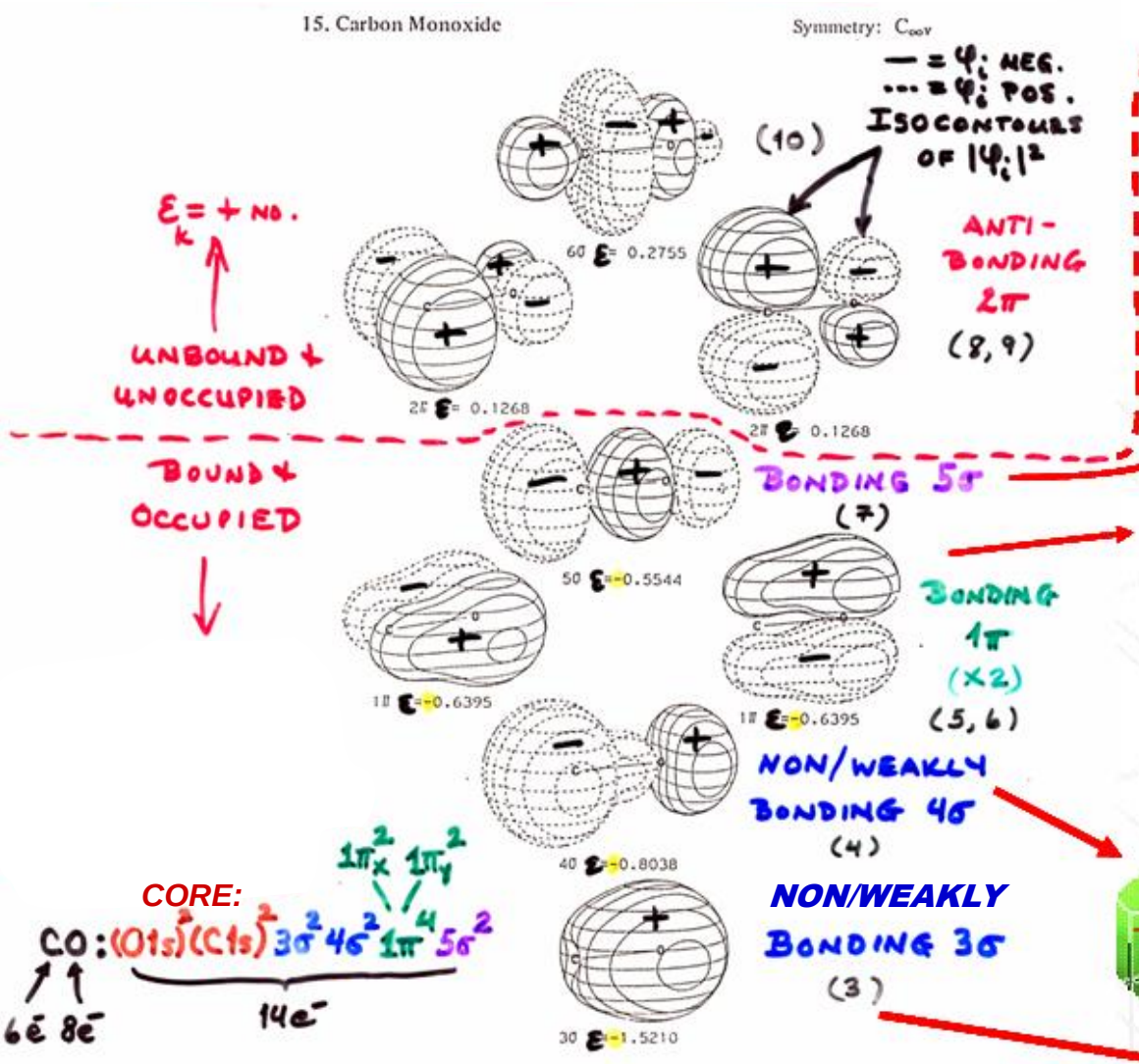

Atomic orbital makeup

$$\varphi_j^{MO}(\vec{r}) = \sum_{\substack{\text{Atoms } A \\ \text{Orbitals } i}} c_{Ai,j}\varphi_{Ai}^{AO}(\vec{r})$$

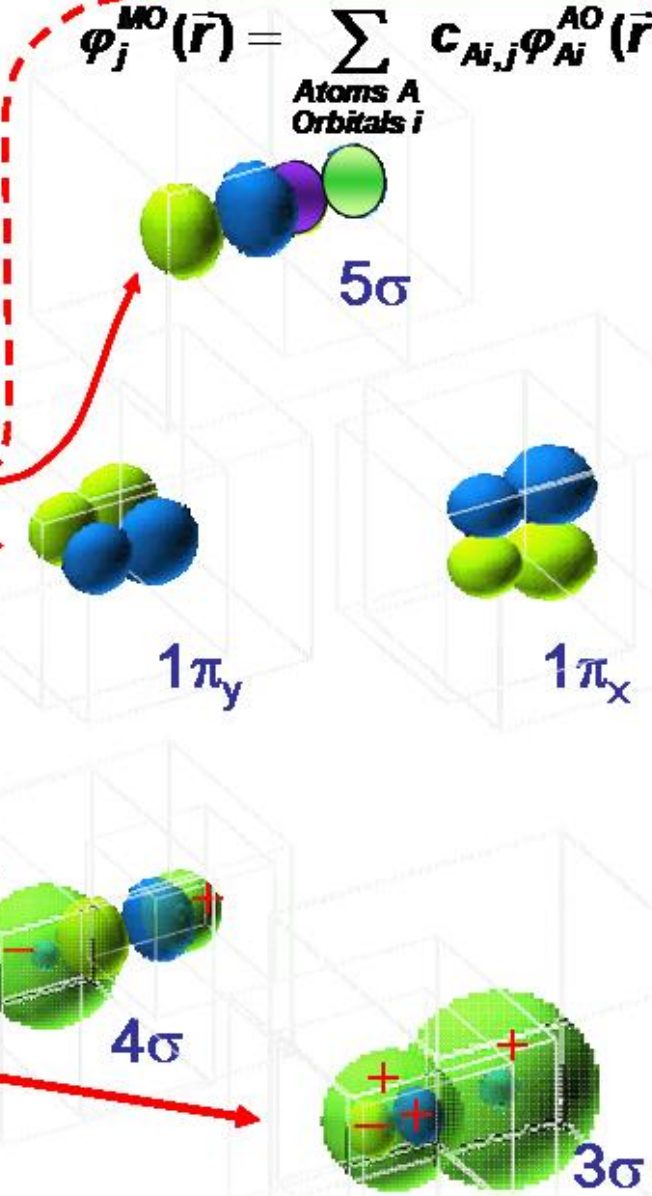

Chemist's picture (no core):

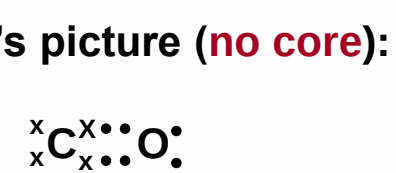

Valence-level Photoelectron spectra of CO adsorbed on various transition metal surfaces

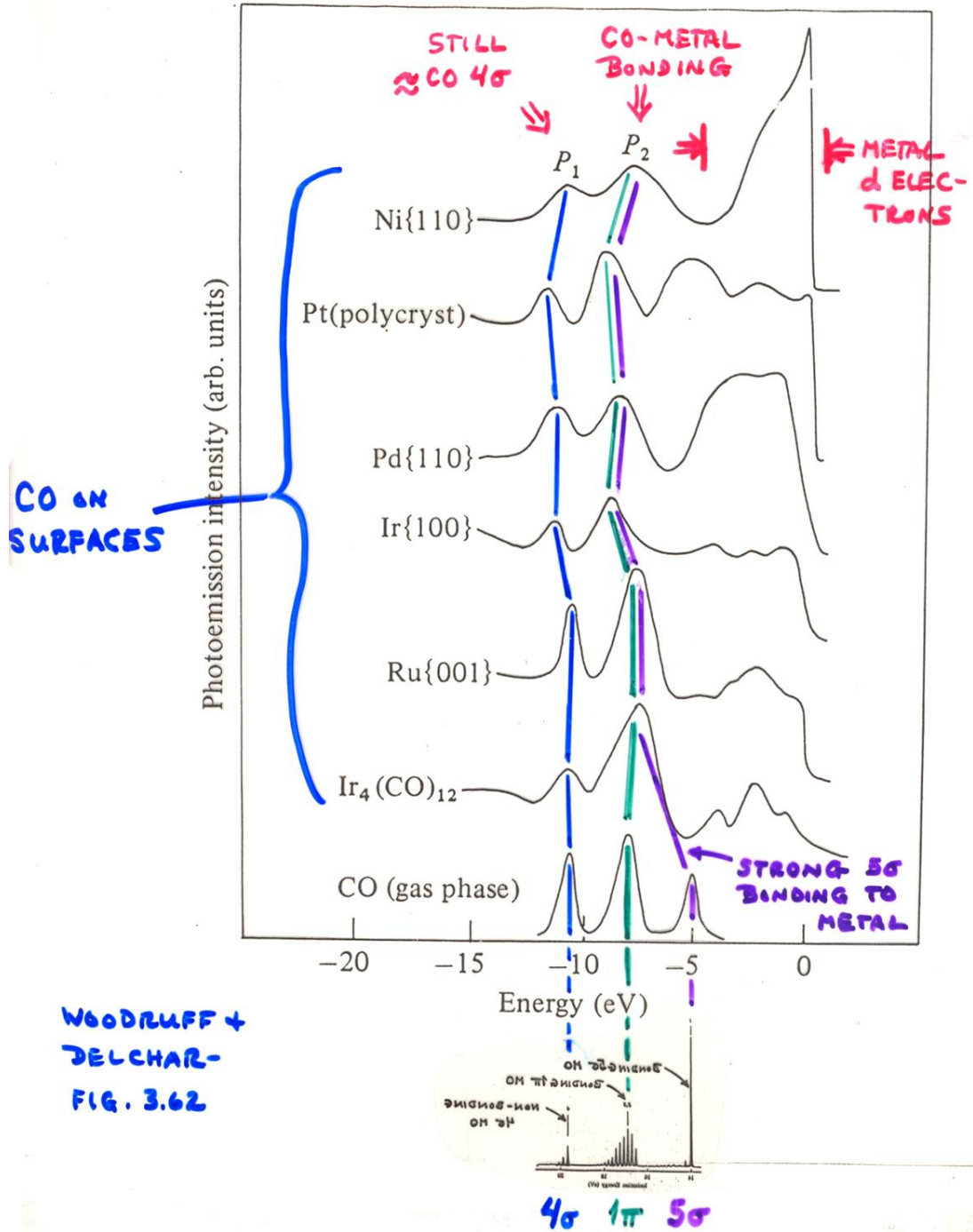

WOODRUFF + DELCHAR-
FIG. 3.62

Theoretical Calculations of charge density for CO bound to Ni(001)- "on-top":

O
|
C
|
Ni

Fig. 12.14. Charge density contour plots appropriate to Ni(100) c(2 × 2)-CO: (*a*) free molecule 5σ orbital; (*b*) free molecule 2π orbital; (*c*) difference between CO/Ni(100) and the superposition of clean Ni(100) and an unsupported CO monolayer. Solid (dashed) lines indicate a gain (loss) of electronic charge (Wimmer, Fu & Freeman, 1985).

CO 5σ

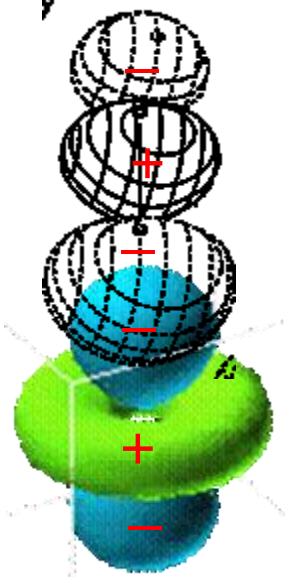

Ni $3d_{z^2}$
σ bond

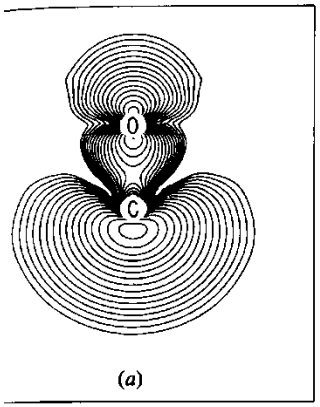

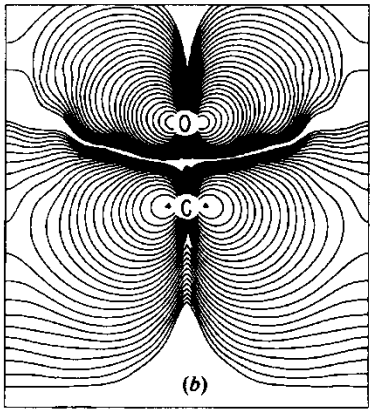

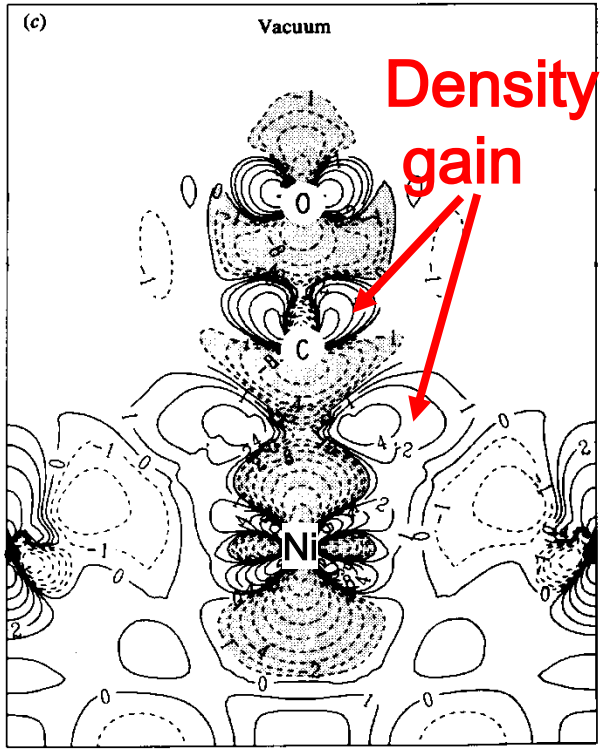

CO 2π = π*

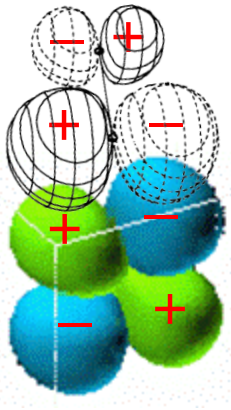

Ni $3d_{xy}$
π "back bond"

Zangwill, p. 307, plus PRL 55, 2618 ('85)

(9) **CO** Carbon Monoxide

UV PHOTOELECTRON SPECTRUM OF CO

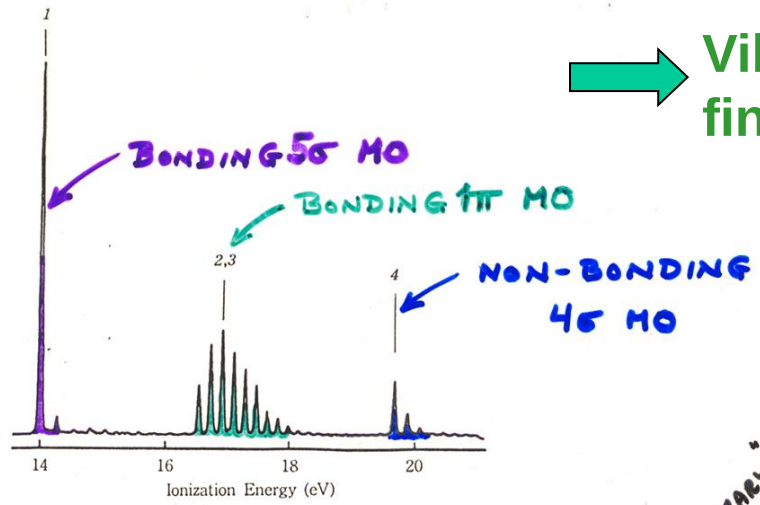

Vibrational fine structure

KOOPMANS' — CI FINAL STATE — "PRIMARY HOLES"

	Exptl.[a]	SCF MO [6-31 G][b]			CI (Ionic State) [6-31 G][c]		
	I_v(eV)	$-\varepsilon$(eV)	MO	Character	E(eV)	State	Configuration
1	14.01	14.99	5σ (7)	σ_{CO}	13.11	$1^2\Sigma^+$	$0.93(7^{-1})$ $-0.15(6^{-1},7^{-1},9^1)_a$ $-0.15(5^{-1},7^{-1},8^1)_a$
2	16.91	17.48	1π (6, 5)	π_{bond}	16.69	$1^2\Pi$	$0.95(6^{-1})$; $0.95(5^{-1})$
3	16.91	17.48					
4	19.72	21.69	4σ (4)	n_O	19.29	$2^2\Sigma^+$	$0.92(4^{-1})$ $+0.16(6^{-1},7^{-1},9^1)_a$ $+0.16(5^{-1},7^{-1},8^1)_a$

RELAX. + CORREL.

a) The spectrum : this work. The I_v's : Turner *et al.* (215). See also other works : Turner and May (215 a) ; Carlson and Jonas (54) ; Gardner and Samson (104) ; Edqvist *et al.* (90) ; Potts and Williams (182 a) ; and Natalis *et al.* (165).
b) We used the bond length reported (A 3) ; symmetry $C_{\infty h}$. $E_{SCF}=-112.6672$ hartree. In 4-31 G calculations, $E_{SCF}=-112.5524$ hartree and $-\varepsilon$(eV)=14.93, 17.41, 17.41, and 21.60.
c) CI-II. (9, 8)=1π. $|N\rangle=0.98$ (SCF). The results obtained in other CI levels are given in Appendix B.

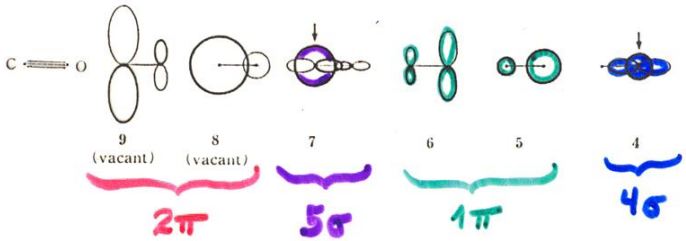

Kimura et al., "Handbook of Hel Photoelectron Spectra"

INTENSITIES IN PHOTOELECTRON SPECTRA:

- GENERAL: FINAL STATE K (K-SUBSHELL + ALL OTHER DESIG.)

$$\text{INT.}_K \propto \left| \hat{e} \cdot \langle \Psi^f_{tot}(N,K) | \sum_{i=1}^{N} \vec{r}_i | \Psi^i(N) \rangle \right|^2 \quad \text{(DIPOLE APPROX.}$$

- BORN-OPPENHEIMER: e^-'s FAST, VIBRATIONS SLOW

$$\text{INT.}_K \propto \underbrace{\left| \langle \Psi^f_{vib,v'} | \Psi^i_{vib,v} \rangle \right|^2}_{\text{FRANCK-CONDON FACTOR}} \left| \hat{e} \cdot \langle \Psi^f_{e^-}(N,K) | \sum_{i=1}^{N} \vec{r}_i | \Psi^i_{e^-}(N) \rangle \right|^2$$

VIBRATIONAL STRUCTURE IN VALENCE-LEVEL (MO) SPECTRA

Diatomic A-B example

(Also applies to core-level emission if equilibrium distance changes on forming core hole)

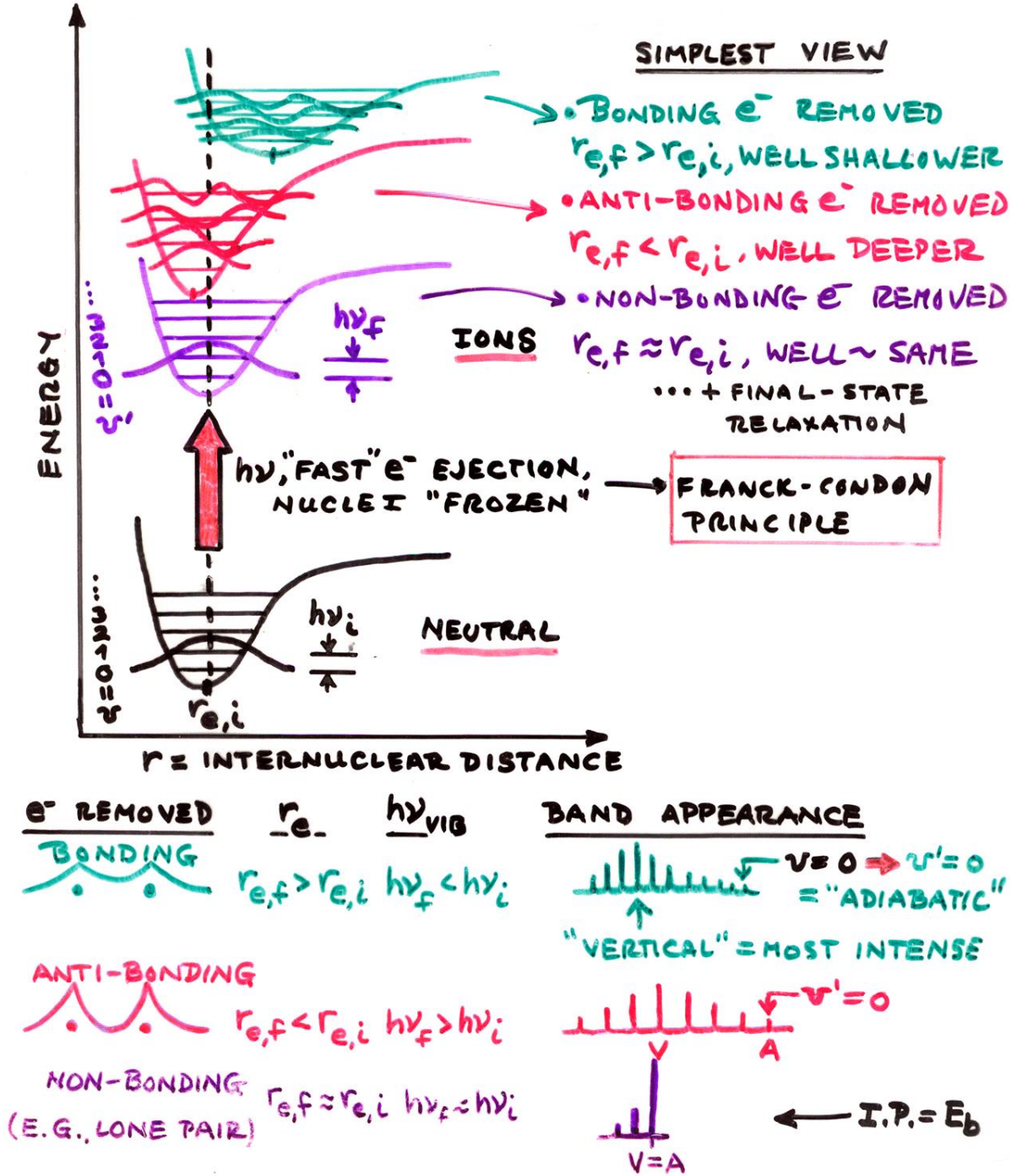

VIBRATIONAL STRUCTURE IN VALENCE-LEVEL (MO) SPECTRA

H_2 Hydrogen

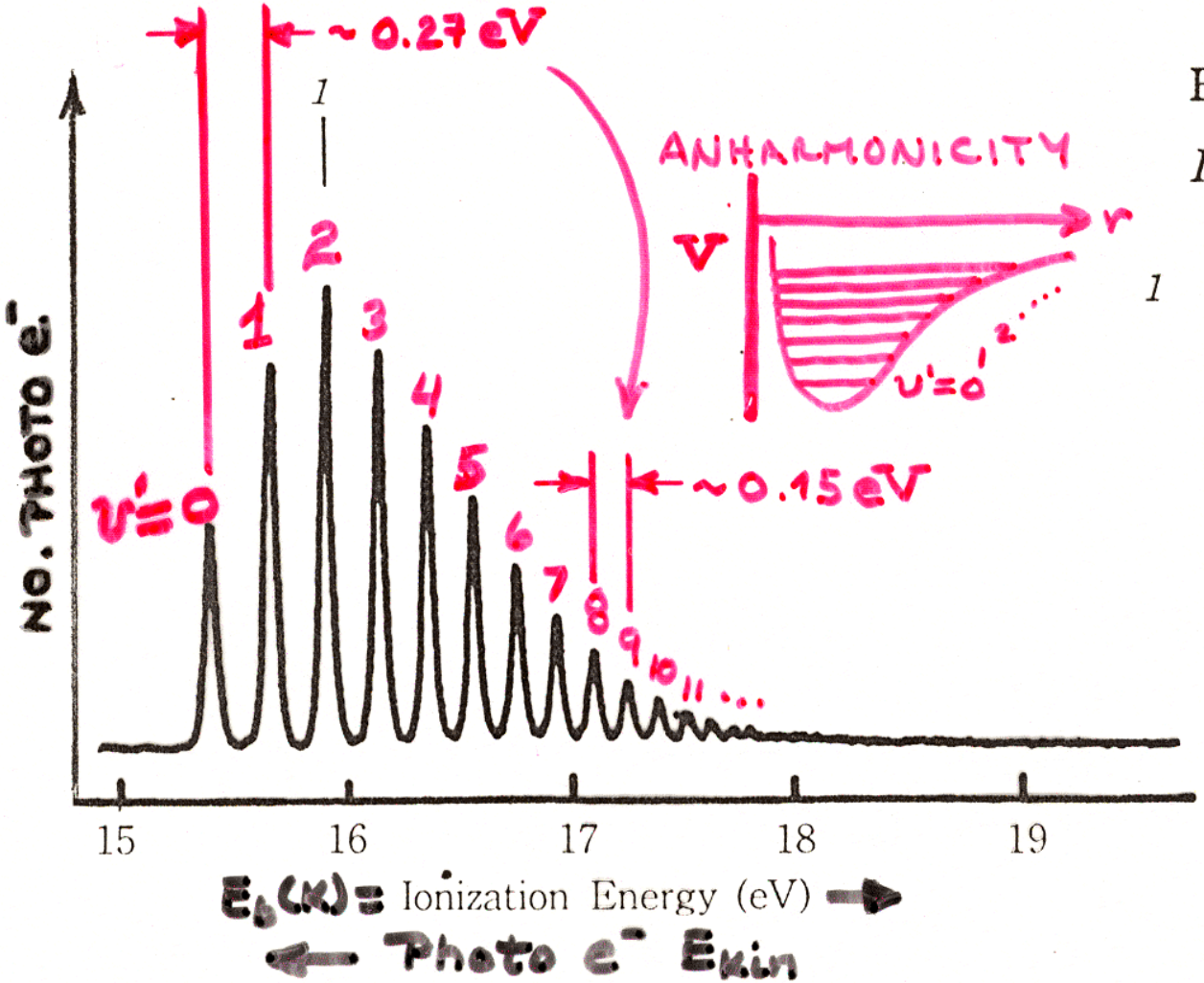

	Exptl.[a] I_v (eV)
1	15.98

INTENSITIES IN PHOTOELECTRON SPECTRA:

- GENERAL: FINAL STATE K (K-SUBSHELL + ALL OTHER DESIG.)

$$\text{INT.}_K \propto \left|\hat{e}\cdot\langle\Psi^f_{tot}(N,K)|\sum_{i=1}^{N}\vec{r}_i|\Psi^i(N)\rangle\right|^2 \quad \text{(DIPOLE APPROX.}$$

- BORN-OPPENHEIMER: e^-'s FAST, VIBRATIONS SLOW

$$\text{INT.}_K \propto \underbrace{|\langle\psi^f_{vib,v'}|\psi^i_{vib,v}\rangle|^2}_{\text{FRANCK-CONDON FACTOR}}\left|\hat{e}\cdot\langle\Psi^f_{e^-}(N,K)|\sum_{i=1}^{N}\vec{r}_i|\psi^i_{e^-}(N)\rangle\right|^2$$

- SUDDEN APPROXIMATION: $\varphi_K \rightarrow \varphi_f$ = PHOTO e^- (FAST)

$$\left.\begin{array}{l}\varphi_1 \rightarrow \varphi_1' \\ \vdots \\ \varphi_{K-1} \rightarrow \varphi_{K-1}' \\ \varphi_{K+1} \rightarrow \varphi_{K+1}' \\ \vdots \\ \varphi_N \rightarrow \varphi_N'\end{array}\right\} \text{(SLOW)}$$

K HOLE →

$$\text{INT.}_K \propto |\langle\psi^f_{vib,v'}|\psi^i_{vib,v}\rangle|^2 \underbrace{|\langle\Psi^f_{e^-}(N-1,K)|\Psi_K(N-1,K)\rangle|^2}_{\text{SAME SUBSHELL COUPLING + TOTAL L,S}\rightarrow\text{"MONOPOLE"}}$$

K MISSING

$$|\hat{e}\cdot\langle\varphi_f|\vec{r}|\varphi_K\rangle|^2$$

↳ NORMAL $\dfrac{d\sigma_K}{d\Omega}$

- SLATER DETS. FOR $\Psi^f_{e^-} = \det(\varphi_1'\varphi_2'\ldots\varphi_{K-1}'\varphi_{K+1}'\ldots\varphi_N')$

$$\Psi_K = \det(\varphi_1\varphi_2\ldots\varphi_{K-1}\varphi_{K+1}\ldots\varphi_N)$$

$$\text{INT.}_K \propto |\langle\psi^f_{vib,v'}|\psi^i_{vib,v}\rangle|^2|\langle\varphi_1'|\varphi_1\rangle|^2|\langle\varphi_2'|\varphi_2\rangle|^2\ldots$$
$$|\langle\varphi_{K-1}'|\varphi_{K-1}\rangle|^2|\langle\varphi_{K+1}'|\varphi_{K+1}\rangle|^2\ldots|\langle\varphi_N'|\varphi_N\rangle|^2.$$

(N-1)e⁻ SHAKE-UP/ SHAKE-OFF→ "MONOPOLE"

spin-orbit +	$\lvert\hat{e}\cdot\langle\varphi_f\lvert\vec{r}\rvert\varphi_K\rangle\rvert^2$
	1e- DIPOLE→$d\sigma/d\Omega$

- PLUS DIFFRACTION EFFECTS IN φ_f ESCAPE

"Basic Concepts of XPS"
Chapter 3.D.

Magnetic Circular Dichroism in X-Ray Absorption (XMCD): Only happens because of the spin-orbit effect

- SPIN-ORBIT SPLITTING OF LEVELS:

$\Rightarrow$ EFFECTIVE $\vec{B}$ (NUCLEUS AROUND e^-) $\propto \vec{L}$

$$\hat{H}_{s\text{-}o} = \xi(r)\,\vec{l}\cdot\vec{s}$$

- SPLITS ALL nl LEVELS $2(2l+1)$ $\rightarrow$ $nlj = l+1/2$ — $2l+2$; $nlj = l-1/2$ — $2l$

- MIXES SPIN + ORBITAL ANGULAR MOM.:

$$\psi_{nljm_j} = C_1\psi_{nl,m_j-1/2}\underbrace{\begin{pmatrix}1\\0\end{pmatrix}}_{m_s=+1/2\ \uparrow} + C_2\psi_{nl,m_j+1/2}\underbrace{\begin{pmatrix}0\\1\end{pmatrix}}_{m_s=-1/2\ \downarrow}$$

WITH C1 AND C2 TABULATED CLEBSCH-GORDAN OR WIGNER 3j SYMBOLS

Example: Photoelectron spin polarization from spin-orbit coupling and circularly-polarized radiation—The Fano Effect

$$\frac{I_{up}-I_{down}}{I_{up}+I_{down}} = \frac{\sqrt{1/3}^2-1^2}{\sqrt{1/3}^2+1^2}\,x100 = \frac{-2/3}{4/3}\,x100 = -50\%$$

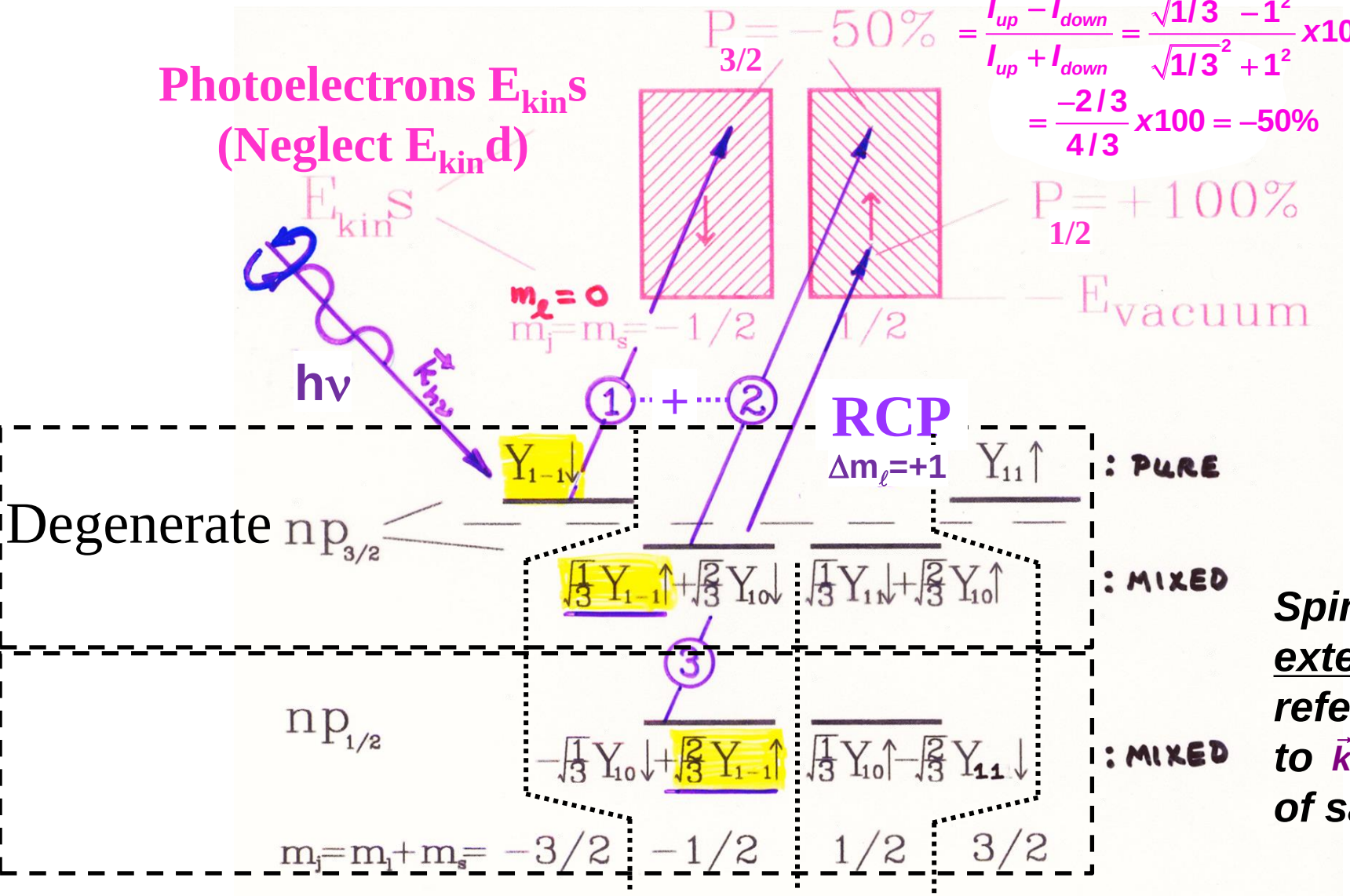

Spin externally referenced to $\vec{k}_{h\nu}$ and $\vec{M}$ of sample

Photoelectron spin polarization from spin-orbit coupling and circularly-polarized radiation—The Fano Effect

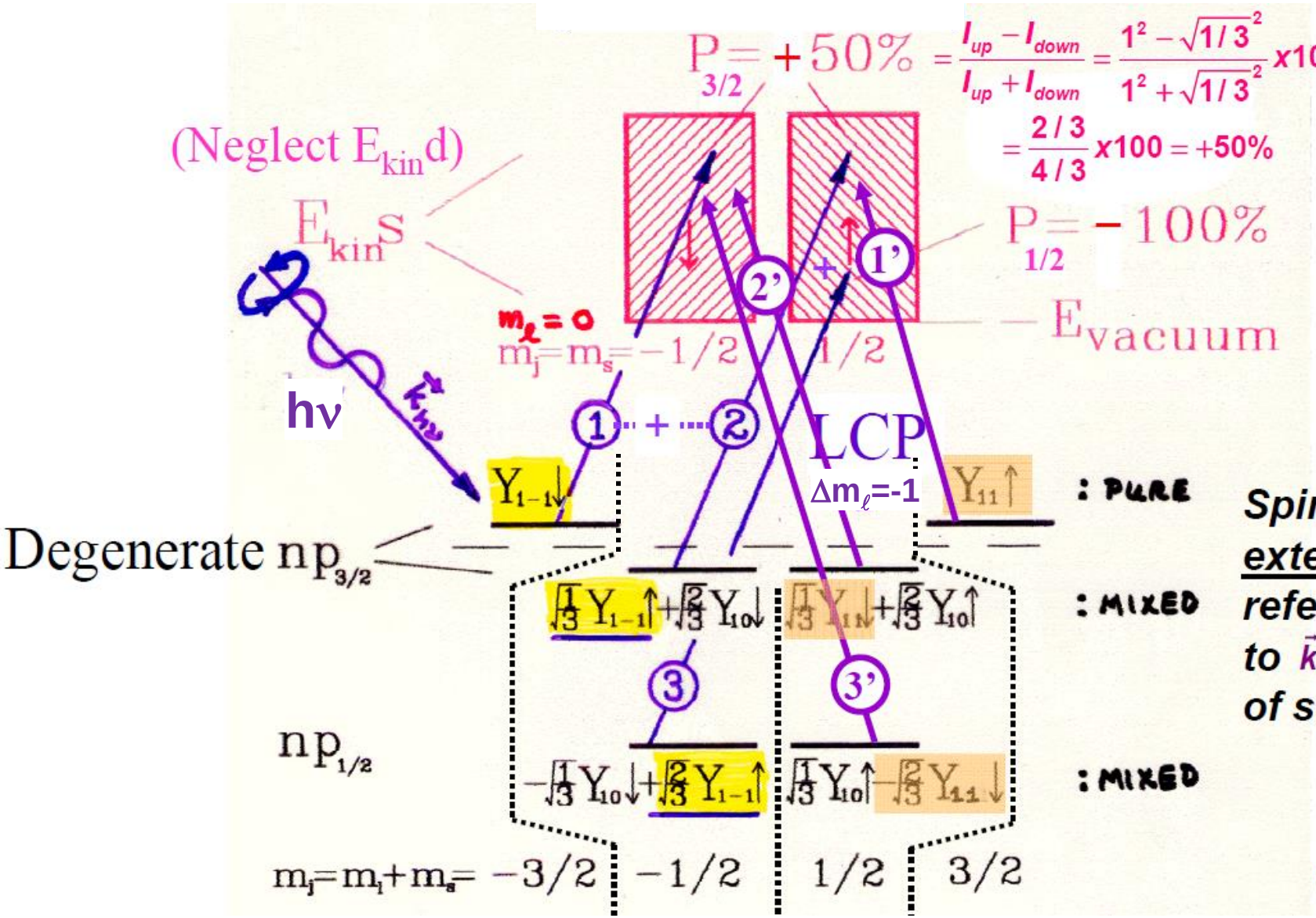

Spin ***externally*** *referenced to* $\vec{k}_{h\nu}$ *and* $\vec{M}$ *of sample*

Measuring Electron Binding Energies

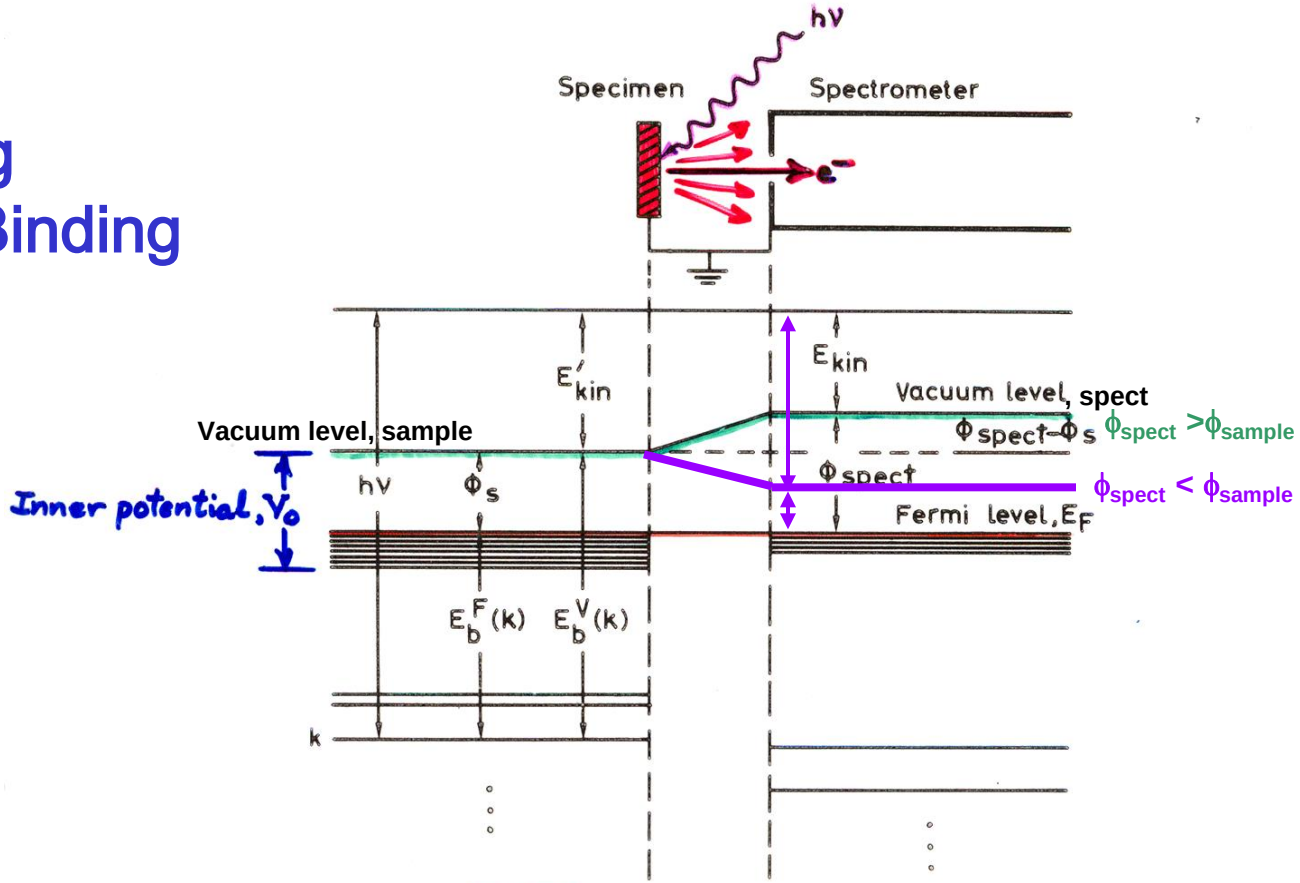

$$h\nu = E_b^V(k) + E'_{kin} = E_b^F(k) + \phi_s + E'_{kin}$$

$$= E_b^F(k) + \phi_{spect} + E_{kin}$$

KNOWN

TWO E_b REFERENCES

MEASURED

Figure 3 -- Energy level diagram for a metallic specimen in electrical equilibrium with an electron spectrometer. The closely spaced levels near the Fermi level E_F represent the filled portions of the valence bands in specimen and spectrometer. The deeper levels are core levels. An analogous diagram also applies to semiconducting or insulating specimens, with the only difference being that E_F lies somewhere between the filled valence bands and the empty conduction bands above.

Paper 1
"Basic Concepts of XPS"
Figure 3

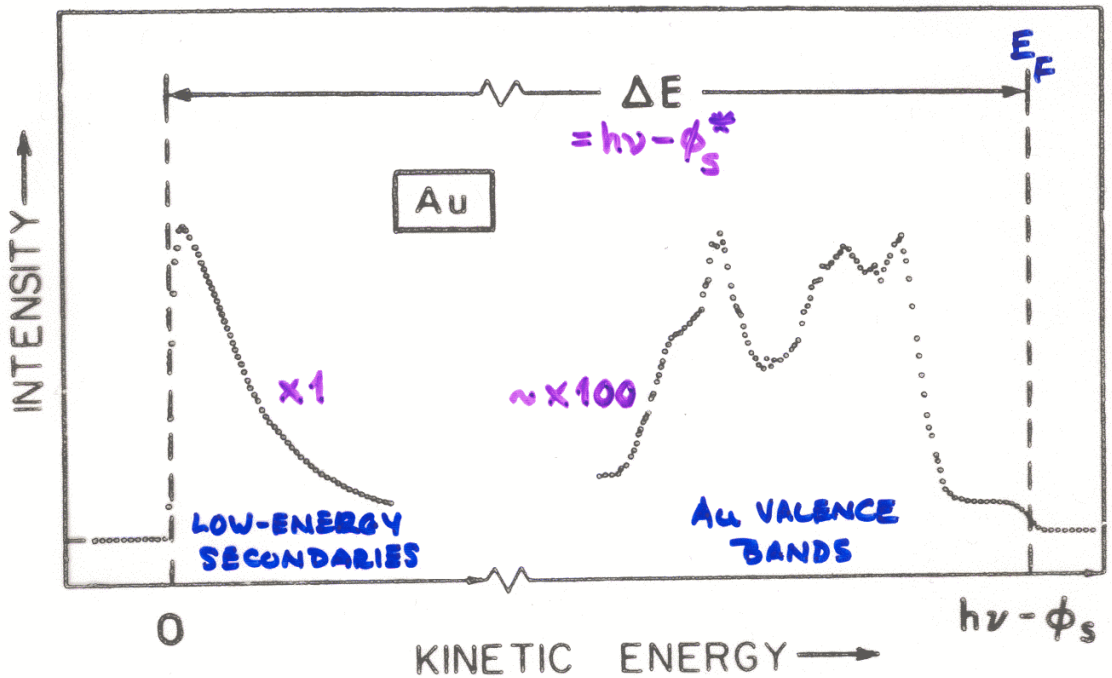

*PROVIDED $\phi_s > \phi_{spect}$ OR, IF $\phi_s < \phi_{spect}$, SAMPLE BIASSED NEGATIVELY BY $V_{BIAS}^{(-)} > \phi_{spect} - \phi_s$

Figure 4 -- Full XPS spectral scan for a polycrystalline Au specimen, showing both the cutoff of the secondary electron peak at zero kinetic energy and the high-energy cutoff for emission from levels at the metal Fermi level. The measureable distance ΔE thus equals $h\nu-\phi_s$, provided that suitable specimen biasing has been utilized. For this case, hν was 1253.6 eV and ϕ_s was 5.1 eV. (From Baer, reference 56).

"Basic Concepts of XPS"
Figure 4

Work functions of the Elements [eV]

After L. Ley and M. Cardona, "Photoemission in Solids", Springer 1979

Low

High

1 H -																	2 He -
3 Li 2.4	4 Be 1.5											5 B 4.5	6 C 4.7	7 N -	8 O -	9 F -	10 Ne -
11 Na 2.35	12 Mg 3.6											13 Al 4.25	14 Si 4.8	15 P -	16 S -	17 Cl -	18 Ar -
19 K 2.2	20 Ca 2.8	21 Sc 3.3	22 Ti 3.95	23 V 4.1	24 Cr 4.6	25 Mn 3.8	26 Fe 4.3	27 Co 4.4	28 Ni 4.5	29 Cu 4.4	30 Zn 4.2	31 Ga 4.0	32 Ge 4.8	33 As 5.1	34 Se 4.7	35 Br -	36 Kr -
37 Rb 2.2	38 Sr 2.35	39 Y 3.3	40 Zr 3.9	41 Nb 4.0	42 Mo 4.3	43 Tc -	44 Ru 4.6	45 Rh 4.75	46 Pd 4.8	47 Ag 4.3	48 Cd 4.1	49 In 3.8	50 Sn 4.4	51 Sb 4.1	52 Te 4.7	53 I -	54 Xe -
55 Cs 1.8	56 Ba 2.5	57 La 3.3	72 Hf 3.5	73 Ta 4.1	74 W 4.5	75 Re 5.0	76 Os 4.7	77 Ir 5.3	78 Pt 5.3	79 Au 4.3	80 Hg 4.5	81 Tl 3.7	82 Pb 4.0	83 Bi 4.4	84 Po -	85 At -	86 Rn -
87 Fr -	88 Ra -	89 Ac -															

58 Ce 2.7	59 Pr -	60 Nd -	61 Pm -	62 Sm -	63 Eu -	64 Gd -	65 Tb -	66 Dy -	67 Ho -	68 Er -	69 Tm -	70 Yb -	71 Lu -
90 Th 3.3	91 Pa -	92 U 3.3	93 Np	94 Pu	95 Am	96 Cm	97 Bk	98 Cf	99 Es	100 Fm	101 Md	102 No	103 Lr

Electron Work Functions of the Elements

From the CRC-Handbook, 73rd edition (1993)

Element	Surface crystallographic orientation	Work function (eV)
Ag	polycrystalline	4.26
	(100)	4.64
	(110)	4.52
	(111)	4.74
Al	polycrystalline	4.28
	(100)	4.41
	(110)	4.06
	(111)	4.24
As		3.75
Au	polycrystalline	5.1
	(100)	5.47
	(110)	5.37
	(111)	5.31
B		4.45
Ba		2.7
Be		4.98
Bi		4.22
C		5.0

Depends on surface orientation

Measuring Electron Binding Energies: Charging Effects For Insulators

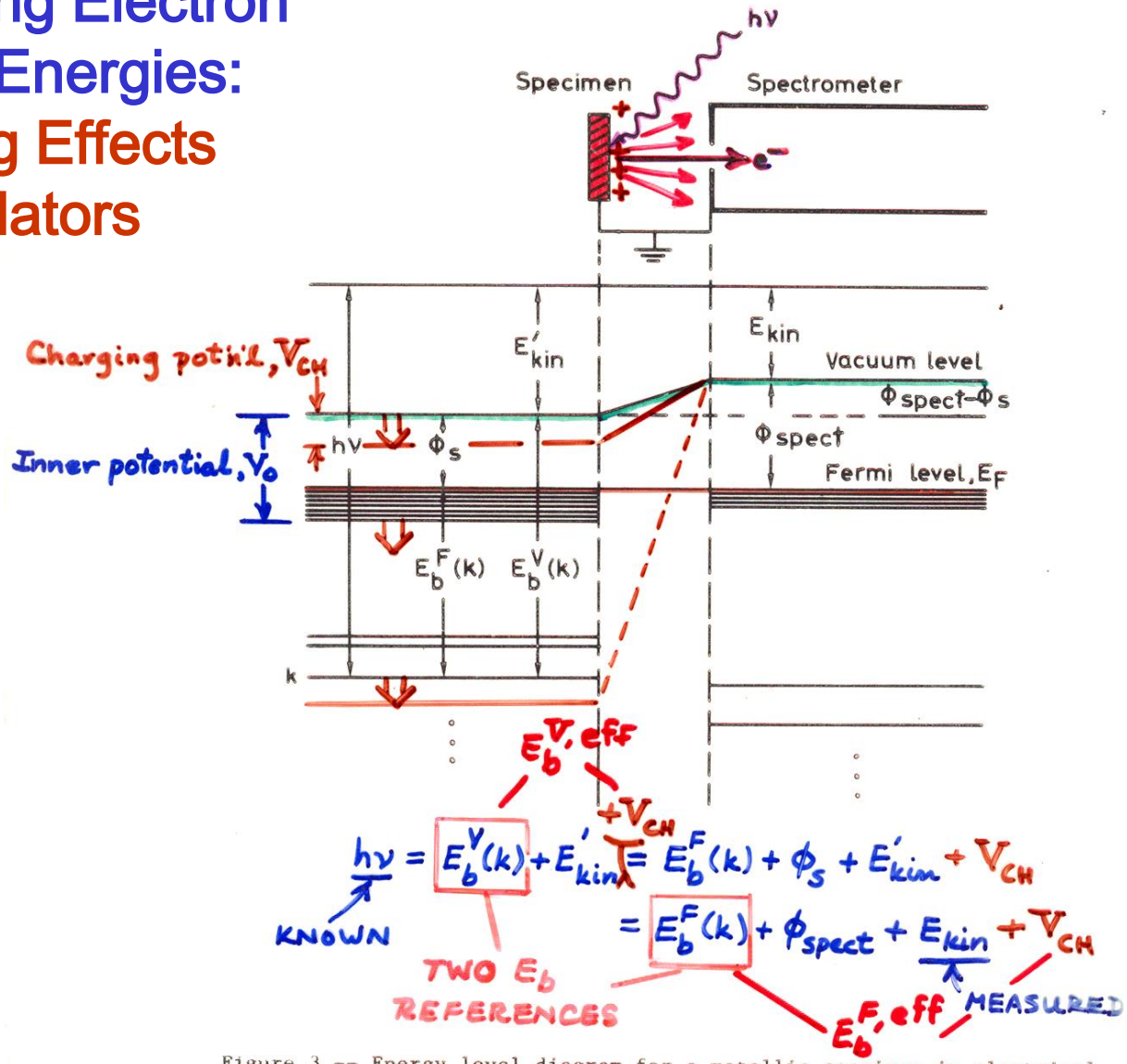

Figure 3 -- Energy level diagram for a metallic specimen in electrical equilibrium with an electron spectrometer. The closely spaced levels near the Fermi level E_F represent the filled portions of the valen bands in specimen and spectrometer. The deeper levels are core levels. An analogous diagram also applies to semiconducting or insulating specimens, with the only difference being that E_F lies somewhere between the filled valence bands and the empty conduction bands above.

"Basic Concepts of XPS"
Figure 3

BEST CURRENT SOLUTION TO AN OLD PROBLEM: CHARGING IN INSULATORS

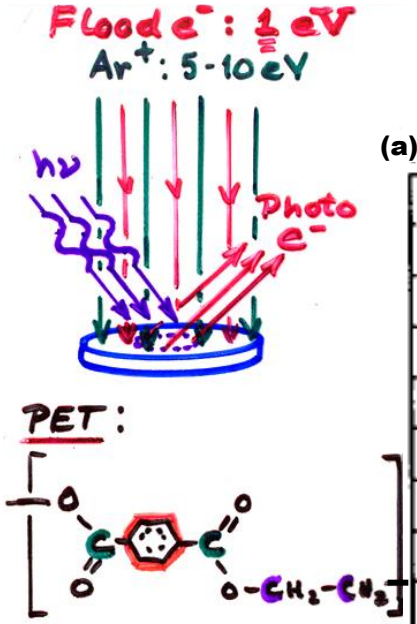

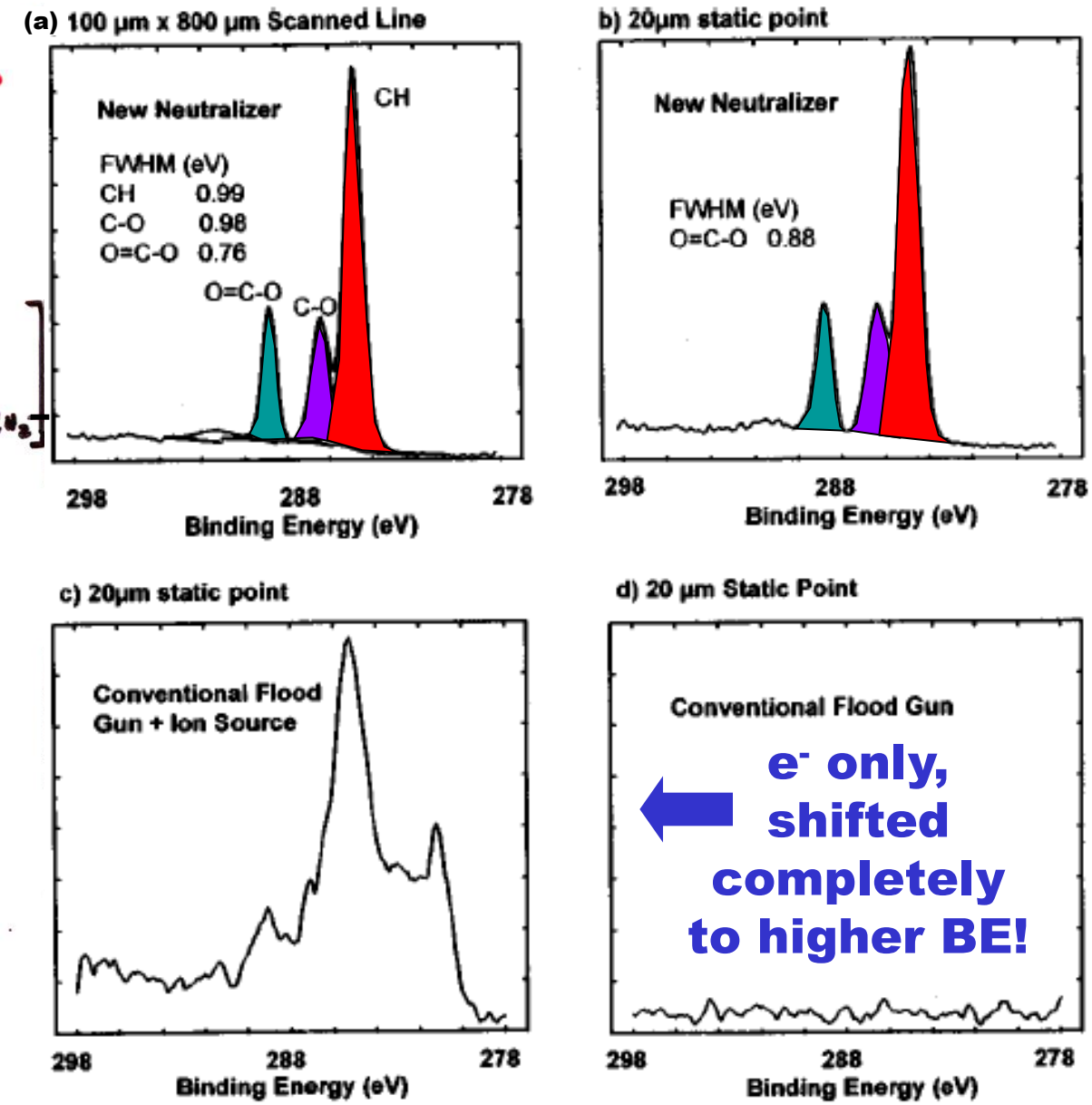

P. LARSON, M. KELLY, J. VAC. SCI. TECH. 16, 3483 ('98)

One-Electron Picture of Photoemission from a Surface

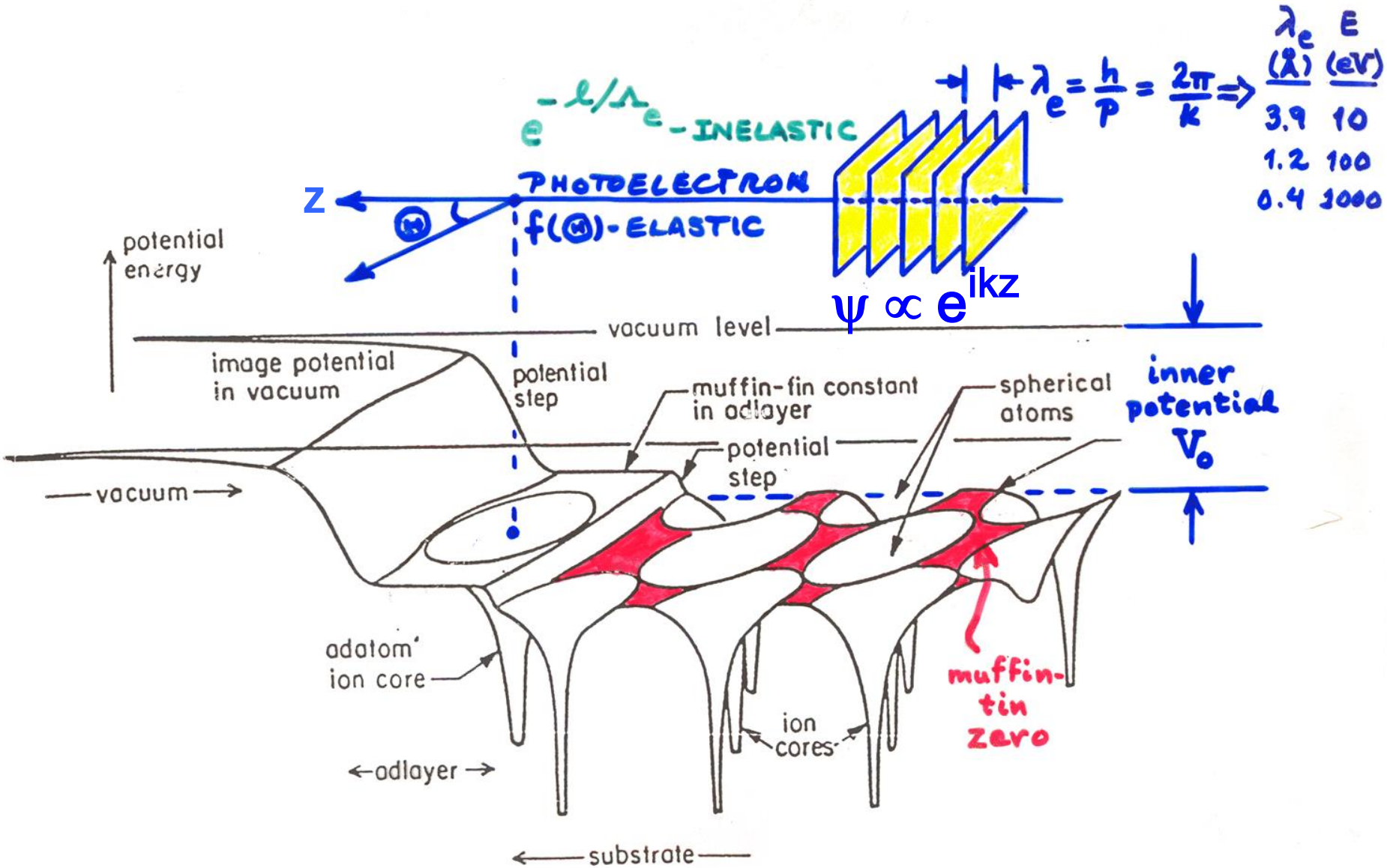

One-Electron Picture of Photoemission from a Surface

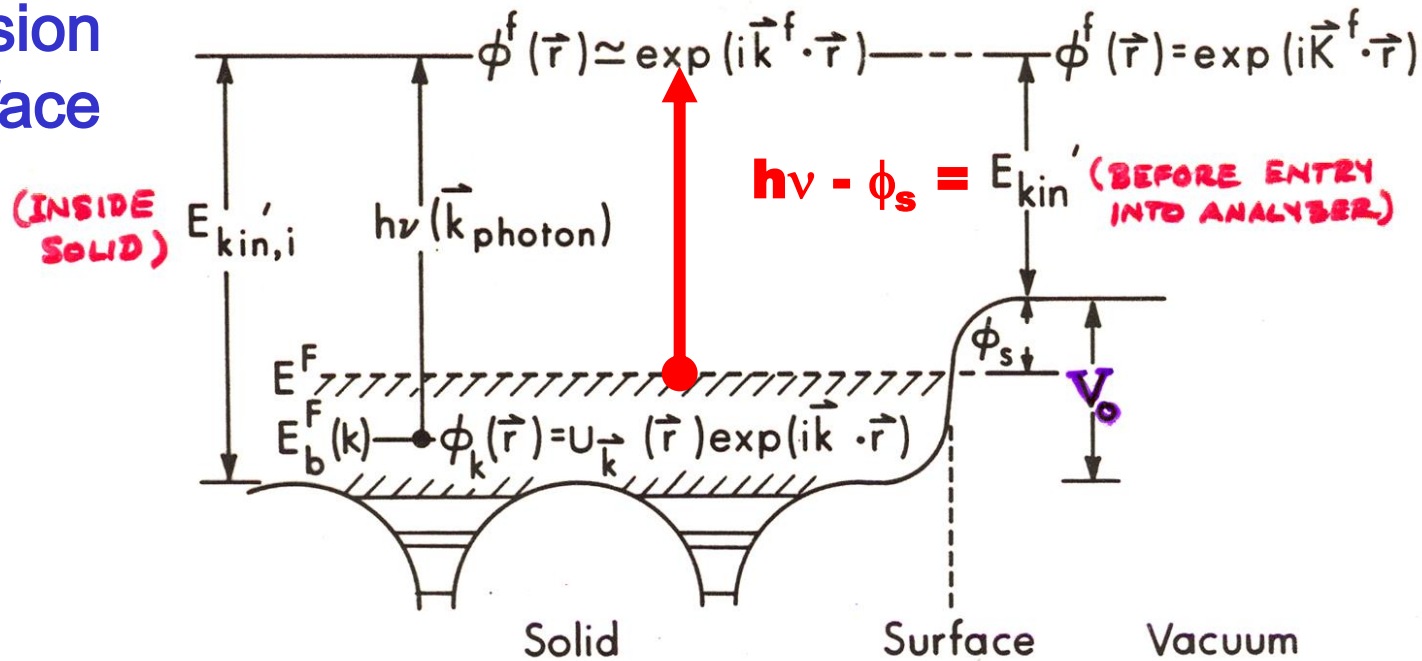

$$(1) \quad E_{kin,i}' = h\nu - E_b^F(k) + V_o - \phi_s \simeq \frac{\hbar^2 (k^f)^2}{2m}$$

$$(2) \quad E_{kin}' = E_{kin,i}' - V_o = \frac{\hbar^2 (K^f)^2}{2m}$$

$$(3) \quad \vec{k} + \underbrace{\vec{k}_{photon}}_{\vec{k}_{h\nu}} + \vec{g} = \vec{k}^f$$

Basic energetics

$$h\nu = E_{binding}^{Vacuum} + E_{kinetic} = E_{binding}^{Fermi} + \varphi_{spectrometer} + E_{kinetic}$$

One-Electron Picture of Photoemission from a Surface

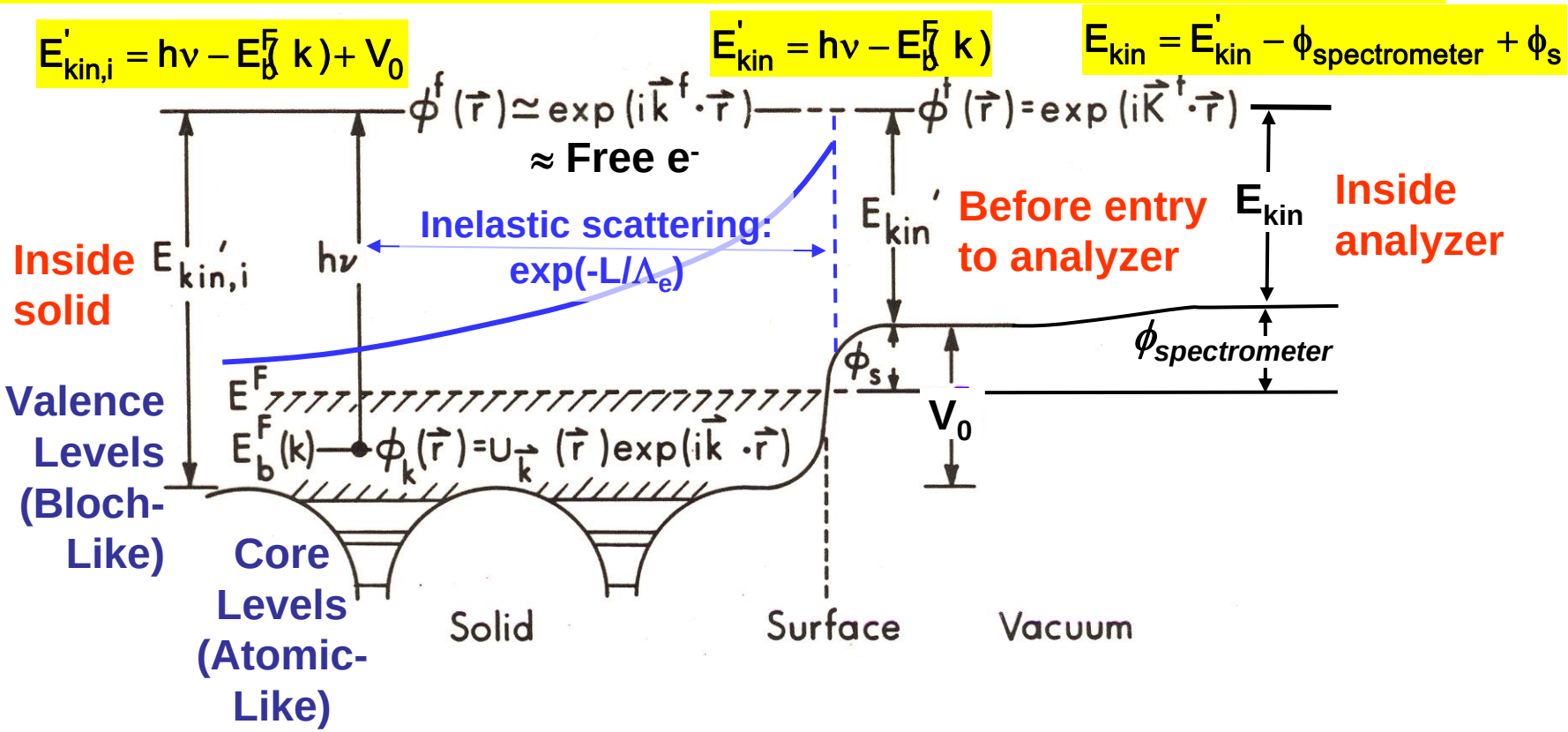

CALCULATION OF V_0 FOR AN IDEAL METAL

Fig. 4.2. Electron density profile at a jellium surface for two choices of the background density, r_s (Lang & Kohn, 1970).

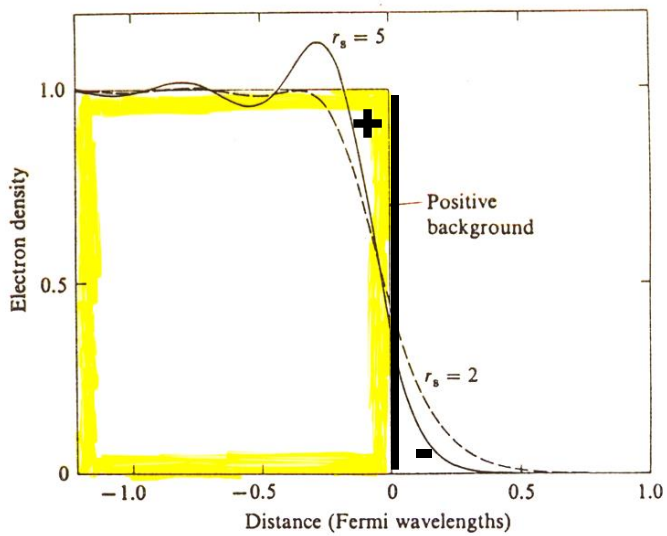

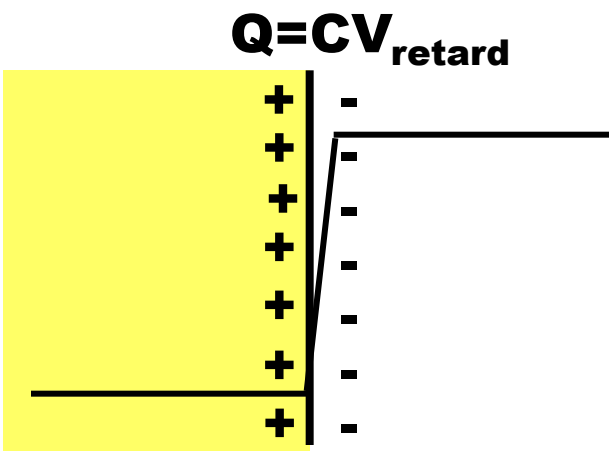

Fig. 4.3. Electrostatic potential, $v(z)$, and total effective one-electron potential, $v_{eff}(z)$, near a jellium surface (Lang & Kohn, 1970).

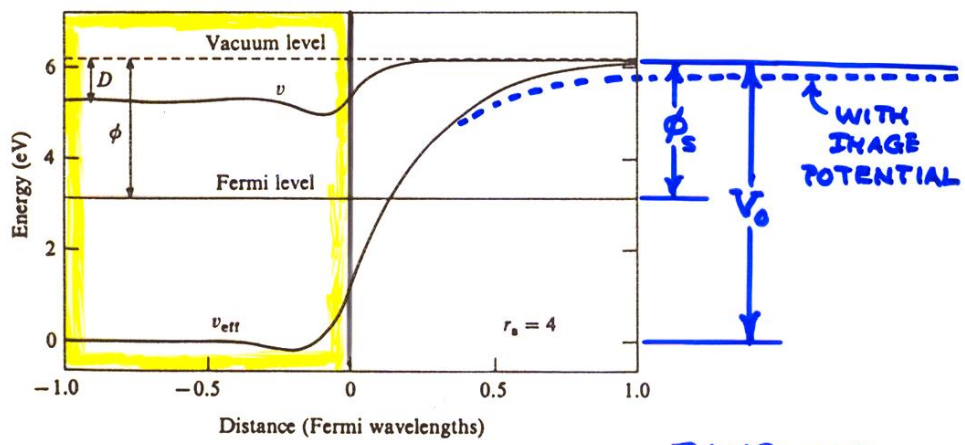

ZANGWILL, "SURFACE PHYSICS"

Electron Spectroscopy—A typical configuration

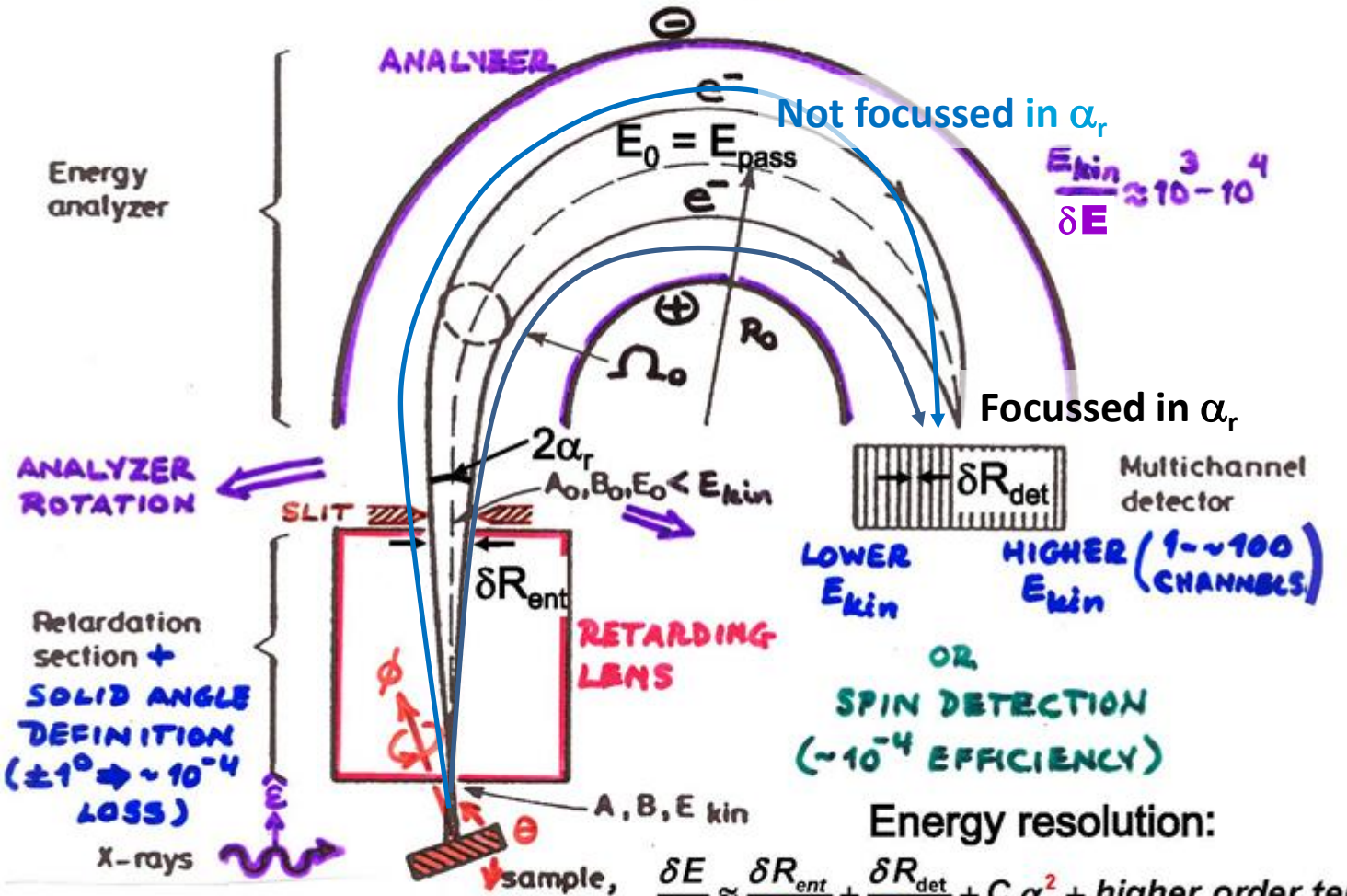

Energy resolution:

$$\frac{\delta E}{E_0} \approx \frac{\delta R_{ent}}{2R_0} + \frac{\delta R_{det}}{2R_0} + C_r \alpha_r^2 + \textit{higher order terms}$$

$$C_r \approx 1.0$$

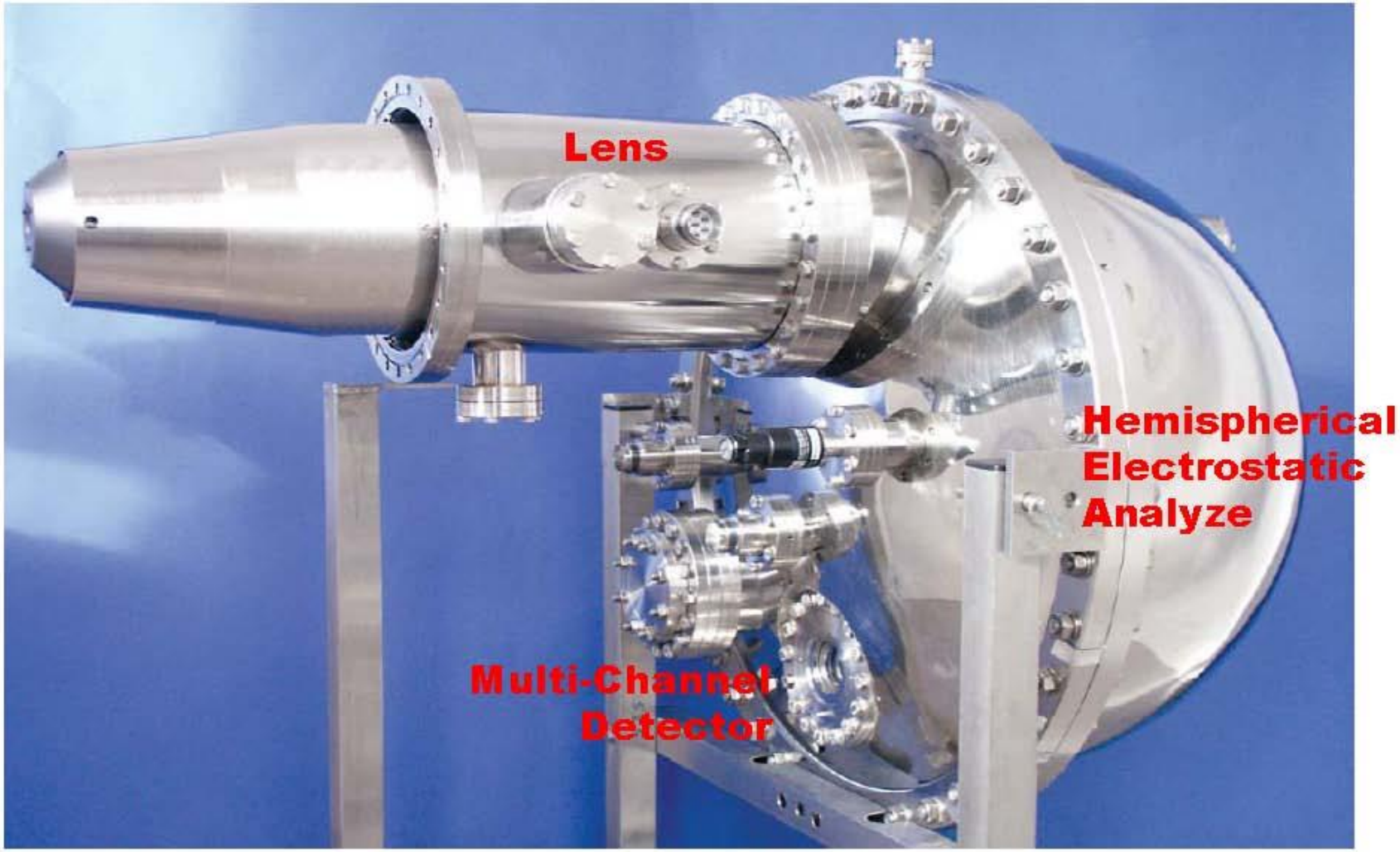

Nilsson et al., Journal of Electron Spectroscopy and Related Phenomena 70 (1994) 117-128

The Scienta R4000

With proper lens imaging in vertical angle- an energy vs angle image at detector

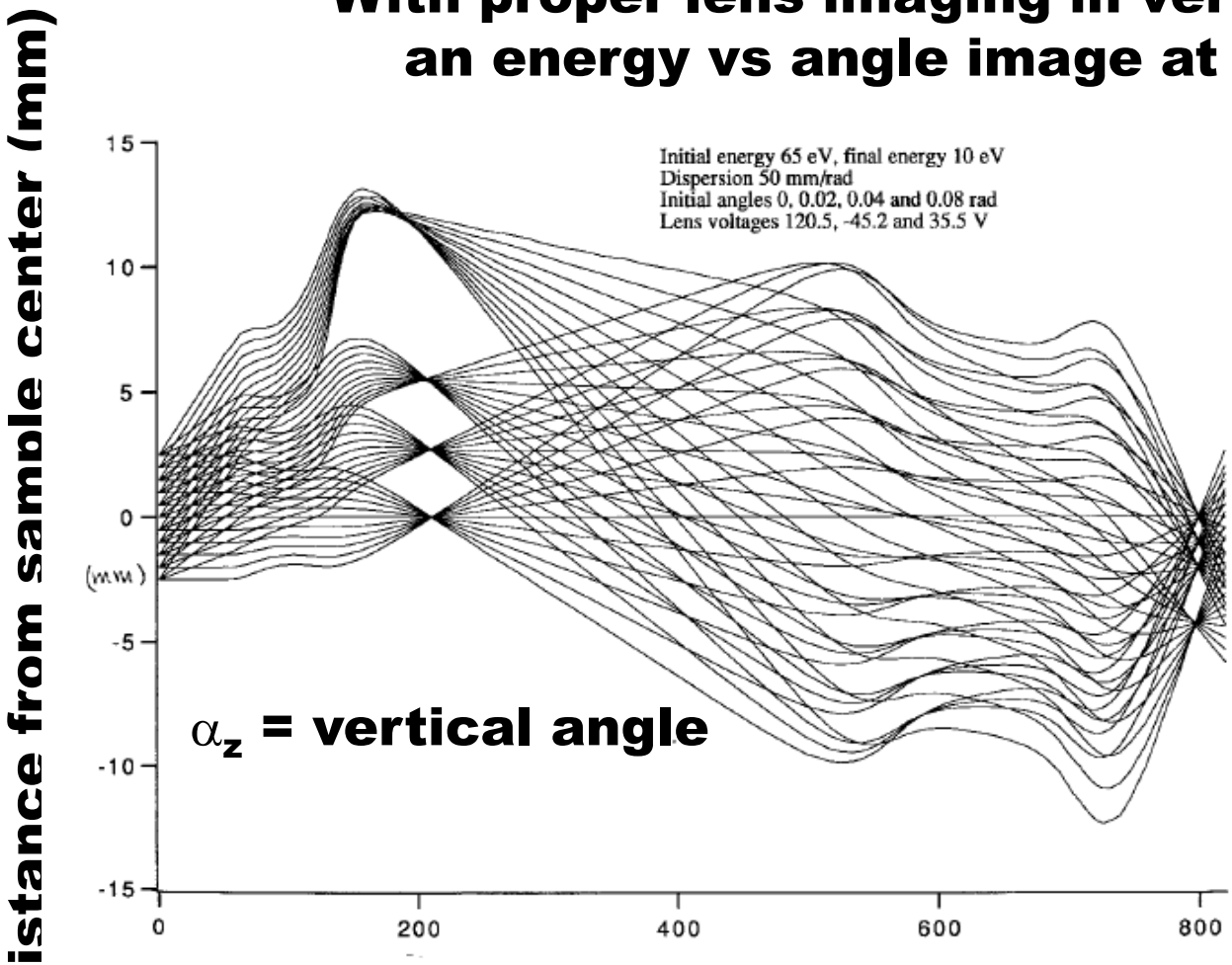

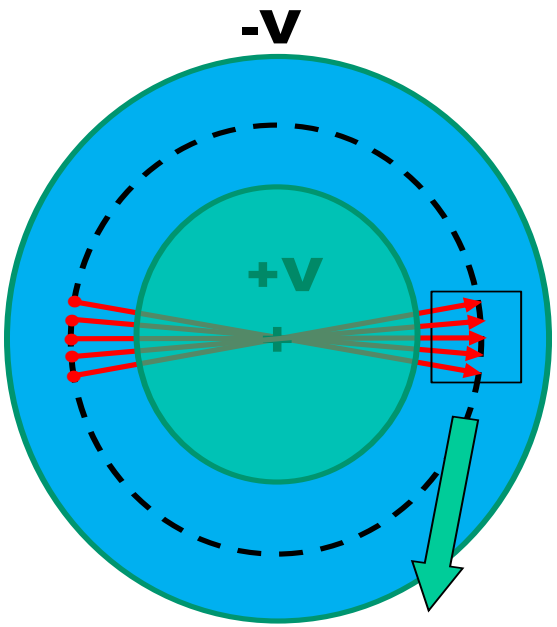

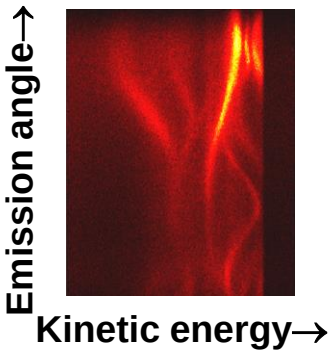

$E,\vec{k}$ band mapping

Graphene- A very special 2D case

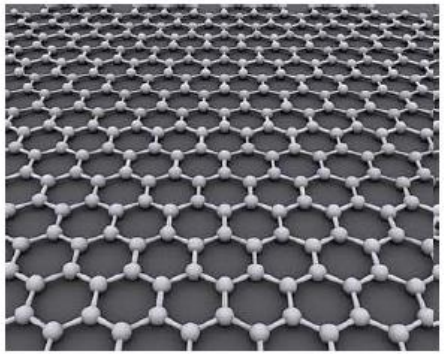

The Nobel Prize in Physics 2010
Andre Geim, Konstantin Novoselov
…"for groundbreaking experiments regarding the two-dimensional material graphene"

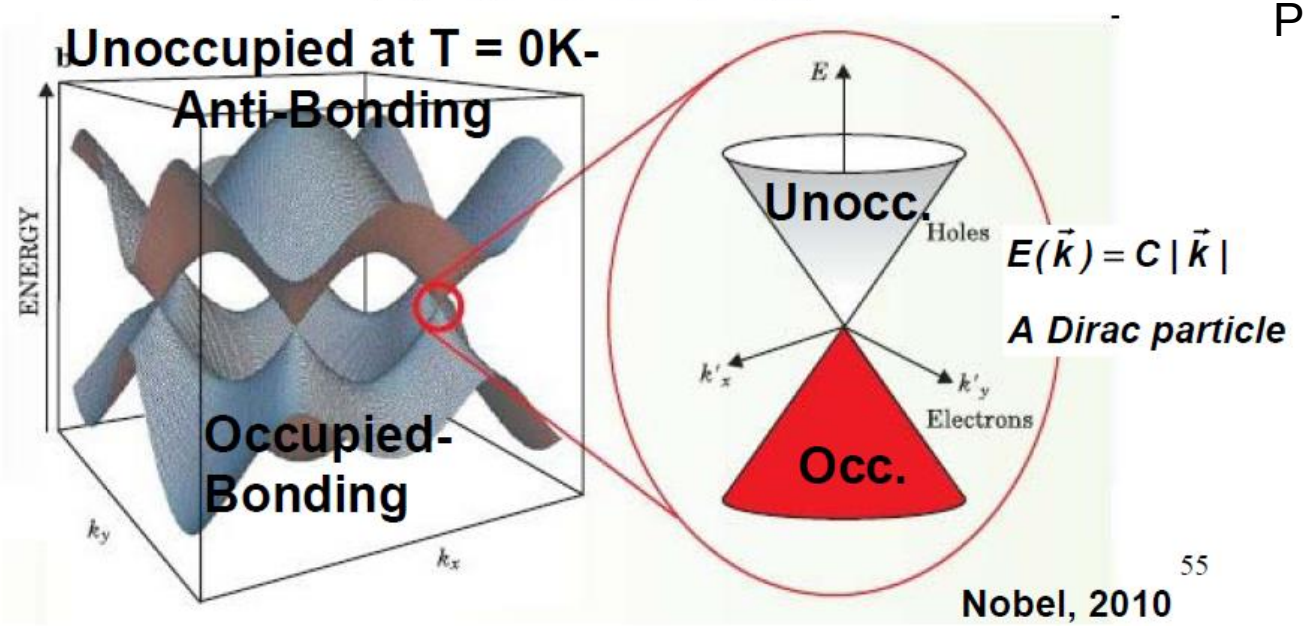

Photoelectron spectroscopy

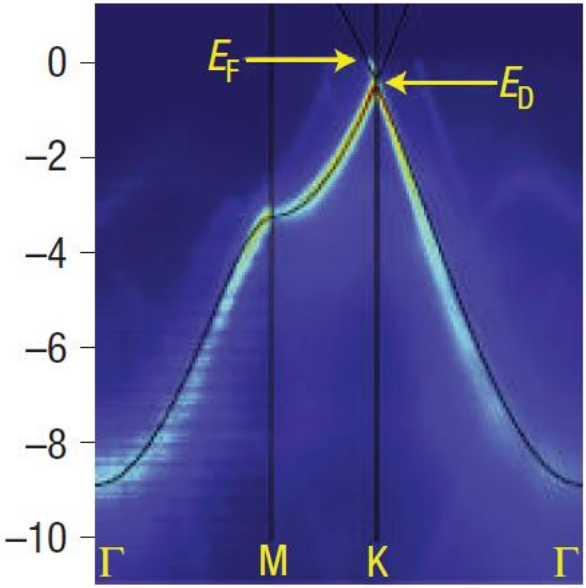

Bostwick et al., Nature Physics 3, 36 - 40 (2007)

MULTICHANNEL DETECTION GEOMETRIES

Multiple channeltrons: brute force

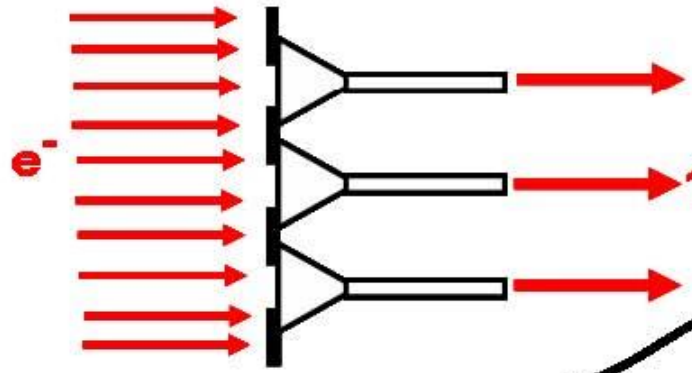

10^6-10^8 e^-

Up to ~ 1-5 MHz per channel

Crossed-wires—2D Up to ~ 1MHz

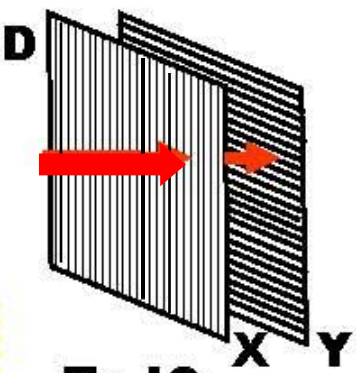

Microchannel plates (MCPs) and

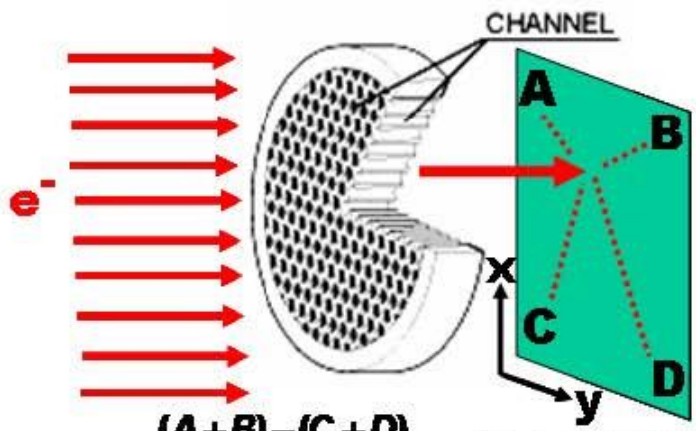

$$x = \frac{(A+B)-(C+D)}{A+B+C+D}$$

$$y = \frac{(B+D)-(A+C)}{A+B+C+D}$$

Resistive Anode—2D: Up to ~1 MHz

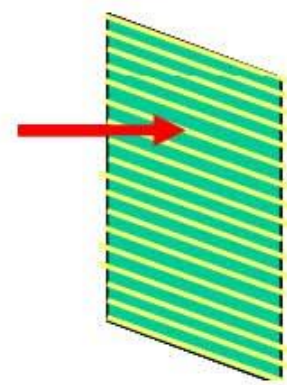

To IC channel

Individual Collectors—1D (Elettra and the ALS): Up to ~ 1GHz

MULTICHANNEL DETECTION GEOMETRIES

Multiple channeltrons: brute force

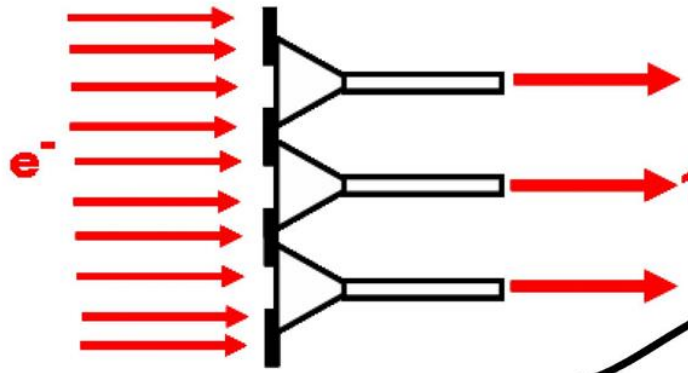

10^6-10^8 e^-

Up to ~ 1-5 MHz per channel

Crossed-wires—2D
Up to ~ 1MHz

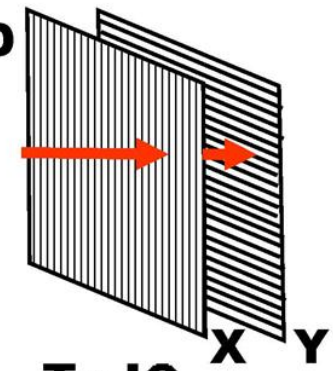

Microchannel plates (MCPs) and

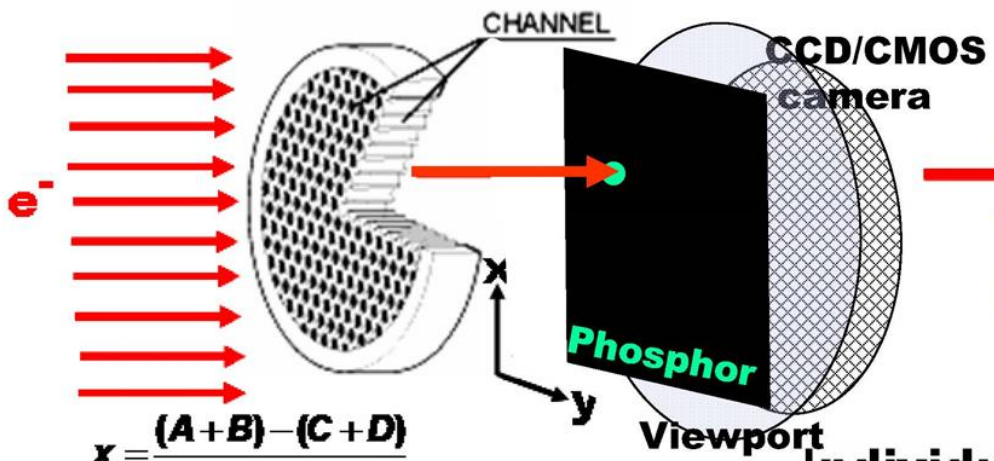

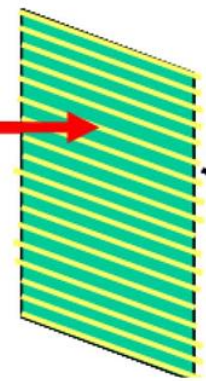

To IC channel

$$x = \frac{(A+B)-(C+D)}{A+B+C+D}$$

$$y = \frac{(B+D)-(A+C)}{A+B+C+D}$$

Phosphor + Video Camera

Individual Collectors—1D (Elettra and the ALS): Up to ~ 1GHz

The Microchannel Plate Electron (and Photon) Multiplier

Diam.
Down to 5
microns

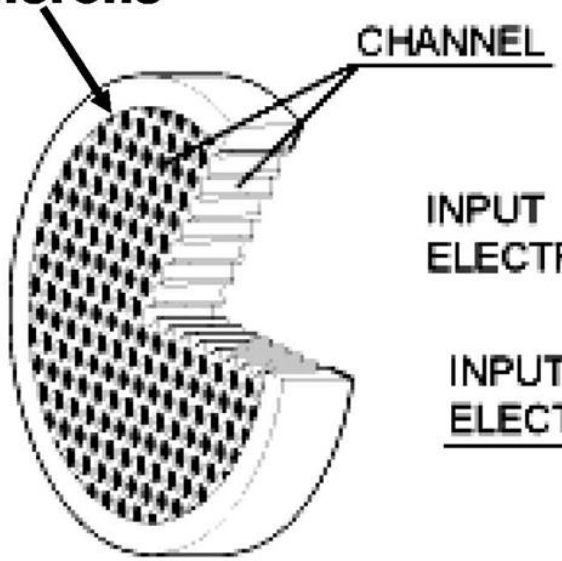

Pb-DOPED GLASS

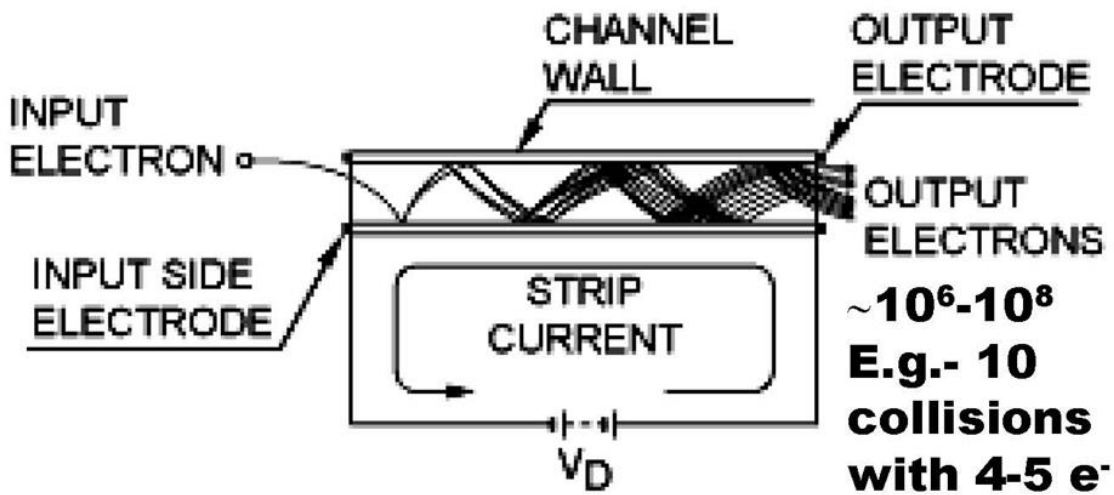

$\sim 10^6$-10^8
E.g.- 10
collisions
with 4-5 e^-
each

The MicroMott Electron Spin Detector

Plus new higher sensitivity via very low energy few-eV exchange scattering from Co(0001)/W(110): Graf et al., http://arxiv.org/pdf/cond-mat/0404720.pdf and Joswiak et al., REVIEW OF SCIENTIFIC INSTRUMENTS 81, 053904 (2010)

Tang et al., Rev. Sci. Inst. 59, 504 (1988); Huang et al., Rev. Sci. Inst. 73, 3778 (2002)

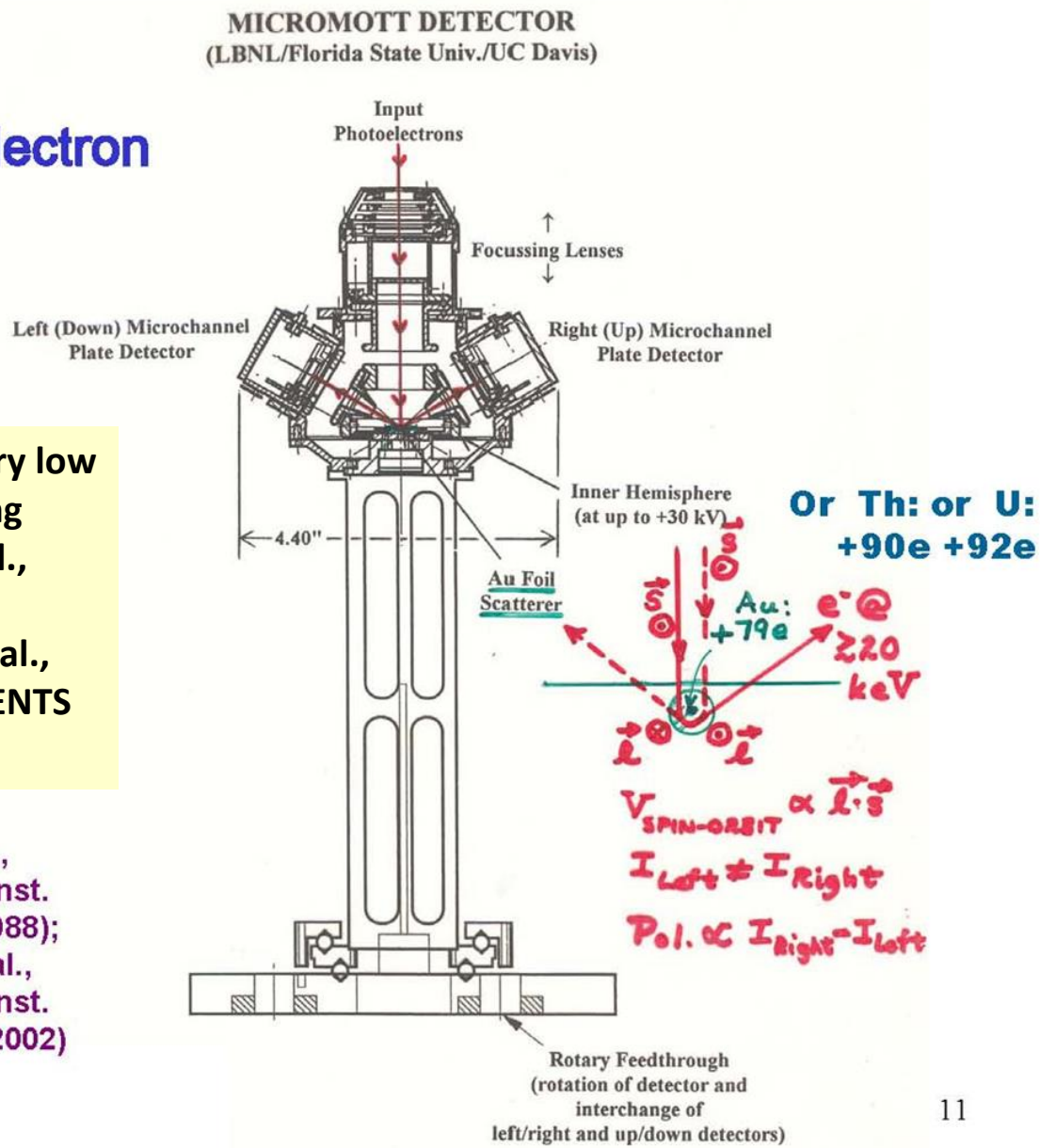

Soft X-Ray Emission Spectroscopy—A typical configuration

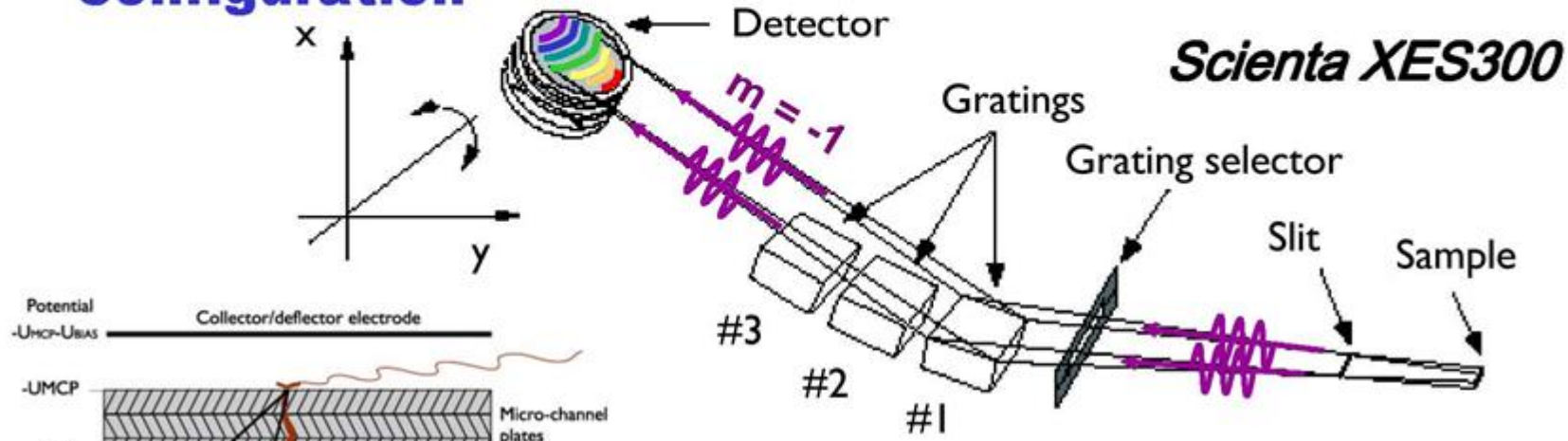

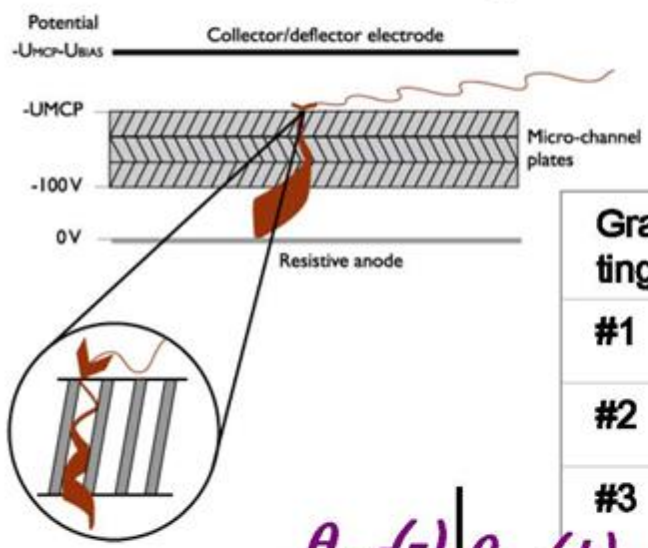

Gra-ting no.	Ra-dius	Groove density.	Incid. angle	Operating range
#1	5 m	1200 l/mm	1.9	300-1500 eV
#2	5 m	400 l/mm	2.6	100-450 eV
#3	3 m	300 l/mm	5.4	20-200 eV

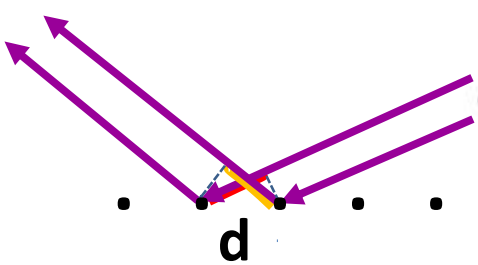

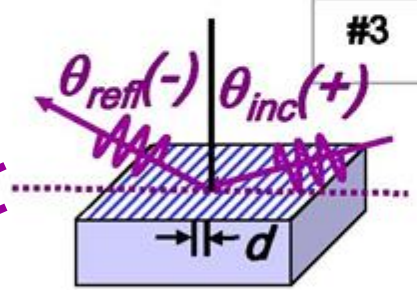

Difference of path lengths =

$$d[\sin(\theta_{inc} = +no.) + \sin(\theta_{refl} = -no.)] = m\lambda_x$$

$$\sin\theta_{inc} + \sin\theta_{refl} = \frac{m\lambda_x}{d}$$

The (Focusing) Rowland Circle
X-Ray Monochromator/Spectrometer Geometry

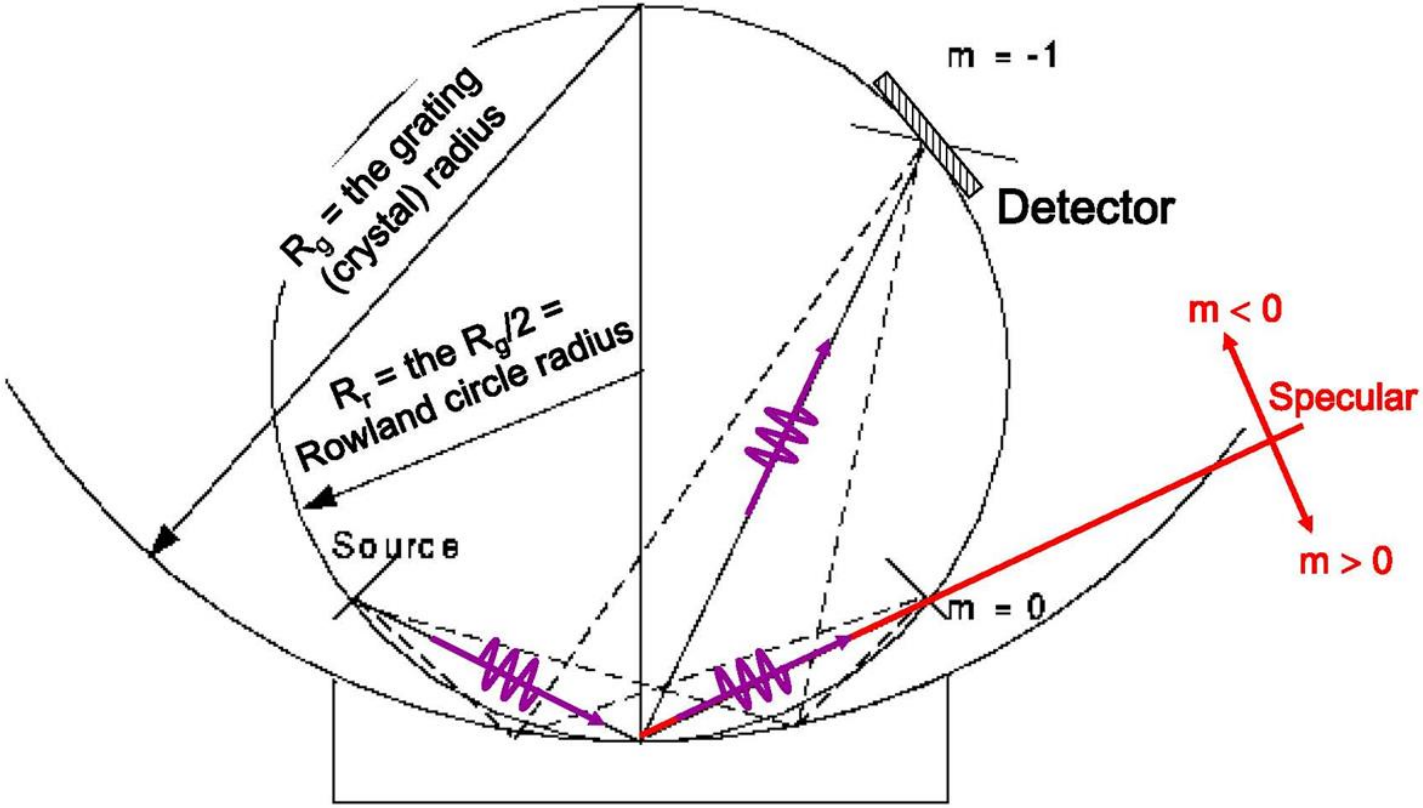

Curved grating (soft x-rays)
or single crystal (hard x-rays)

One commercial soft x-ray spectrometer—Scienta XES 300

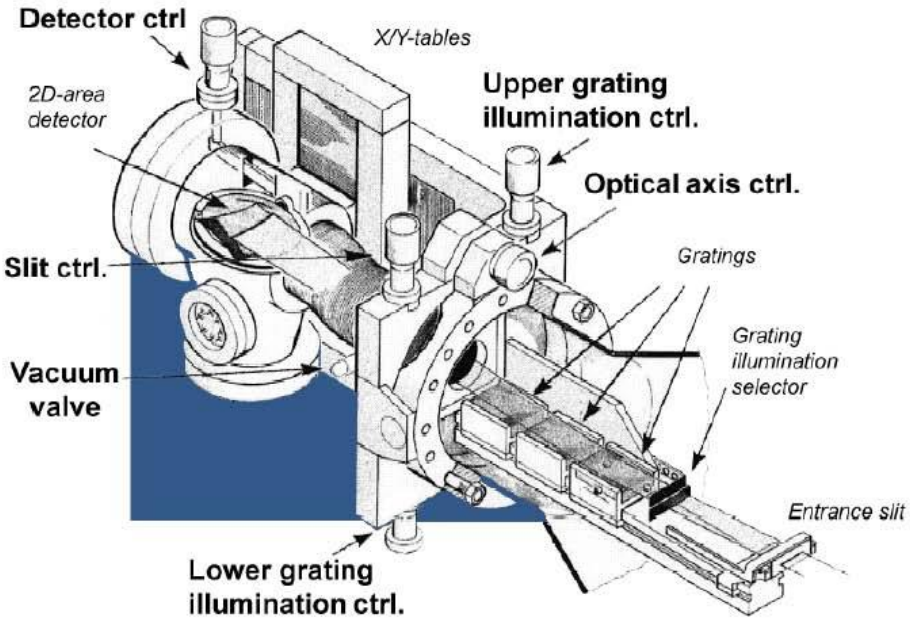

Hard X-ray Photoemission at the Advanced Light Source: The Multi-Technique Spectrometer/ Diffractometer (MTSD)

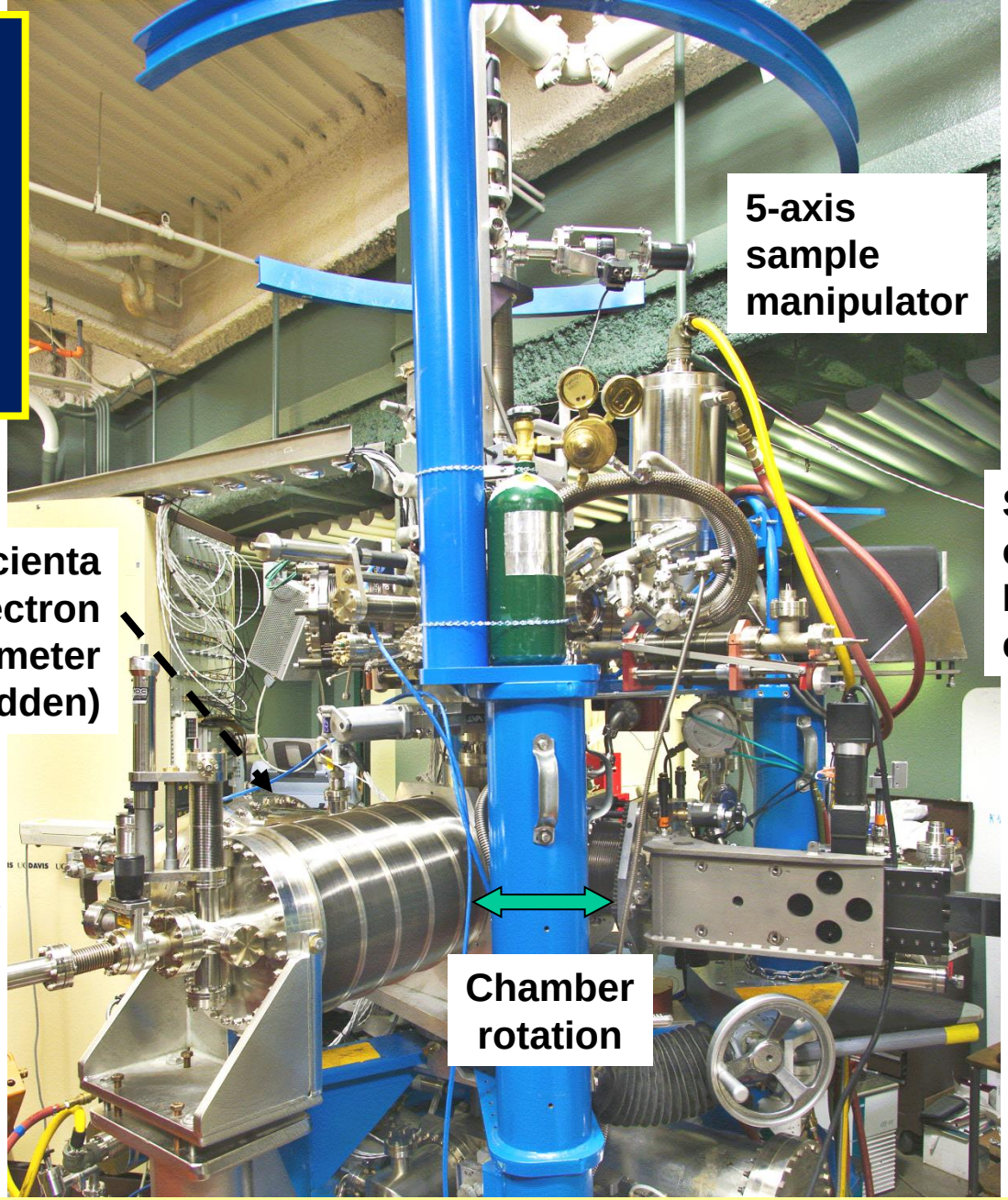

ALS
BL 9.3.1
$h\nu$ = 2-5 keV

Permits using all relevant spectroscopies on a single sample:
XPS (incl. Al and Mg Kα), HXPS, XPD; XAS (e^- or photon detection), soft XES/RIXS

Hard X-ray Photoemission at the Advanced Light Source: The Multi-Technique Spectrometer/ Diffractometer (MTSD)

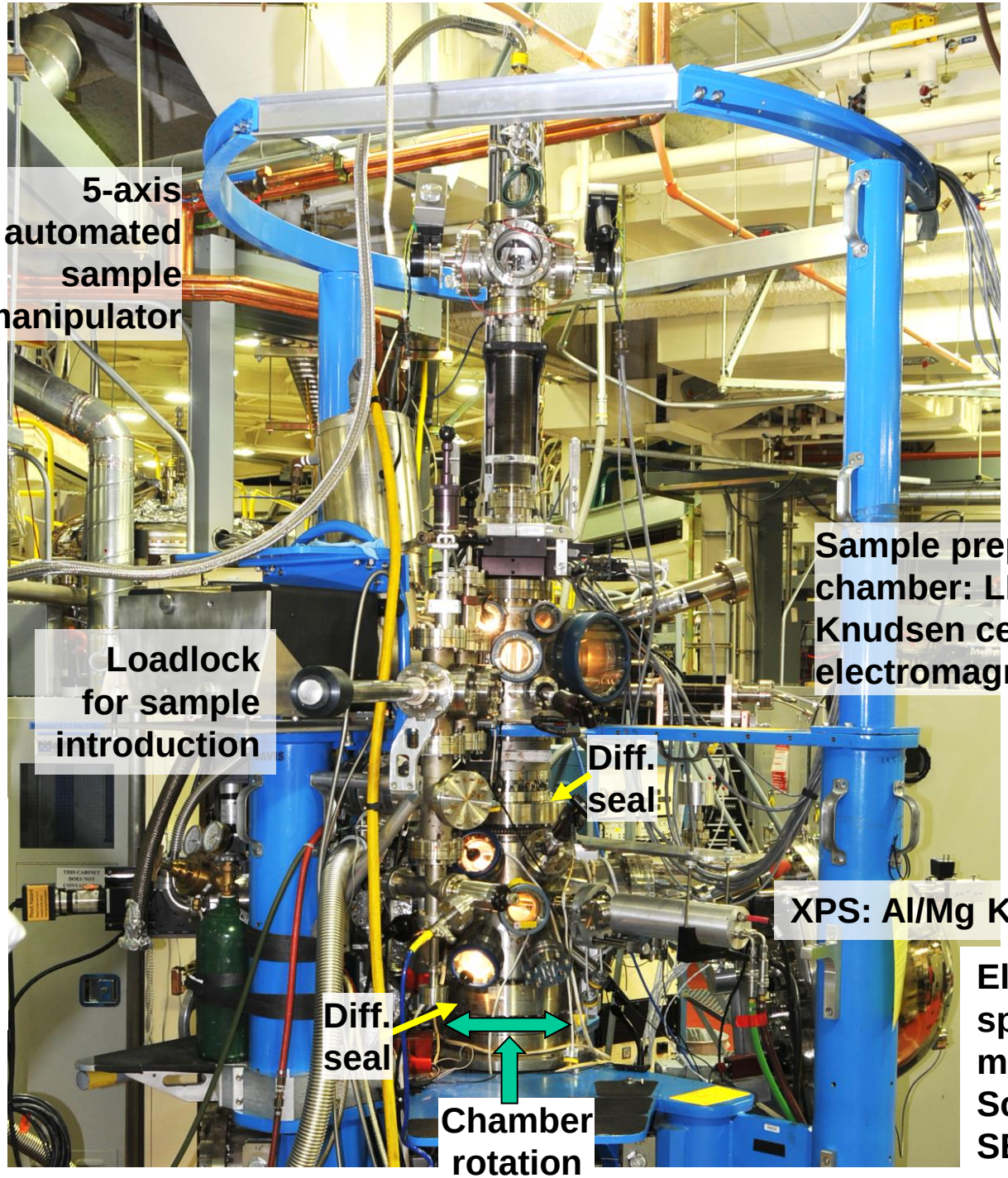

Basic energetics

$$h\nu = E_{binding}^{Vacuum} + E_{kinetic} = E_{binding}^{Fermi} + \varphi_{spectrometer} + E_{kinetic}$$

One-Electron Picture of Photoemission from a Surface

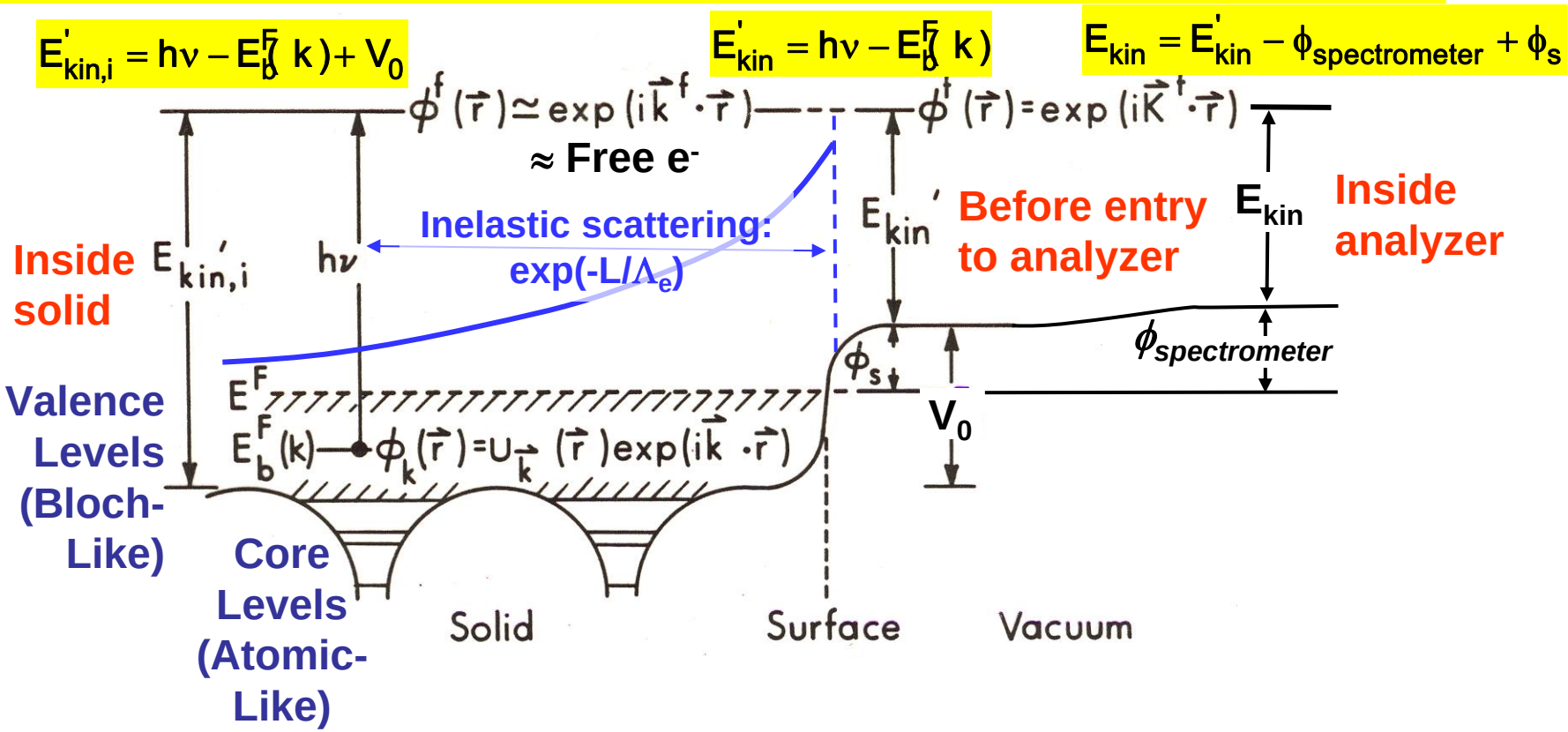

Complete Reading and Problem Assignments for Physics 243A
Surface Physics of Materials: Spectroscopy, Fall, 2016

READING:

- **WOODRUFF AND DELCHAR, "MODERN TECHNIQUES OF SURFACE SCIENCE", 2ND EDITION--**
  - **Chapter 1**
  - **Chapter 2: Sections 2.1, pp.22 (bottom)-23(top) on Wood notation for surface structures, 2.4, and 2.5 (pp. 31-37), 2.9.6 on standing waves**
  - **Chapter 6: 6.9, 6.10, 6.11**
  - **Chapter 3: Sections 3.1, 3.2, 3.3, 3.5**
- **ZANGWILL, "PHYSICS AT SURFACES", DOWNLOADABLE CHAPTERS 1-5 (SEE COURSE WEBSITE)--**
  - **Chapter 1: Everything except "The roughening transition"**
  - **Chapter 3: pp. 28-34, pp. 49-52 on STM, Pages 85-8, 192-196, 204-212**
  - **Chapter 2: All**
  - **Chapter 4: Introduction, with lighter reading of *The jellium model*, *One-dimensional band theory, and Three-dimensional band theory*, and detailed reading of *Photoelectron spectroscopy, Metals, and Alloys***
- **IBACH, "PHYSICS OF SURFACES AND INTERFACES", DOWNLOADABLE BOOK (SEE COURSE WEBSITE)—**
  - **Chapter 2: 2.1, 2.2**
  - **Chapter 8: 8.2**
- **DESJONQUERES AND SPANJAARD, "CONCEPTS OF SURFACE PHYSICS", EXCERPTS DOWNLOADABLE FROM COURSE WEBSITE:**
  - **On equilibrium shapes of surfaces, thermodynamics, kinetics and adsorption isotherms,STM current calculation, photoelectron diffraction and Debye-Waller factors. No need to follow every step, but as needed to fill in the line of arguments in lecture and Zangwill**
- **FADLEY, "BASIC CONCEPTS OF XPS", HANDED OUT, BUT ALSO DOWNLOADEABLE—**
  - **Read all of it**
- **FADLEY, "THE STUDY OF SURFACE STRUCTURES BY PHOTOELECTRON DIFFRACTION AND AUGER ELECTRON DIFFRACTION", PAGES 421-450 only, DOWNLOADABLE FROM COURSE WEBSITE with other examples and exercises using the EDAC web program introduced in lecture**
- **ATTWOOD, DOWNLOADEABLE EXCERPT ON SYNCHROTRON RADIATION FROM THE BOOK "Soft X-Rays and Extreme Ultraviolet Radiation" (see course website)**
- **SIX READING DOWNLOADS FROM THE COURSE WEBSITE: <u>If needed for comprehension at level of lectures or to use programs</u>**
  1. **Molecular orbital basics**
  2. **Tight-binding basics**
  3. **Core-Hole Multiplets with Charge Transfer--Basic Theory, or similar pages from Book by de Groot and Kotani**
  4. **Brief Manual for SESSA spectral simulation program**
  5. **Brief Manual for CTM4XAS20 charge-transfer multiplet simulation program**

  [7) <u>Optional only for physics students</u>: Basic theory for the Hubbard Model of bonding }

PROBLEM ASSIGNMENT 4-FINAL: Not all problems assigned

Problem Asst. 4—4.5, 4.7(a) only, 5.1, 5.2, 5.3. 5.4, 5.7, 5.8, 5.9, 5.10, due Friday, December 2nd

REMAINING LECTURE SCHEDULE:

22 November, Happy Thanksgiving!, 29 November and 1 December

FINAL EXAMINATION: TUESDAY, DECEMBER 6TH, 10:30-12:30 PM, PHYSICS 185

Open book: You may use lecture notes, copies of lecture slides, textbooks, and laptops, with signed affirmation as follows:

I will not make use of any hardcopy or online material from prior versions of this course that is not posted at the current course website.

Copying from such material will be considered as cheating.

CALCULATION OF PHOTOELECTRON INTENSITIES—THE 3-STEP MODEL

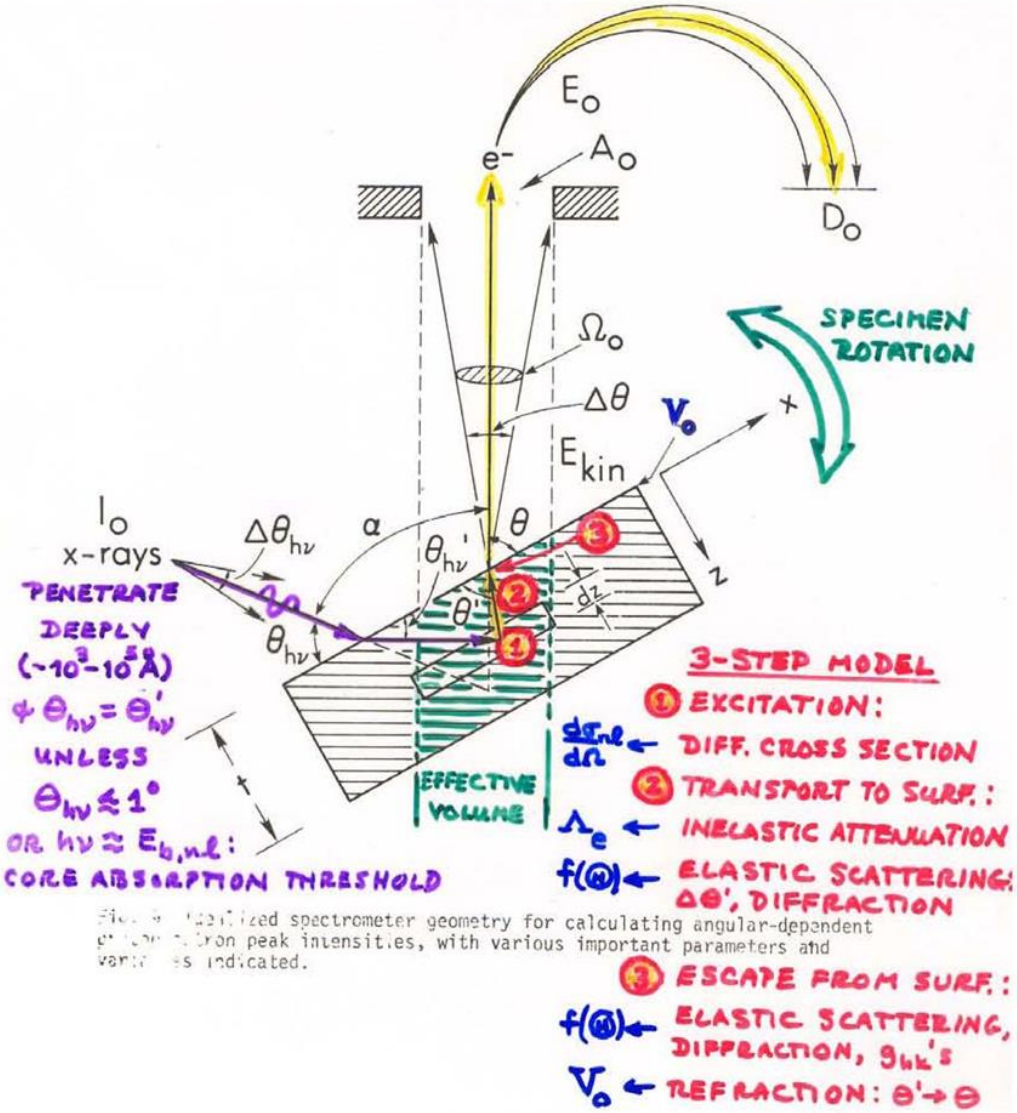

Fig. 4. Idealized spectrometer geometry for calculating angular-dependent photoelectron peak intensities, with various important parameters and variables indicated.

CALCULATING INTENSITIES IN PHOTOELECTRON SPECTRA

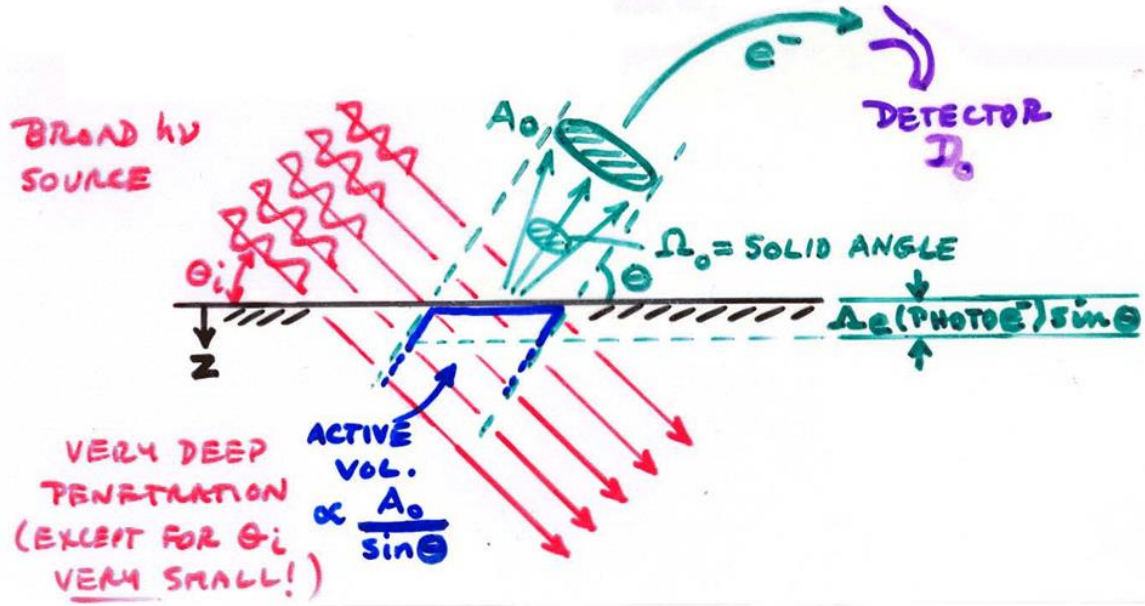

$$\text{INTENSITY} \propto \underset{\left(\frac{\text{NO.}}{\text{CM}^2\text{-SEC}}\right)}{\begin{bmatrix}\text{INCIDENT}\\ \text{EXCITING}\\ \text{FLUX}\end{bmatrix}} \cdot \underset{\left(\frac{\text{NO.}}{\text{CM}^3}\right)}{\begin{bmatrix}\text{DENSITY OF}\\ \text{ATOMS EX-}\\ \text{CITED}\end{bmatrix}} \cdot \underset{(\text{CM}^3)}{\begin{bmatrix}\text{ACTIVE}\\ \text{VOLUME}\end{bmatrix}} \cdot$$

$$\underset{(\text{CM}^2)}{\begin{bmatrix}\text{"CROSS}\\ \text{SECTION"}\\ \text{PER ATOM}\\ \text{FOR EXCITATION}\\ \text{INTO ANALYZER}\end{bmatrix}} \cdot \underset{= e^{-z/\Lambda_e \sin\theta}}{\begin{bmatrix}\text{PROBABILITY}\\ \text{FOR}\\ \text{NO-LOSS}\\ \text{ESCAPE}\end{bmatrix}} \cdot \underset{\equiv D_0}{\begin{bmatrix}\text{PROBABILITY}\\ \text{FOR}\\ \text{DETECTION}\\ \text{IN}\\ \text{ANALYZER}\end{bmatrix}}$$

ATOMIC (CORE) PHOTOELECTRON INTENSITIES: THE THREE-STEP MODEL

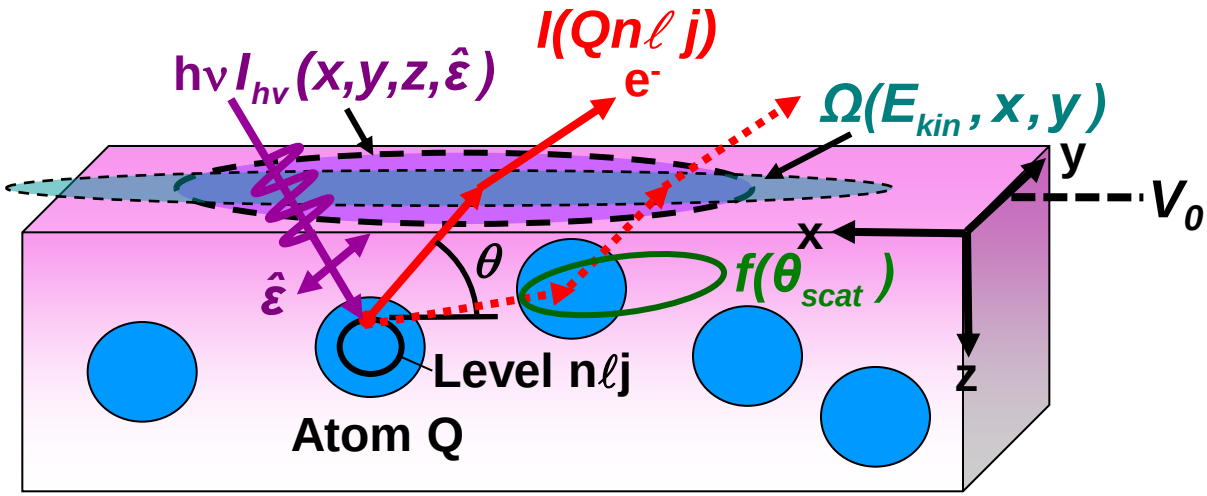

$I(Qn\ell j) =$

$$C\int_0^\infty I_{hv}(x,y,z,\hat{\varepsilon})\rho_Q(x,y,z)\frac{d\sigma_{Qn\ell j}(hv,\hat{\varepsilon})}{d\Omega}\exp\left[-\frac{z}{\Lambda_e(E_{kin})\sin\theta}\right]\Omega(E_{kin},x,y)dxdydz$$

$I_{hv}(x,y,z,\hat{\varepsilon})$ = x-ray flux, $\hat{\varepsilon}$ = polarization

$\rho_Q(x,y,z)$ = density of atoms Q → quantitative analysis

$\frac{d\sigma_{Qn\ell j}(hv,\hat{\varepsilon})}{d\Omega}$ = energy-dependent differential photoelectric cross section for subshell $Qn\ell j$

$\Lambda_e(E_{kin})$ = energy-dependent inelastic attenuation length + elastic scattering: $f(\theta_{scat})$

→ Effective Attenuation Length (EAD) → Mean Emission Depth (MED)

$\Omega(E_{kin},x,y)$ = energy-dependent spectrometer acceptance solid angle

$\iint \Omega(E_{kin},x,y)dxdy = T(E_{kin})$ = transmission function

V_0 = inner potential

E.g.-Eqns. (113) and (114) of Basic Concepts of XPS

VALENCE-BAND PHOTOELECTRON INTENSITIES IN THE DENSITY-OF-STATES(XPS)LIMIT

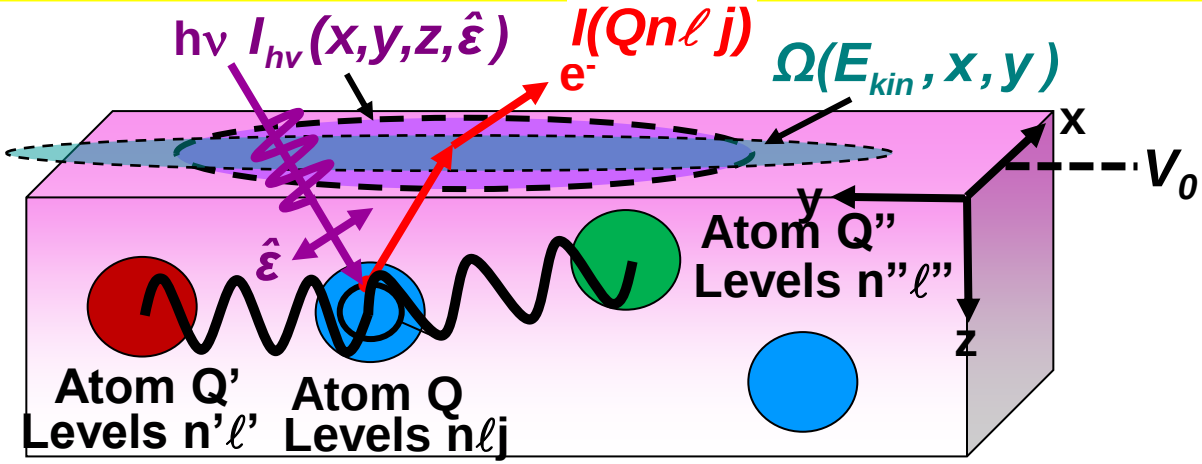

For a given subshell:

$$I(E_{kin},Qn\ell j) = C'\int_0^\infty I_{hv}(x,y,z,\hat{\varepsilon})\rho_{Qn\ell}(E_b,x,y,z)\frac{d\sigma_{Qn\ell}(hv,\hat{\varepsilon})}{d\Omega}\exp\left[-\frac{z}{\Lambda_e(E_{kin})\sin\theta}\right]\Omega(E_{kin},x,y)dxdydz$$

$I_{hv}(x,y,z)$ = x-ray flux, $\hat{\varepsilon}$ = x-ray polarization

$\rho_{Qn\ell}(E_b,x,y,z)$ = density of states, projected onto $Qn\ell$ character

$\frac{d\sigma_{Qn\ell j}(hv,\hat{\varepsilon})}{d\Omega}$ = energy-dependent differential photoelectric cross section for subshell $Qn\ell j$

$\Lambda_e(E_{kin})$ = energy-dependent inelastic attenuation length

→ Mean Emission Depth

$\Omega(E_{kin},x,y)$ = energy-dependent spectrometer acceptance solid angle

For the total VB intensity:

$$I_{total}(E_{kin}) = \sum_{Qn\ell} I(E_{kin},Qn\ell)$$

E.g.-Pages 56-57 of Basic Concepts of XPS
Solterbeck et al., Phys. Rev. Lett. 79, 4681 (1997)

Copper densities of states-total and projected onto orbital type

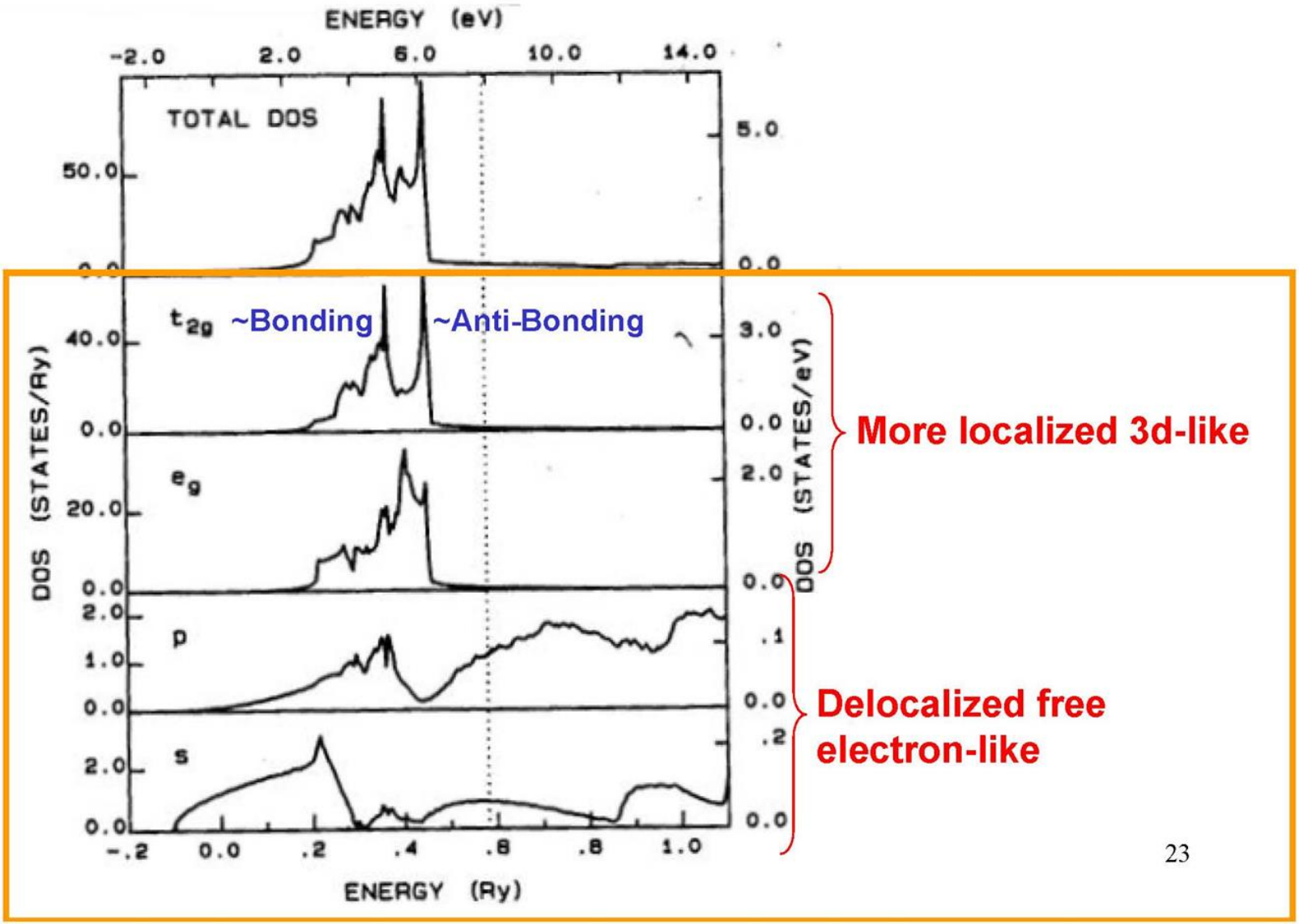

$SrTiO_3$ and $La_{0.67}Sr_{0.33}MnO_3$ band structures and DOS

$SrTiO_3$-band insulator

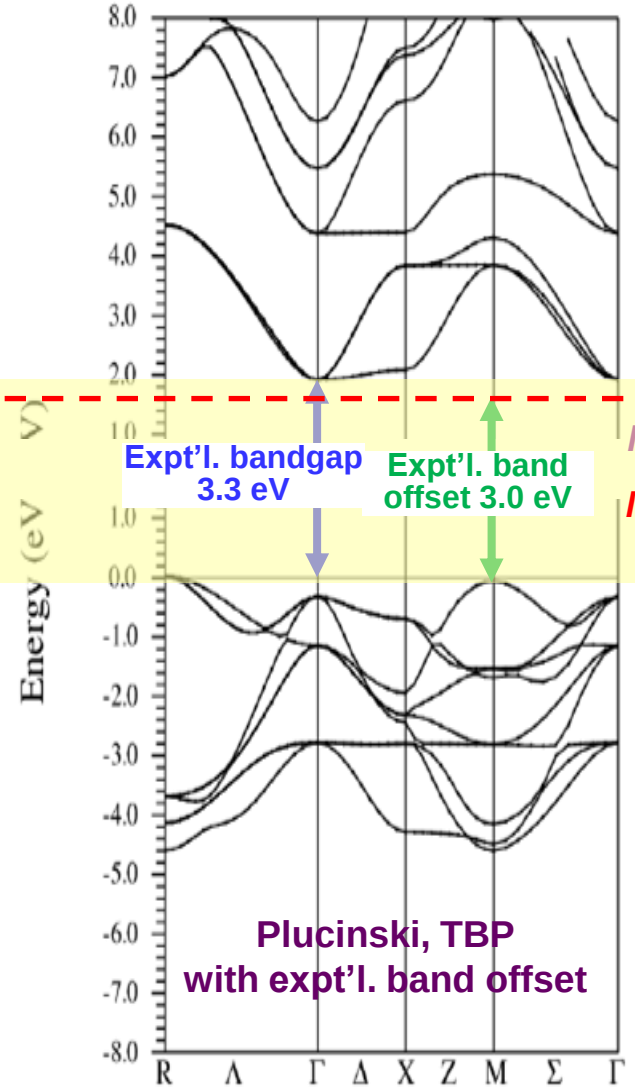

Plucinski, TBP
with expt'l. band offset

$La_{0.67}Sr_{0.33}MnO_3$- Half-Metallic Ferromagnet

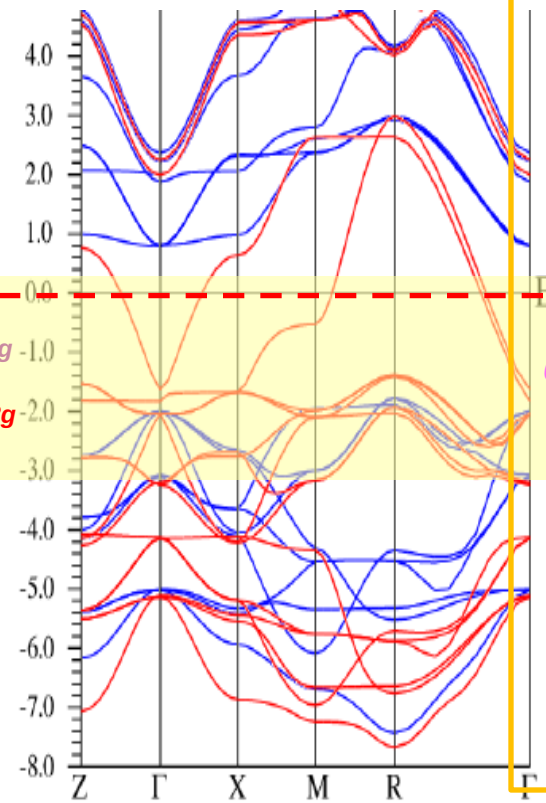

Spin-up
Spin-down

Chikamatsu et al., PRB 73, 195105 (2006); Plucinski, TBP

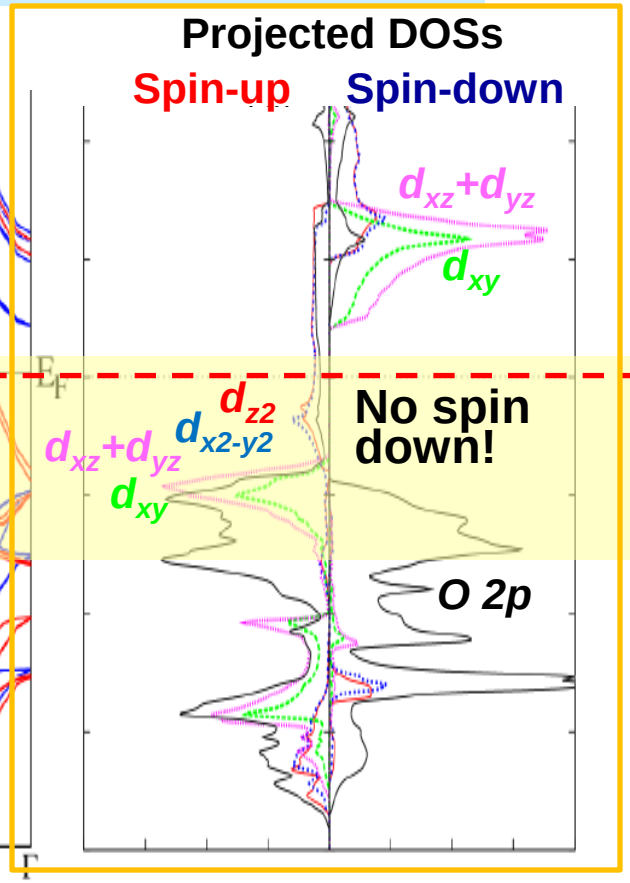

Zheng, Binggeli, J. Phys. Cond. Matt. 21, 115602 (2009)
Plucinski, TBP

PHOTOELECTRON INTENSITIES FOR SOME USEFUL CASES

(a) Semi-infinite specimen, atomically clean surface, peak k with $E_{\mathrm{kin}} \equiv E_k$:

$$N_k(\theta) = I_0 \Omega_0(E_k) A_0(E_k) D_0(E_k) \rho \, d\sigma_k/d\Omega \; \Lambda_e(E_k) \quad (115)$$

(NO θ DEP.)

This case corresponds to an optimal measurement on a homogeneous specimen for which no surface contaminant layer is present.

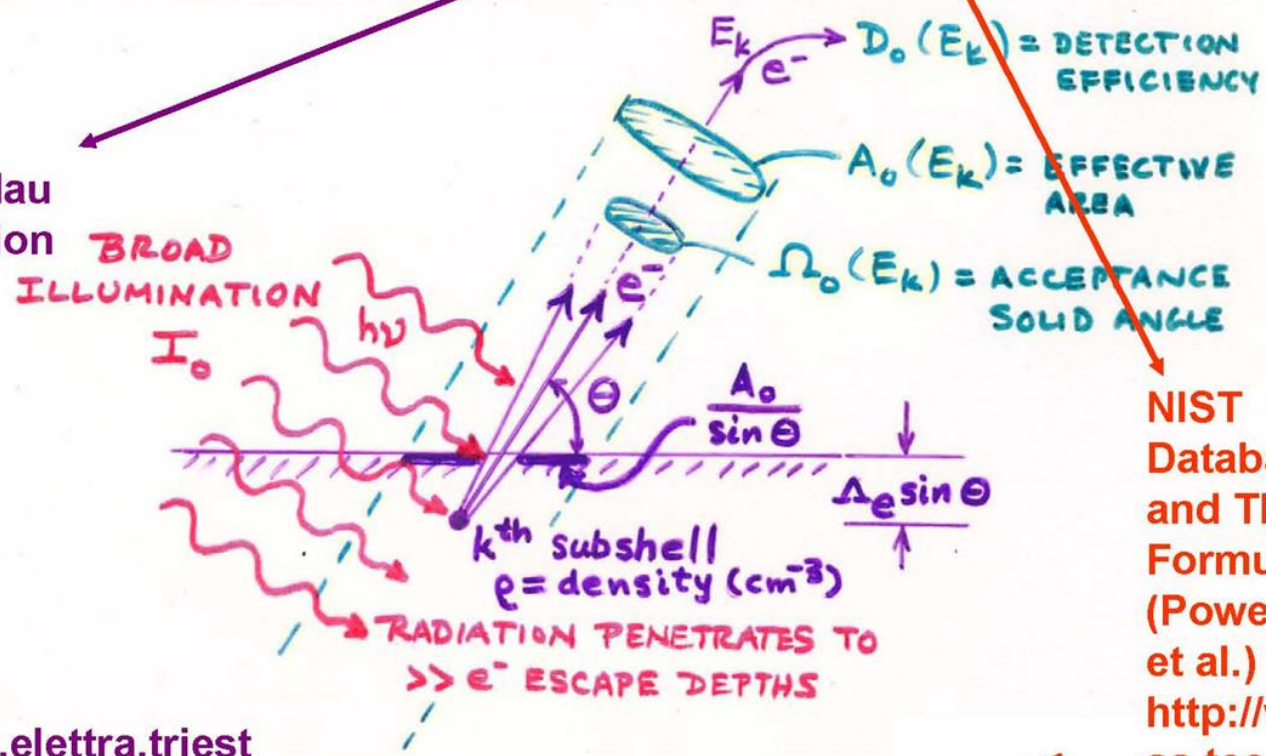

Yeh & Lindau cross section table

http://ulisse.elettra.trieste.it/services/elements/WebElements.html

+ SESSA Program (more later)

NIST Database and TPP-2M Formula (Powell et al.) E.g.- http://www.ss.teen.setsunan.ac.jp/e-imfp2.html

http://www.quases.com/products/quases-imfp-tpp2m/

(b) Specimen of thickness t, atomically clean surface, peak k with $E_{\mathrm{kin}} \equiv E_k$:

$$N_k(\theta) = I_0 \Omega_0(E_k) A_0(E_k) D_0(E_k) \rho \; \mathrm{d}\sigma_k/\mathrm{d}\Omega \; \Lambda_e(E_k) \times [1 - \exp(-t/\Lambda_e(E_k) \sin\theta)] \qquad (116)$$

Here, the intensity of a peak originating in a specimen of finite thickness is predicted to increase with decreasing θ.

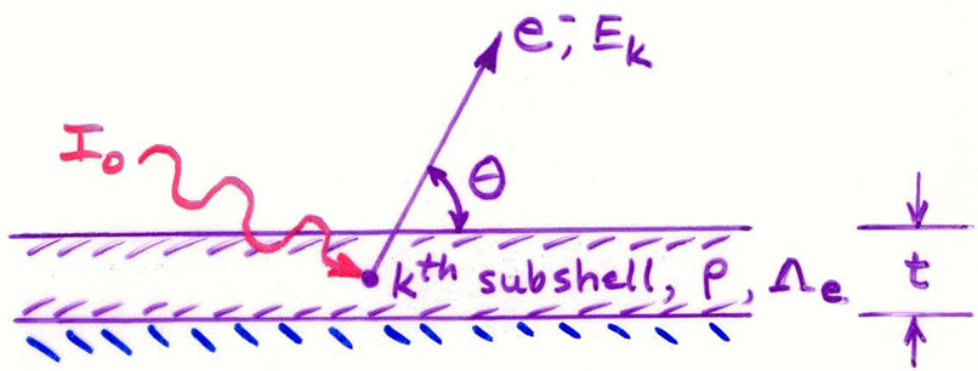

(c) Semi-infinite substrate with uniform overlayer of thickness t - Peak k from substrate with $E_{\mathrm{kin}} \equiv E_{\mathrm{k}}$:

$$N_k(\theta) = I_0 \Omega_0(E_k) A_0(E_k) D_0(E_k) \rho \, \mathrm{d}\sigma_k/\mathrm{d}\Omega \; \Lambda_{\mathrm{e}}(E_k) \times \exp\left(-t/\Lambda_{\mathrm{e}}'(E_k) \sin\theta\right) \qquad (117)$$

Peak l from overlayer with $E_{\mathrm{kin}} \equiv E_l$:

$$N_l(\theta) = I_0 \Omega_0(E_l) A_0(E_l) D_0(E_l) \rho' \, \mathrm{d}\sigma_l/\mathrm{d}\Omega \; \Lambda_{\mathrm{e}}'(E_l) \times \left[1 - \exp\left(-t/\Lambda_{\mathrm{e}}'(E_l) \sin\theta\right)\right] \qquad (118)$$

where

$\Lambda_{\mathrm{e}}(E_k)$ = an attenuation length in the substrate

$\Lambda_{\mathrm{e}}'(E_k)$ = an attenuation length in the overlayer

ρ = an atomic density in the substrate

ρ' = an atomic density in the overlayer.

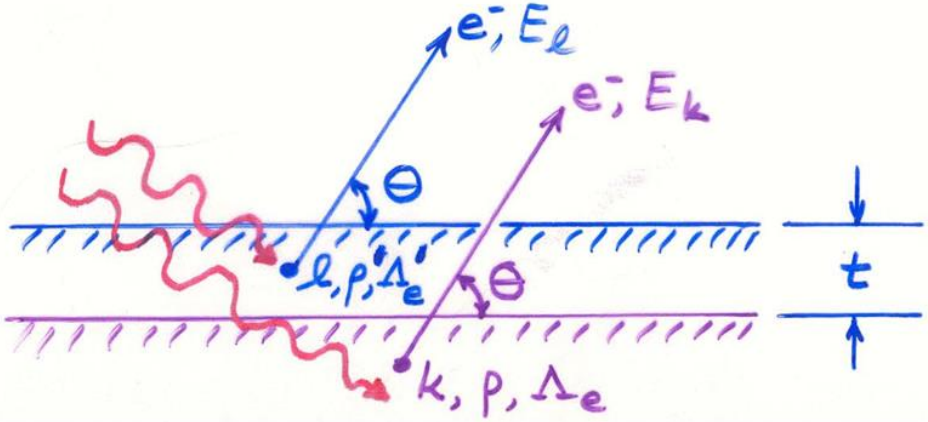

(d) Semi-infinite substrate with a non-attenuating overlayer at fractional monolayer coverage—Peak k from substrate: Eq. (115).

Peak l from overlayer:

$$N_l(\theta) = I_0 \Omega_0(E_l) A_0(E_l) D_0(E_l)\, s'(\mathrm{d}\sigma_l/\mathrm{d}\Omega)(\sin\theta)^{-1} \tag{120a}$$

Overlayer/substrate ratio:

$$\frac{N_l(\theta)}{N_k(\theta)} = \frac{\Omega_0(E_l) A_0(E_l) D_0(E_l) s'(\mathrm{d}\sigma_l/\mathrm{d}\Omega)}{\Omega_0(E_k) A_0(E_k) D_0(E_k) s\ \mathrm{d}\sigma_k/\mathrm{d}\Omega\ (\Lambda_e(E_k)\sin\theta/d)}$$

$$= \left[\frac{s'}{s}\right] \cdot \frac{D_0(E_l)\Omega_0(E_l) A_0(E_l)(\mathrm{d}\sigma_l/\mathrm{d}\Omega) d}{D_0(E_k)\Omega_0(E_k) A_0(E_k)\ \mathrm{d}\sigma_k/\mathrm{d}\Omega\ \Lambda_e \sin\theta} \tag{120b}$$

with

s' = the mean surface density of atoms in which peak l originates in cm^{-2}

s = the mean surface density of substrate atoms in cm^{-2}

s'/s = the fractional monolayer coverage of the atomic species in which peak l originates

d = the mean separation between layers of density s in the substrate (calculable from s/ρ).

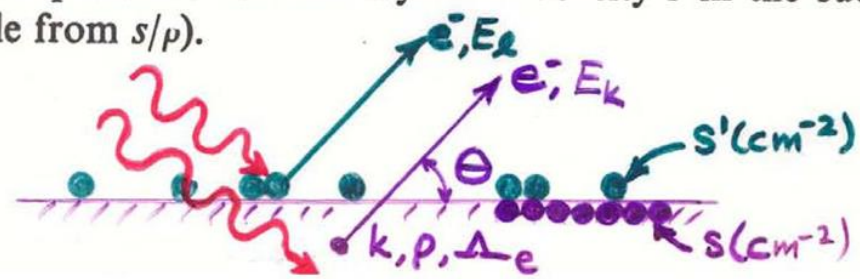

Surface sensitivity enhancement for grazing exit angles

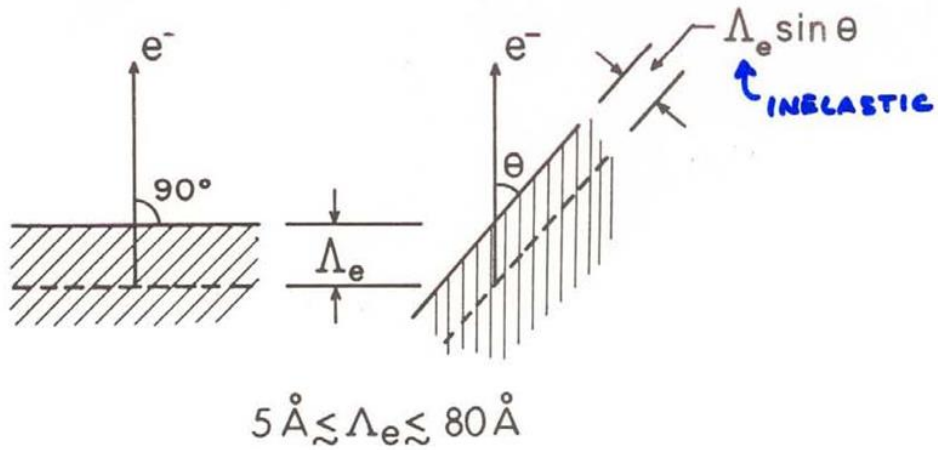

Fig. 5. Illustration of the basic mechanism producing surface sensitivity enhancement for low electron exit angles θ. The average depth for no-loss emission as measured perpendicular to the surface is $\Lambda_e \sin\theta$.

E.g.- $\Lambda_e = 28$ Å in Au(s) at 1400 eV

	θ	Mean Depth	No. layers
"BULK" →	90°	28 Å	~9
"SURFACE" →	10°	~4.4 Å	~1.5

... BUT REFRACTION AT SURFACE AND ELASTIC SCATTERING CAN REDUCE SURFACE ENHANCEMENT, ESP. AT LOW $\theta \lesssim 30°$

Surface sensitivity enhancement for grazing exit angles

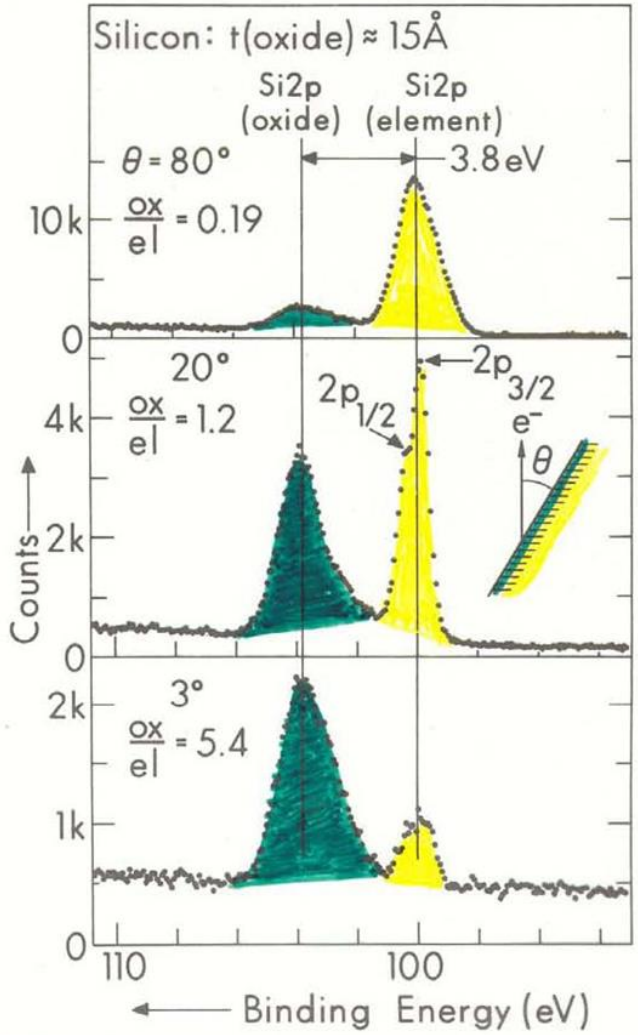

Fadley, Progress in Surface Science, 16, 275 ('84)

Fig. 7. Si2p spectra at three electron exit angles for a Si specimen with a 15-Å thick oxide overlayer. Note the complete reversal of the relative intensities of oxide and element between high and low θ. (From Hill et al., ref. (19).)

Surface sensitivity enhancement for grazing exit angles

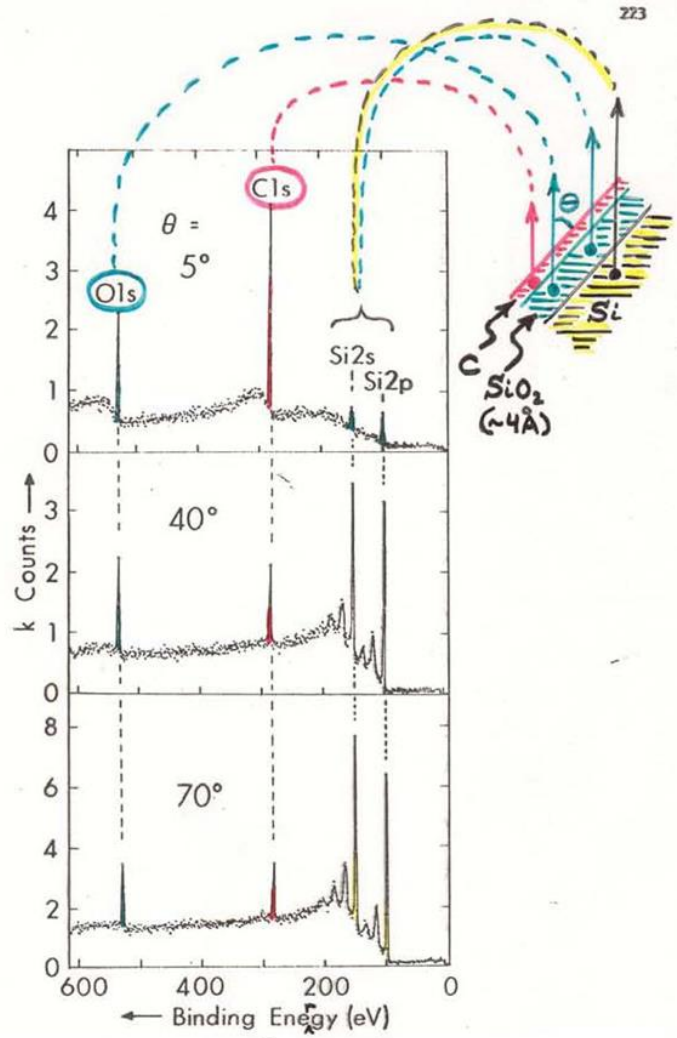

Figure 44 -- Broad-scan core spectra at low and high exit angles for a Si specimen with a thin oxide overlayer (~ 4Å) and an outermost carbon contaminant overlayer approximately 1-2 monolayers in thickness. The C1s and O1s signals are markedly enhanced in relative intensity at low θ due to the general effect presented in Figure 43. (From Fadley, reference 17.)

CALCULATION OF PHOTOELECTRON INTENSITIES—THE 3-STEP MODEL

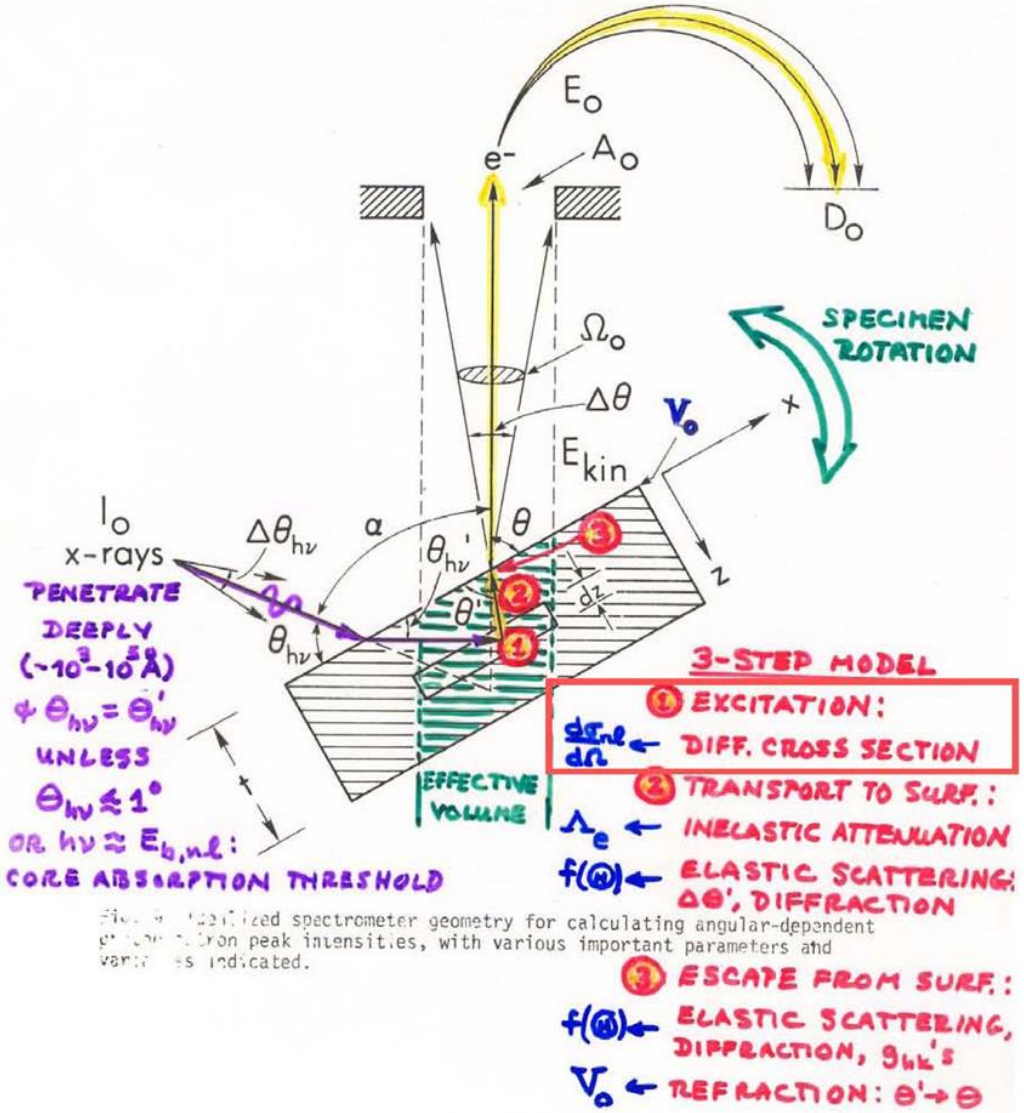

Fig. 4. Idealized spectrometer geometry for calculating angular-dependent photoelectron peak intensities, with various important parameters and variables indicated.

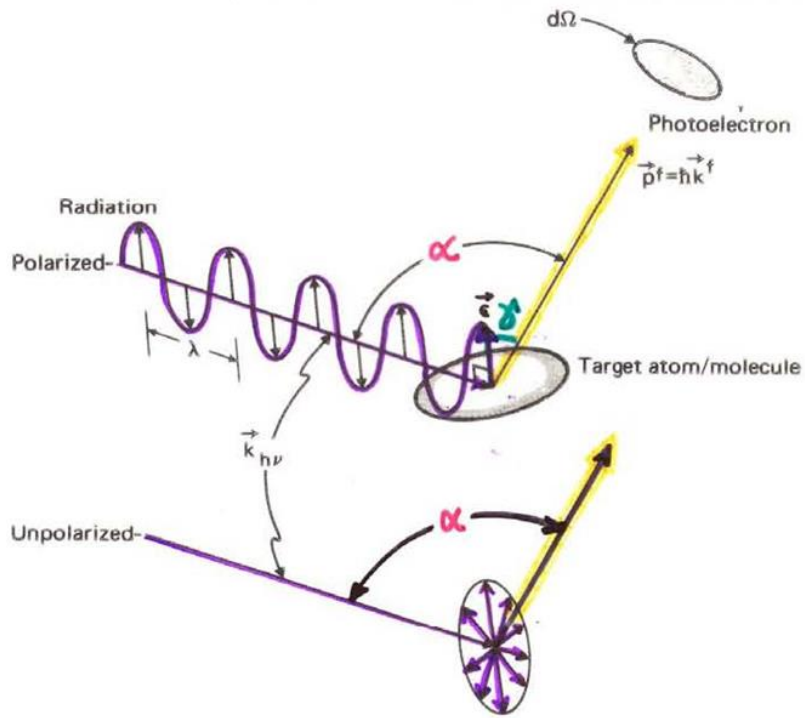

FOR ATOMIC-LIKE EMISSION:

LIN. POLARIZED: $\frac{d\sigma_{n\ell}(E_f)}{d\Omega} = \frac{\sigma_{n\ell}(E_f)}{4\pi}\left[1 + \beta_{n\ell}(E^f)\left(\frac{3}{2}\cos^2\gamma - \frac{1}{2}\right)\right]$

UNPOLARIZED: $\frac{d\sigma_{n\ell}(E_f)}{d\Omega} = \frac{\sigma_{n\ell}(E_f)}{4\pi}\left[1 + \frac{1}{2}\beta_{n\ell}(E^f)\left(\frac{3}{2}\sin^2\alpha - 1\right)\right]$

Figure 7 -- General geometry for defining the differential cross section $d\sigma/d\Omega$, showing both polarized and unpolarized incident radiation. The polarization vector $\vec{e}$ is parallel to the electric field $\vec{E}$ of the radiation. In order for the dipole approximation to be valid, the radiation wave length λ should be much larger than typical target dimensions (that is, the opposite of what is shown here).

WITH:

$\sigma_{n\ell}$ = TOTAL CROSS SECTION

$\beta_{n\ell}$ = ASYMMETRY PARAMETER

$\sigma_{n\ell}$, $\beta_{n\ell}$ TABULATIONS IN: GOLDBERG ET AL., J. ELECT. SPECT. & YEH, LINDAU, AT. NUC. DATA 32, 1 ('85) & 21, 285 ('91)

TOTAL SUBSHELL CROSS SECTION: $\int_{4\pi} \frac{d\sigma_{nl}}{d\Omega} d\Omega =$

$$\sigma_{nl}(E^f) = \frac{4\pi\alpha_0 a_0^2}{3}(h\nu)[lR_{l-1}^2(E^f) + (l+1)R_{l+1}^2(E^f)]$$

= SUM OVER ALL m_l, m_s IN SUBSHELL nl

RADIAL MATRIX ELEMENTS TO $l \pm 1$ CHANNELS:

$$R_{l\pm1}(E^f) = \int_0^\infty R_{nl}(r) r R_{E^f,\, l\pm1}(r) r^2\, dr = \int_0^\infty P_{nl}(r) r P_{E^f,\, l\pm1}(r)\, dr$$

DIFFERENTIAL CROSS SECTION: UNPOLARIZED

$$\frac{d\sigma_{nl}}{d\Omega}(E^f) = \frac{\sigma_{nl}}{4\pi}[1 - \tfrac{1}{2}\beta_{nl}(E^f)P_2(\cos\alpha)]$$

$$= \frac{\sigma_{nl}}{4\pi}[1 + \tfrac{1}{2}\beta_{nl}(E^f)(\tfrac{3}{2}\sin^2\alpha - 1)]$$

$$= A + B\sin^2\alpha$$

ASYMMETRY PARAMETER:

TERM FOR $l \pm 1$ INTERFERENCE

$$\beta_{nl}(E^f) = \frac{\{l(l-1)R_{l-1}^2(E^f) + (l+1)(l+2)R_{l+1}^2(E^f) - 6l(l+1)R_{l+1}(E^f)R_{l-1}(E^f)\cos[\delta_{l+1}(E^f) - \delta_{l-1}(E^f)]\}}{(2l+1)[lR_{l-1}^2(E^f) + (l+1)R_{l+1}^2(E^f)]}$$

$\delta_{l\pm1}(E^f)$ = CONTINUUM ORBITAL PHASE SHIFTS IN ATOMIC POTENTIAL $V(r)$

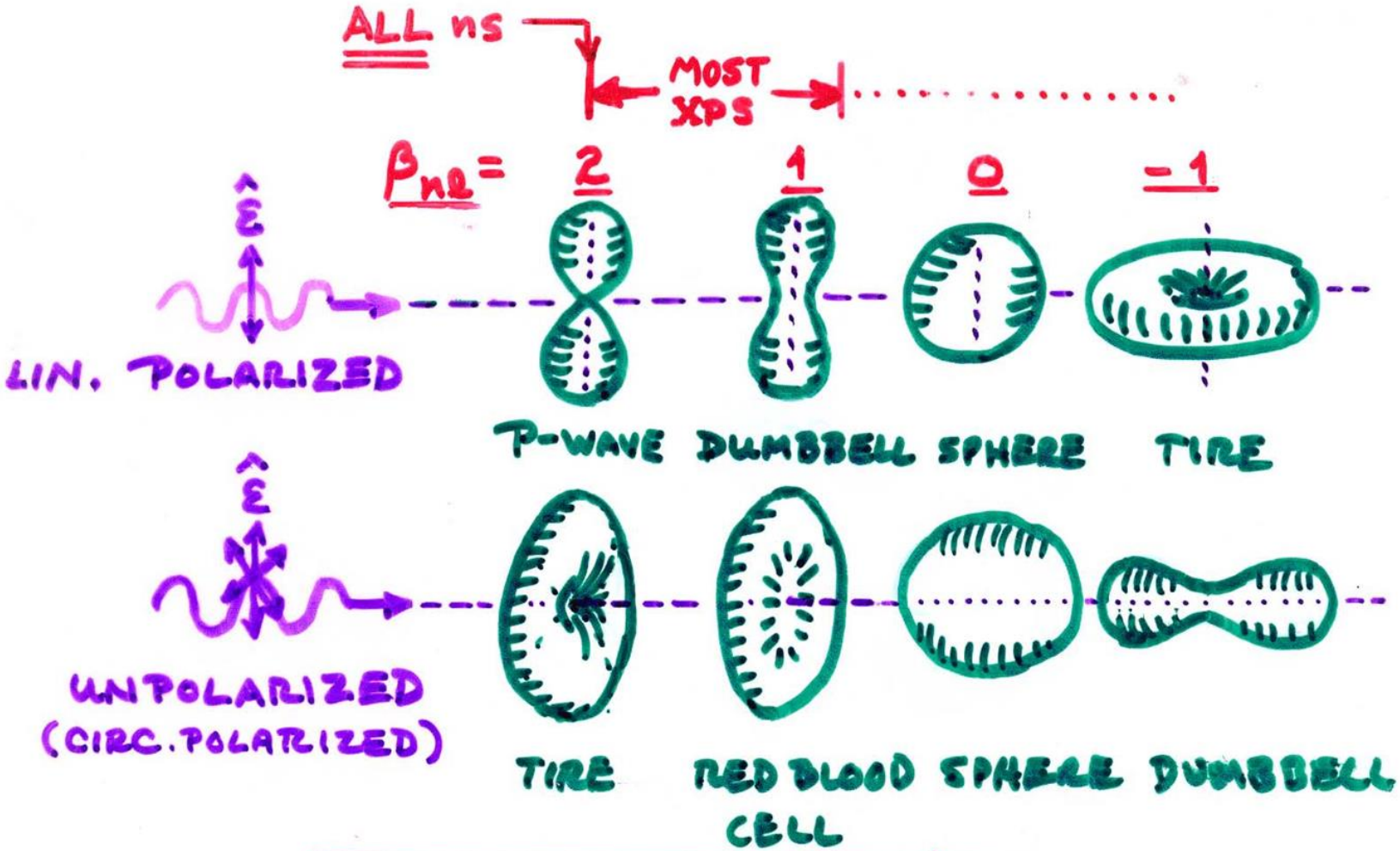

RANGE OF SHAPES OF $\frac{d\sigma}{d\Omega}$

Intraatomic electron screening in many-electron atoms--a self-consistent Q.M. calculation

Plus radial one-electron functions:
$P_{n\ell}(r) \equiv rR_{n\ell}(r)$

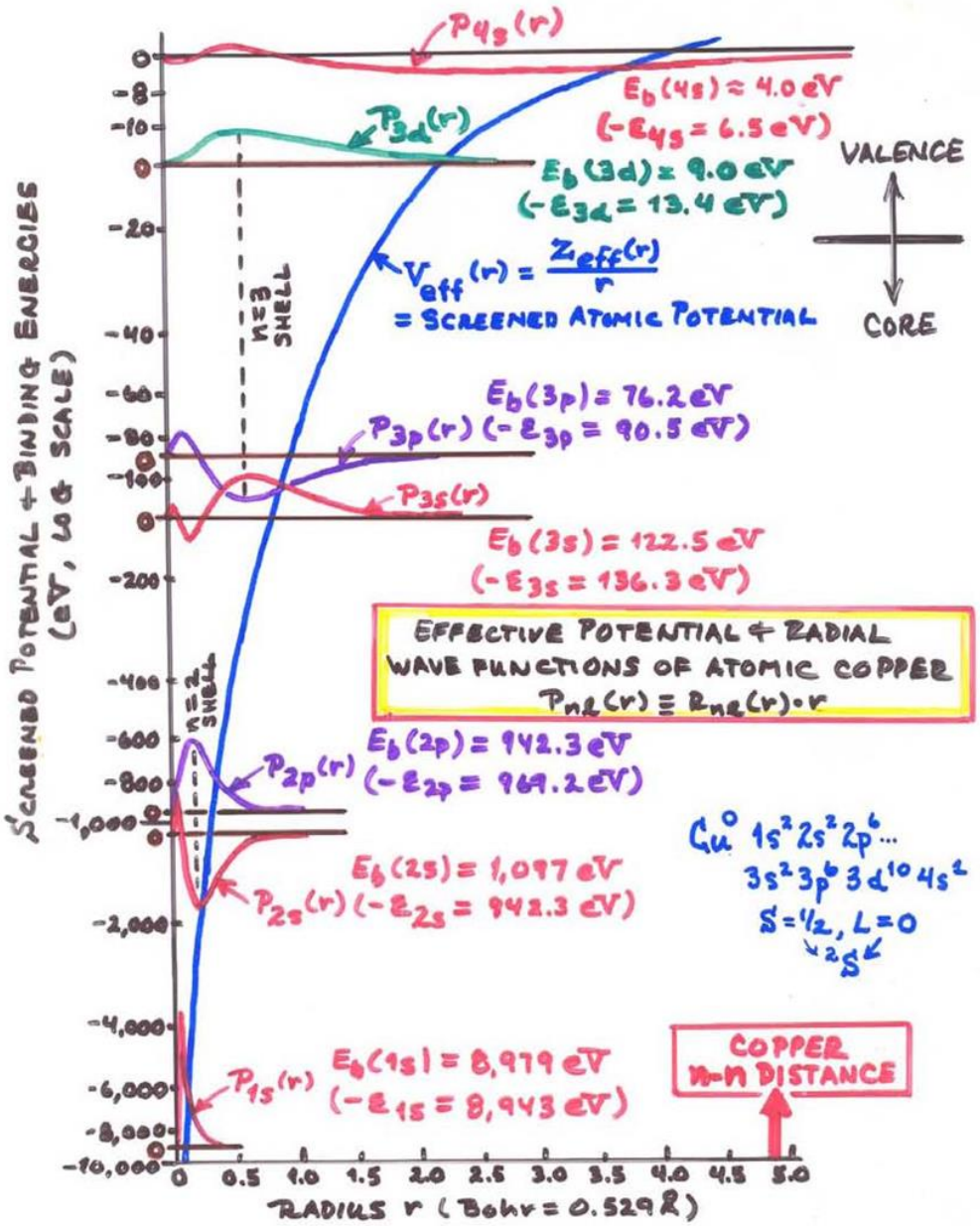

The one-electron wave functions $P_{n\ell}(r)$ and $P_{E^f,\ell\pm1}(r)$ for 2p emission from Carbon

RADIAL MATRIX ELEMENTS TO $\ell \pm 1$ = s and d CHANNELS:

$$R_{s(d)}(E^f) = \int_0^\infty R_{2p}(r) r R_{E^f,s(d)}(r) r^2 dr$$

$$= \int_0^\infty P_{2p}(r) r P_{E^f,s(d)}(r) dr$$

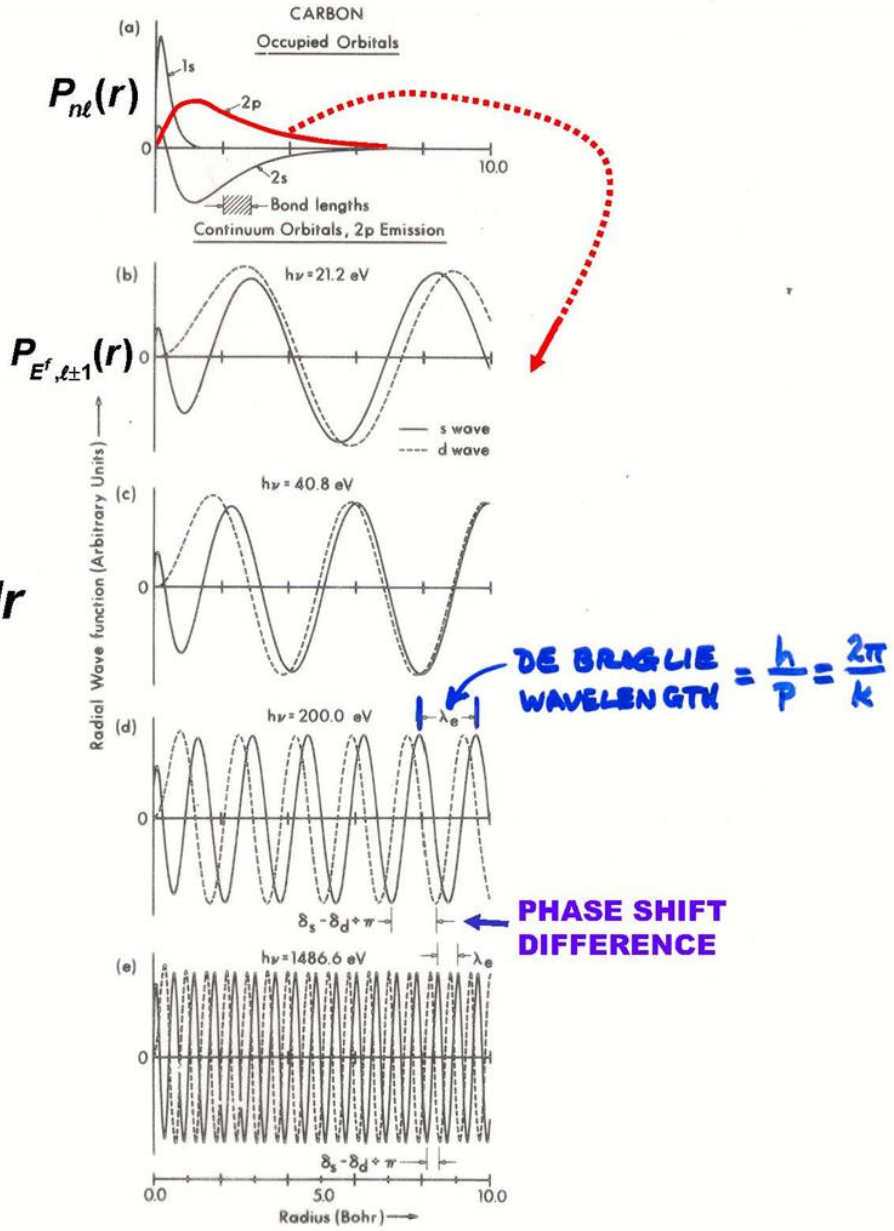

"Basic Concepts of XPS"
Figure 9

GRAPH I. Atomic Subshell Photoionization Cross Sections for 0–1500 eV, $1 \leq Z \leq 103$
See page 6 for Explanation of Graphs

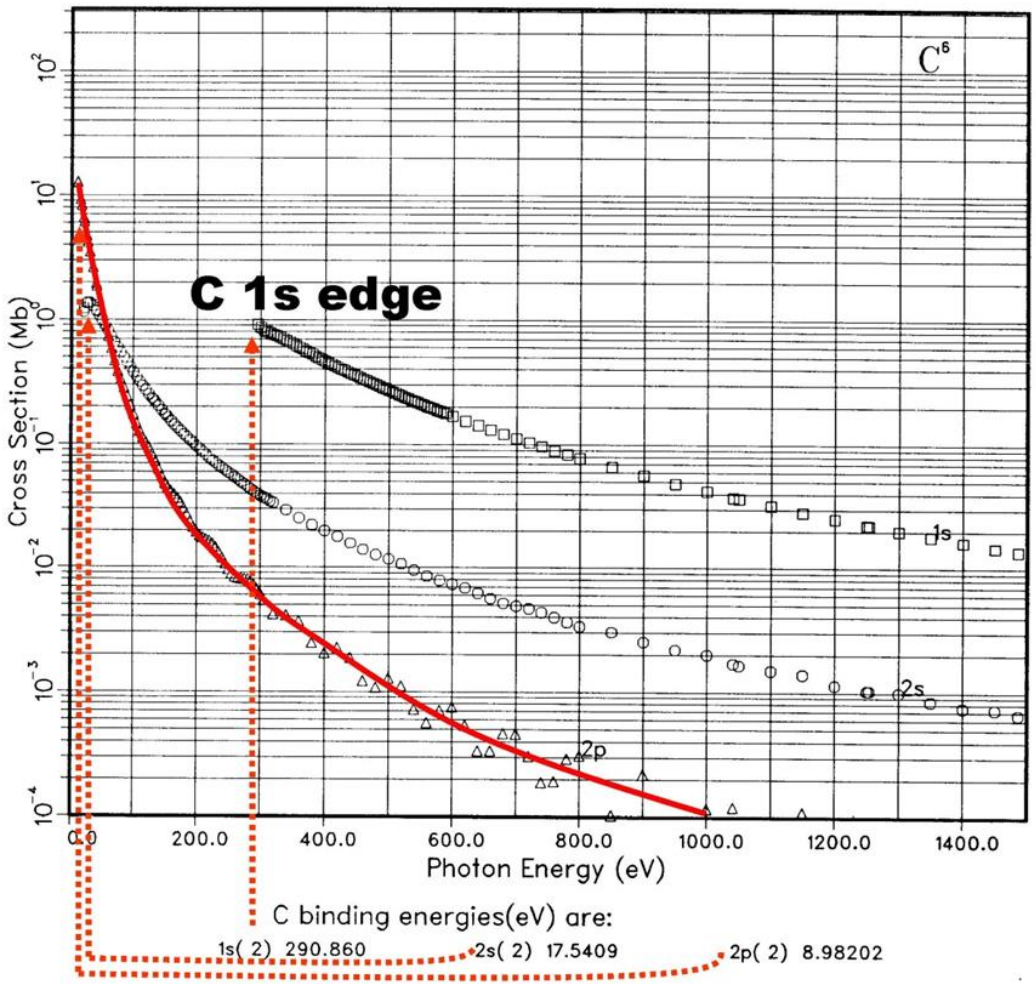

Plus other Examples from Yeh and Lindau in Sec. 1.5 of X-Ray Data Booklet, and plots for all elements at: http://ulisse.elettra.trieste.it/elements/WebElements.html

The five ways in which x-rays Interact with Matter:

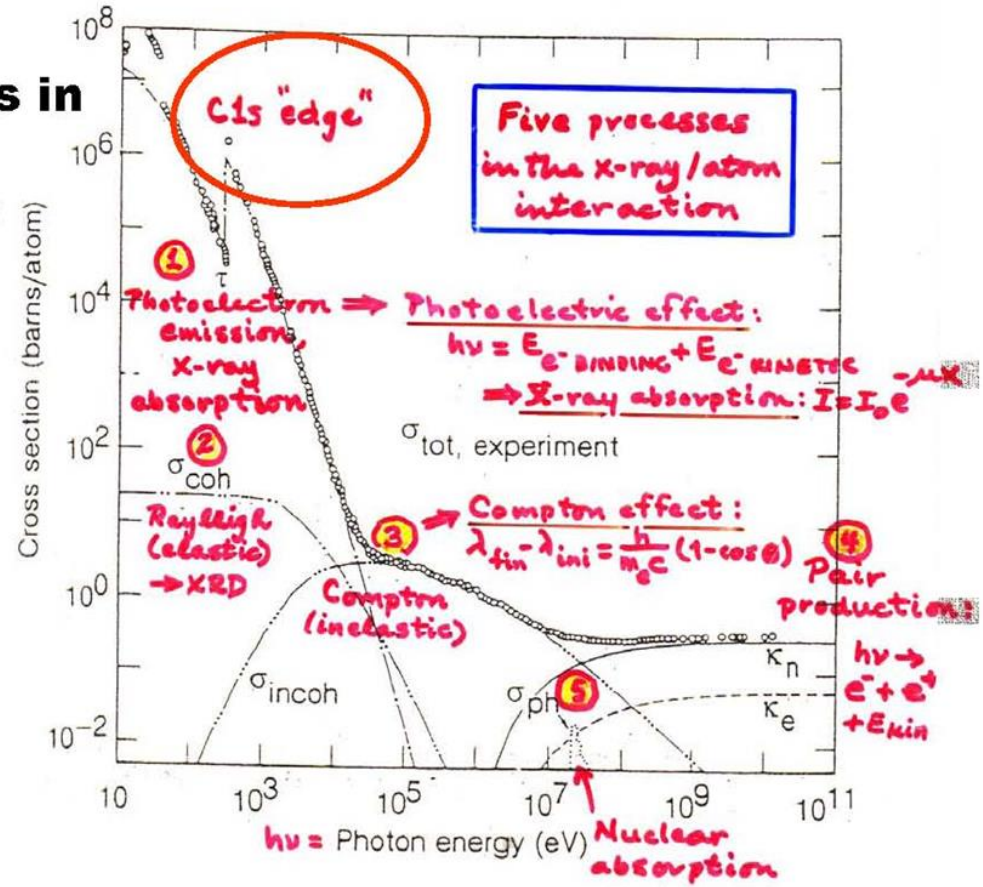

Fig. 3-1. *Total photon cross section σ_{tot} in carbon, as a function of energy, showing the contributions of different processes: τ, atomic photo-effect (electron ejection, photon absorption); σ_{coh}, coherent scattering (Rayleigh scattering—atom neither ionized nor excited); σ_{incoh}, incoherent scattering (Compton scattering off an electron) κ_n, pair production, nuclear field; κ_e, pair production, electron field; σ_{ph}, photonuclear absorption (nuclear absorption usually followed by emission of a neutron or other particle). (From Refs; figure courtesy of J. H. Hubbell.)*

"X-Ray Data Booklet"
Section 3.1

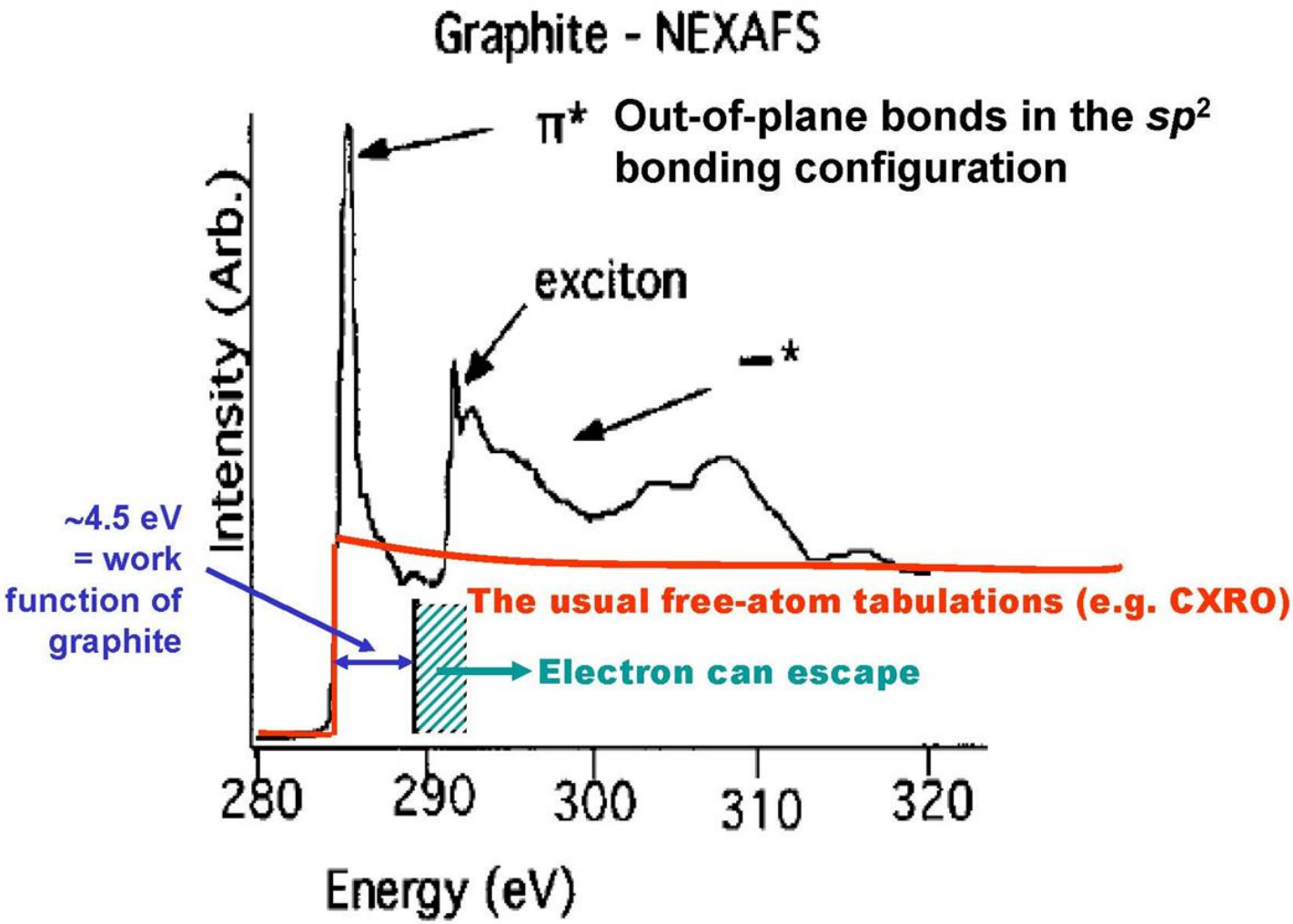

Appl. Phys. Lett. **69** (4), 22 July 1996, p. 568

Ethane: C 1s NEXAFS

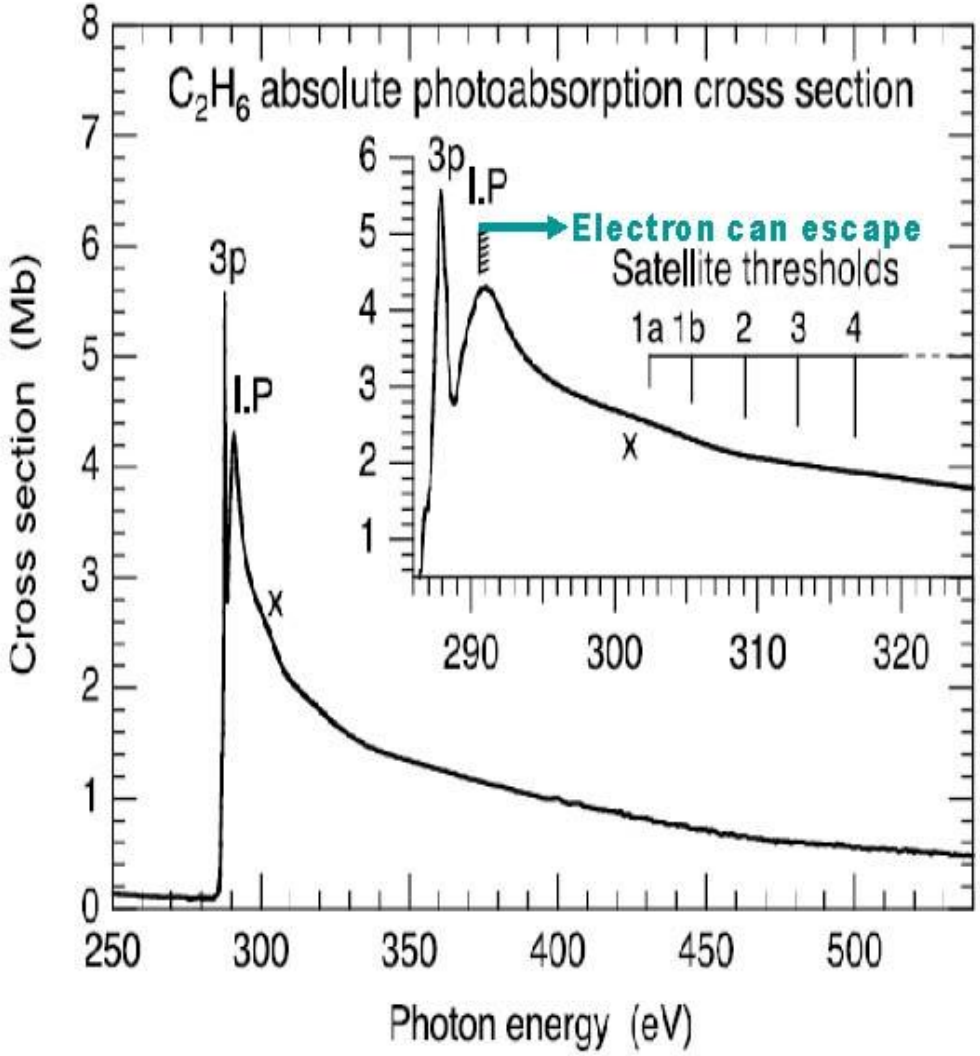

Rennie et al., J. Phys. B: At. Mol. Opt. Phys. 32 (1999) 2691

COMPARISON OF SCANNED-ENERGY PD TO EXTENDED X-RAY ABSORPTION FINE STRUCTURE

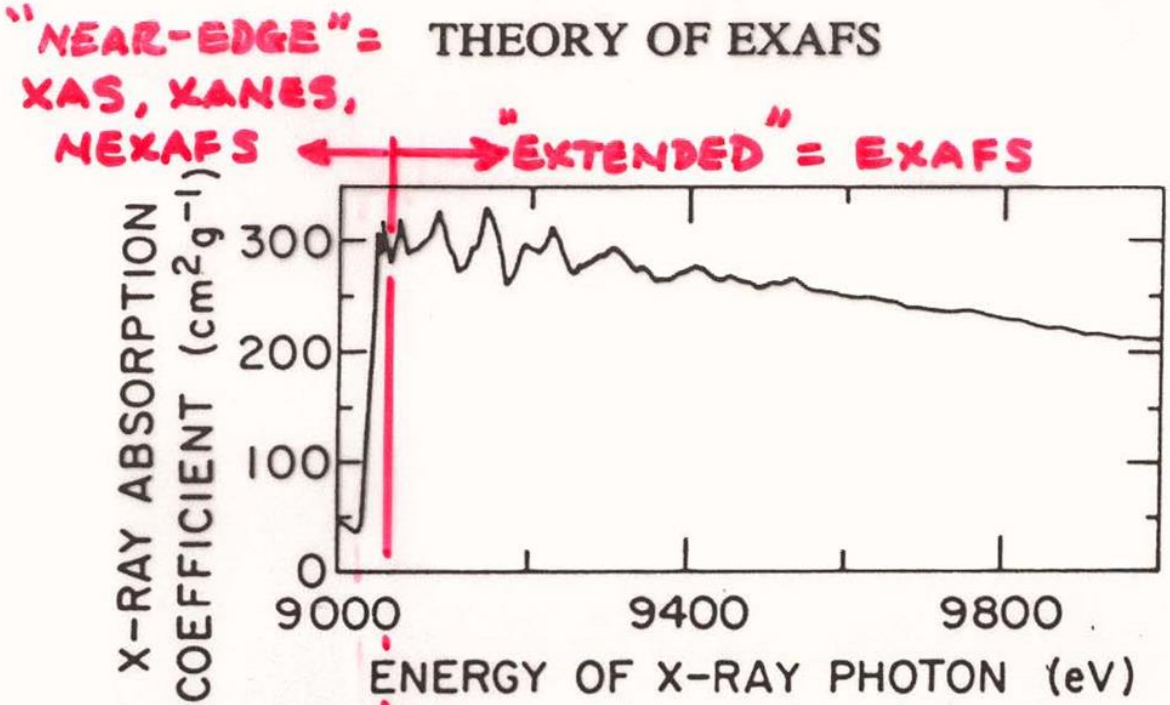

Figure 1.1. The x-ray absorption coefficient for the *K*-edge of copper metal.

~ COPPER 1S BINDING ENERGY

Also scanned-energy, but integrates over all electron emission directions

WebCrossSections - Microsoft Internet Explorer

File Edit View Favorites Tools Help

Back Search Favorites Media

Address http://ulisse.elettra.trieste.it/elements/WebElements.html Go Links

Search Web Mail My Yahoo! Games Yahoo! Personals LAUNCH Sign In

Atomic Calculation of Photoionization Cross-Sections and Asymmetry Parameters

This periodic table interface was developed to easily acces the calculated atomic cross sections for photoionization and the related asymmetry parameters. The data are taken from: J.J. Yeh, *Atomic Calculation of Photoionization Cross-Sections and Asymmetry Parameters,* Gordon and Breach Science Publishers, Langhorne, PE (USA), 1993 and from J.J. Yeh and I.Lindau, *Atomic Data and Nuclear Data Tables*, **32**, 1-155 (1985). The data shown here are those calculated in the dipole length approximation.

This is a beta version: comments are welcome.

Group	1	2	3	4	5	6	7	8	9	10	11	12	13	14	15	16	17	18
	1A	2A	3B	4B	5B	6B	7B	8B			1B	2B	3A	4A	5A	6A	7A	8A
Period																		
1	1 H																	2 He
2	3 Li	4 Be											5 B	6 C	7 N	8 O	9 F	10 Ne
3	11 Na	12 Mg											13 Al	14 Si	15 P	16 S	17 Cl	18 Ar
4	19 K	20 Ca	21 Sc	22 Ti	23 V	24 Cr	25 Mn	26 Fe	27 Co	28 Ni	29 Cu	30 Zn	31 Ga	32 Ge	33 As	34 Se	35 Br	36 Kr

Internet

Graph - Microsoft Internet Explorer

File Edit View Favorites Tools Help

Back Search Favorites Media

Address http://ulisse.elettra.trieste.it/elements/mnu_elem.cgi?ACTION=SHOWGRAPH&ELEMENT=c&C0=1s&C1=2p&C2=2s

Go Links

Search Web Mail My Yahoo! Games Yahoo! Personals LAUNCH Sign In

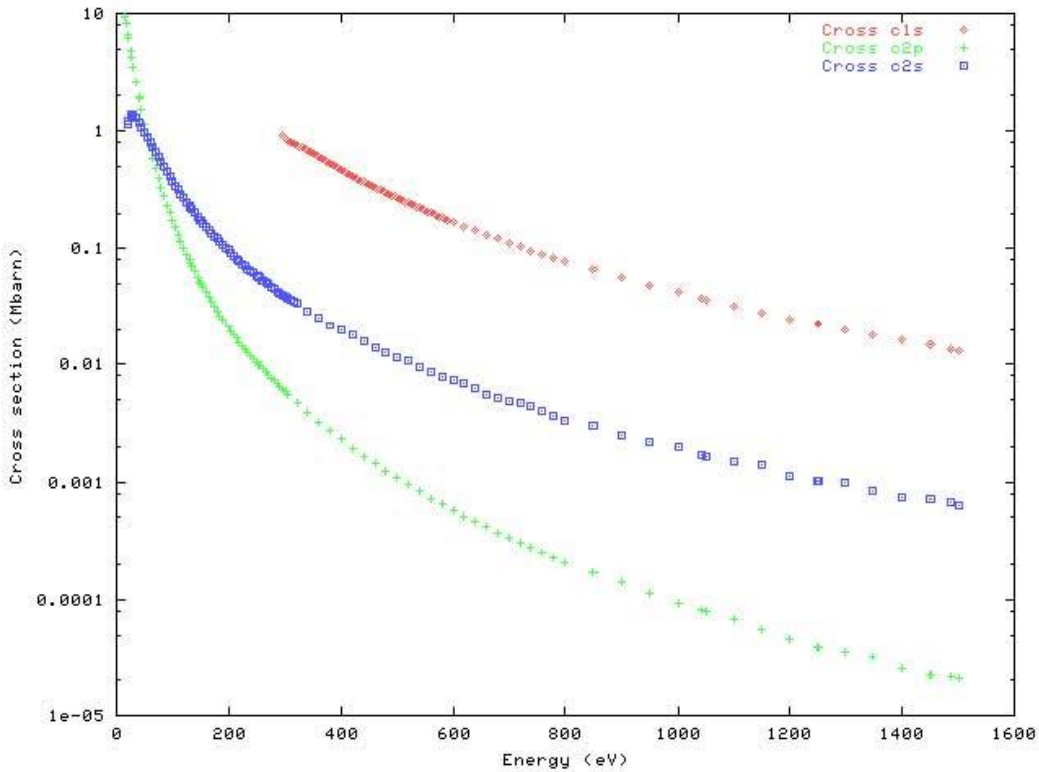

Done Internet

Start 11:17 AM

GRAPH I. Atomic Subshell Photoionization Cross Sections for 0–1500 eV, $1 \leq Z \leq 103$

See page 6 for Explanation of Graphs

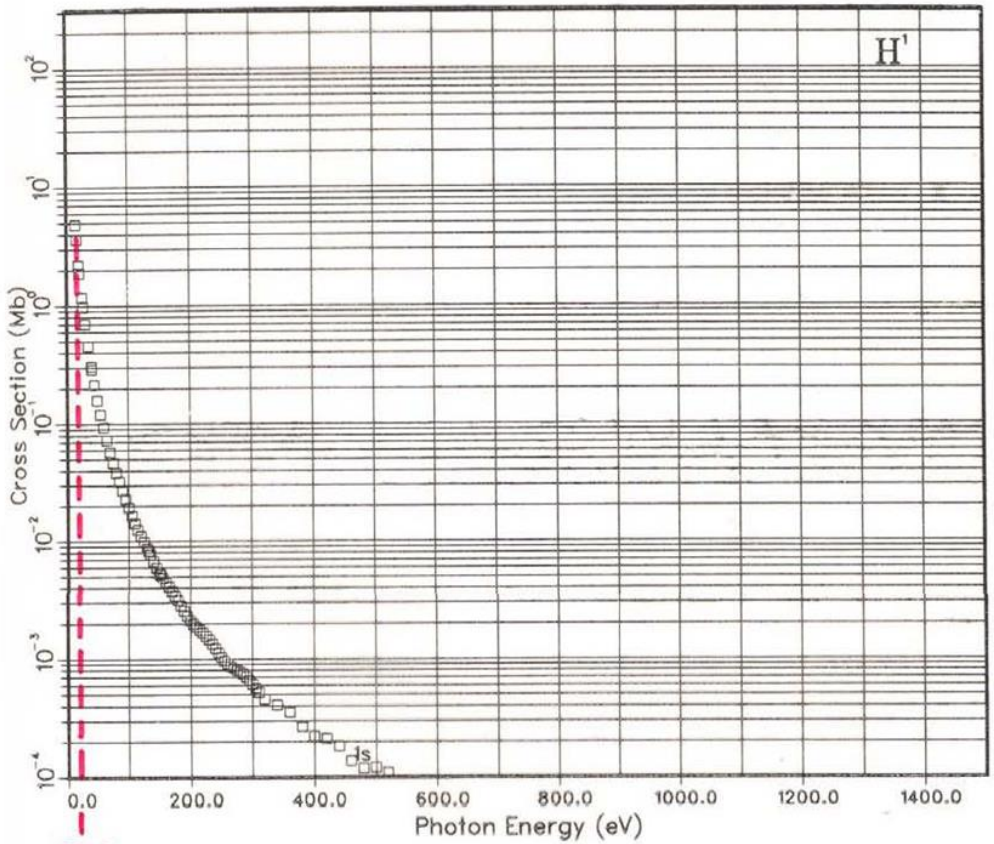

13.6 eV = THRESHOLD FOR e⁻ EMISSION

H binding energies(eV) are:

1s(1) 13.6050

GRAPH I. Atomic Subshell Photoionization Cross Sections for 0–1500 eV, $1 \leq Z \leq 103$

See page 6 for Explanation of Graphs

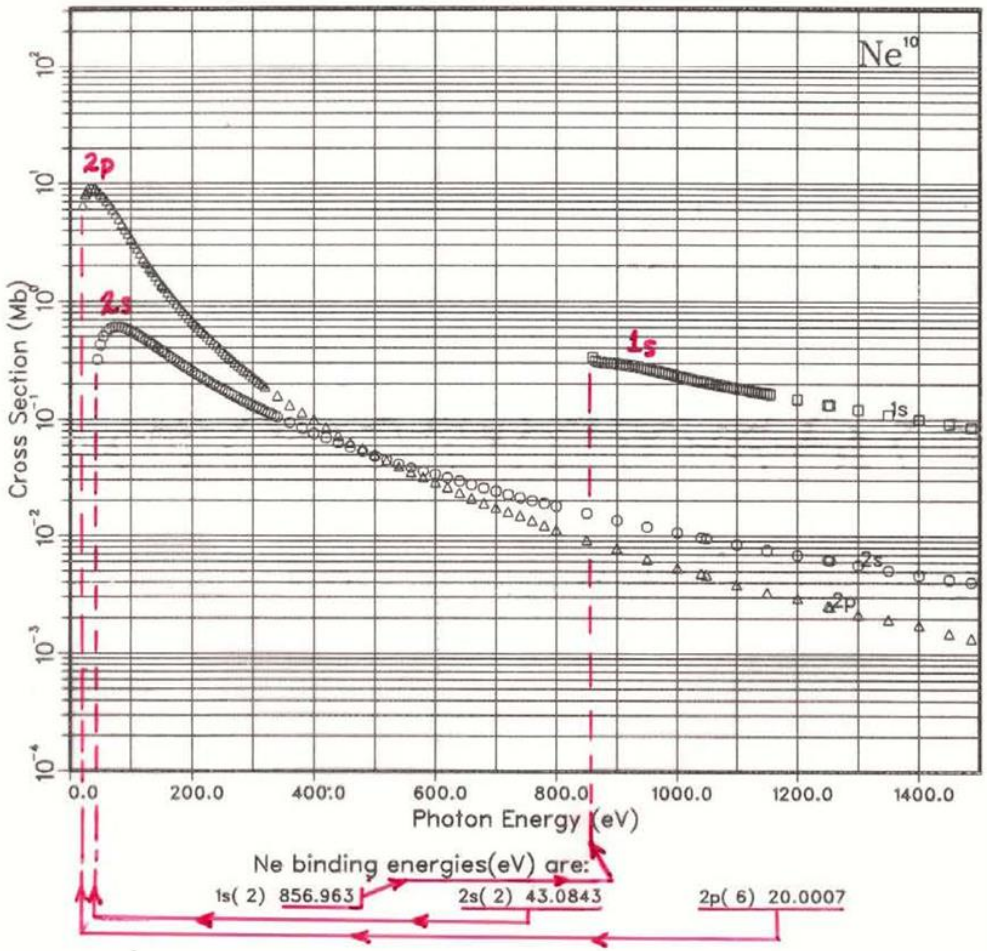

GRAPH I. Atomic Subshell Photoionization Cross Sections for 0–1500 eV, $1 \leq Z \leq 103$

See page 6 for Explanation of Graphs

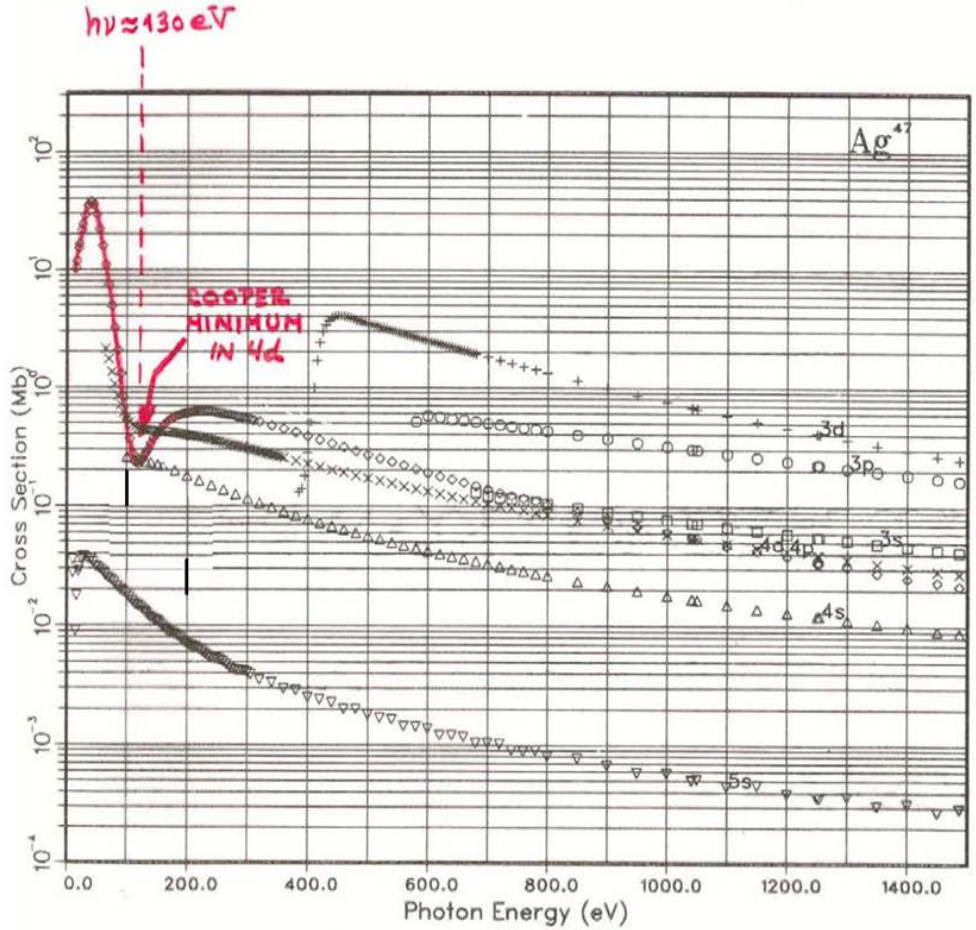

Ag binding energies(eV) are:

1s(2) 24693.5	2s(2) 3591.17	2p(6) 3352.94
3s(2) 665.102	3p(6) 567.203	4s(2) 94.2146
3d(10) 384.360	4p(6) 62.9041	4d(10) 12.6499
5s(1) 6.42700		

COOPER MINIMUM IN Ag 4d (Z = 47) CROSS SECTION : Expt. & Theory

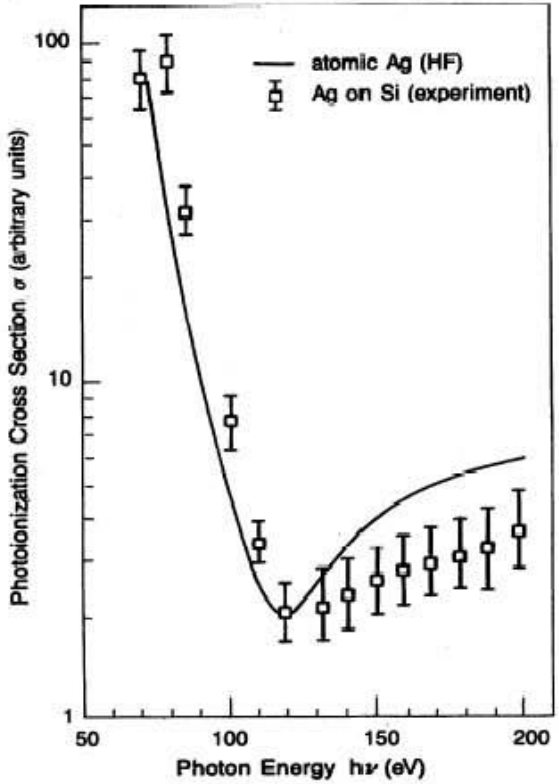

FIG. 5. Partial photoionization cross section for 4*d* electrons of Ag in logarithmic scale. Our experimental data for the Ag/Si interface (squares) are compared with the Hartree-Fock results for atomic Ag by Yeh and Lindau (solid line). Note that our experimental data are normalized at the minimum to the theoretical value.

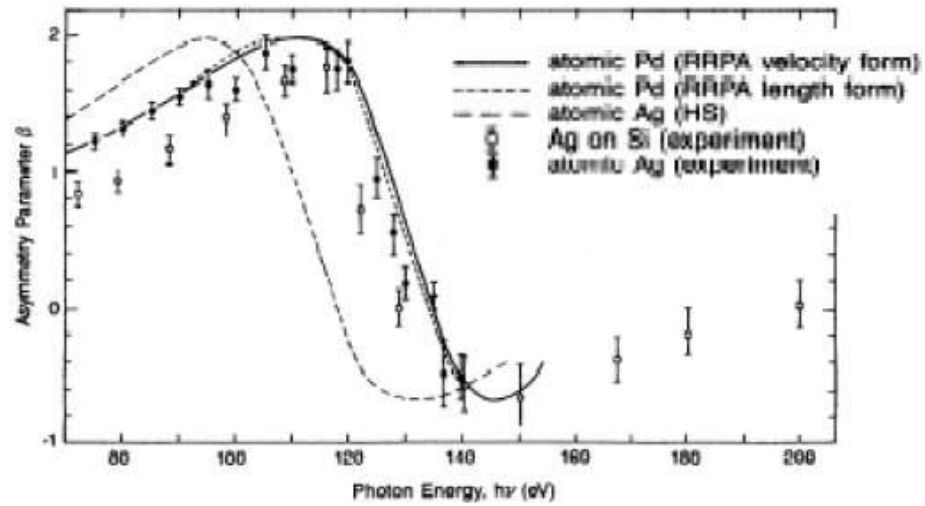

FIG. 6. Asymmetry parameter for 4*d* electrons of Ag. Our experimental data for the Ag/Si interface (squares) are compared with the data for atomic Ag (circles), the RRPA prediction for atomic Pd by Radojevic and Johnson (solid line, velocity form; short-dashed line, length form), and the HS calculations for atomic Ag by Manson (long-dashed line).

M. Ardehali et al., Phys. Rev. B 39, 8107 (1989)

TOTAL SUBSHELL CROSS SECTION: $\int_{4\pi} \frac{d\sigma_{nl}}{d\Omega} d\Omega =$

$$\sigma_{nl}(E^f) = \frac{4\pi\alpha_0 a_0^2}{3}(h\nu)[lR_{l-1}^2(E^f) + (l+1)R_{l+1}^2(E^f)]$$

= SUM OVER ALL m_l, m_s IN SUBSHELL nl

If either $R_{\ell+1}$ or $R_{\ell-1}$ goes to zero, get a Cooper minimum

RADIAL MATRIX ELEMENTS TO $l \pm 1$ CHANNELS:

$$R_{l\pm1}(E^f) = \int_0^\infty R_{nl}(r) r R_{E^f,\, l\pm1}(r) r^2\, dr = \int_0^\infty P_{nl}(r) r P_{E^f,\, l\pm1}(r)\, dr$$

DIFFERENTIAL CROSS SECTION: UNPOLARIZED

$$\frac{d\sigma_{nl}}{d\Omega}(E^f) = \frac{\sigma_{nl}}{4\pi}[1 - \tfrac{1}{2}\beta_{nl}(E^f)P_2(\cos\alpha)]$$

$$= \frac{\sigma_{nl}}{4\pi}[1 + \tfrac{1}{2}\beta_{nl}(E^f)(\tfrac{3}{2}\sin^2\alpha - 1)]$$

$$= A + B\sin^2\alpha$$

ASYMMETRY PARAMETER:

TERM FOR $l \pm 1$ INTERFERENCE

$$\beta_{nl}(E^f) = \frac{\{l(l-1)R_{l-1}^2(E^f) + (l+1)(l+2)R_{l+1}^2(E^f) - 6l(l+1)R_{l+1}(E^f)R_{l-1}(E^f)\cos[\delta_{l+1}(E^f) - \delta_{l-1}(E^f)]\}}{(2l+1)[lR_{l-1}^2(E^f) + (l+1)R_{l+1}^2(E^f)]}$$

$\delta_{l\pm1}(E^f)$ = CONTINUUM ORBITAL PHASE SHIFTS IN ATOMIC POTENTIAL $V(r)$

COOPER MINIMUM IN In 4d (Z = 49) CROSS SECTION—Radial Matrix Element Variation

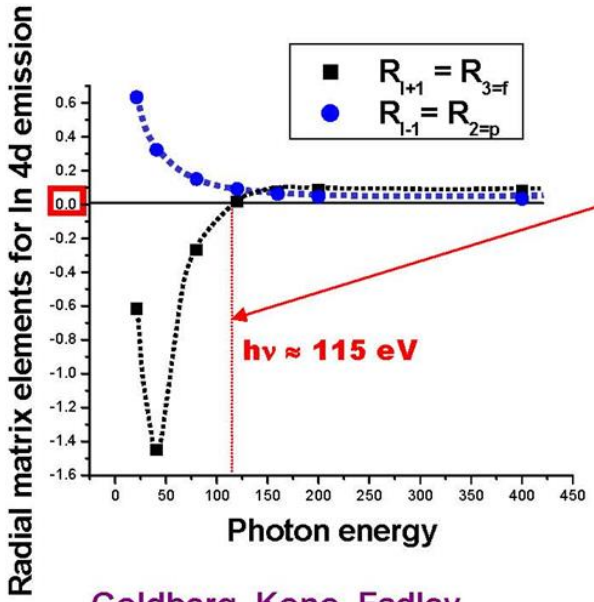

Goldberg, Kono, Fadley
J. Elect. Spect. 21, 285 ('81)

GRAPH I. Atomic Subshell Photoionization Cross Sections for 0–1500 eV, $1 \leq Z \leq 103$
See page 6 for Explanation of Graphs

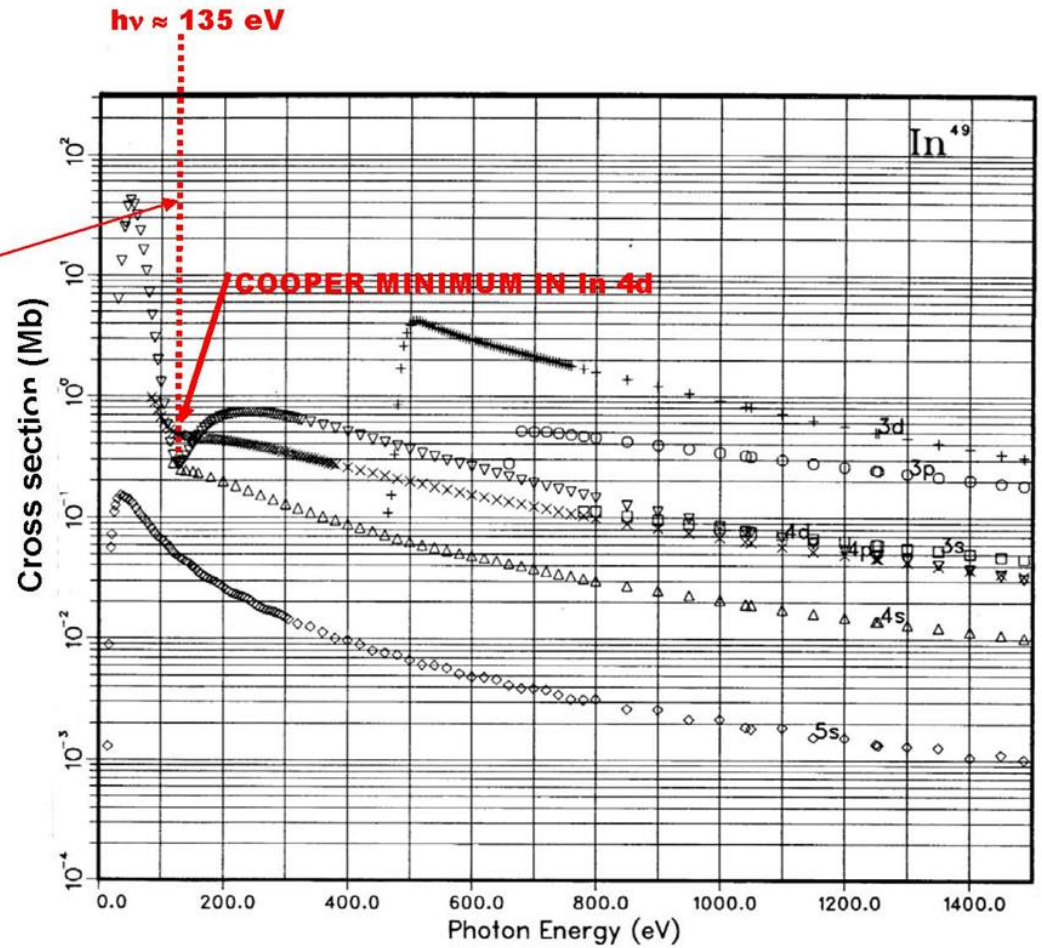

In binding energies(eV) are:

1s(2) 26971.5	2s(2) 3983.01	2p(6) 3731.41
3s(2) 764.232	3p(6) 659.286	4s(2) 118.953
3d(10) 462.909	4p(6) 84.0558	5s(2) 10.1384
4d(10) 26.2168	5p(1) 4.69781	

An additional many-elecron effect: Resonant photoemission

J. J. YEH and I. LINDAU Subshell Photoionization Cross Sections

ATOMIC + NUCLEAR DATA TABLES 32, 45 (1985)

GRAPH I. Atomic Subshell Photoionization Cross Sections for 0–1500 eV, $1 \leq Z \leq 103$

See page 6 for Explanation of Graphs

THEORETICAL ATOMIC CROSS SECTIONS: ENTIRE PERIODIC TABLE

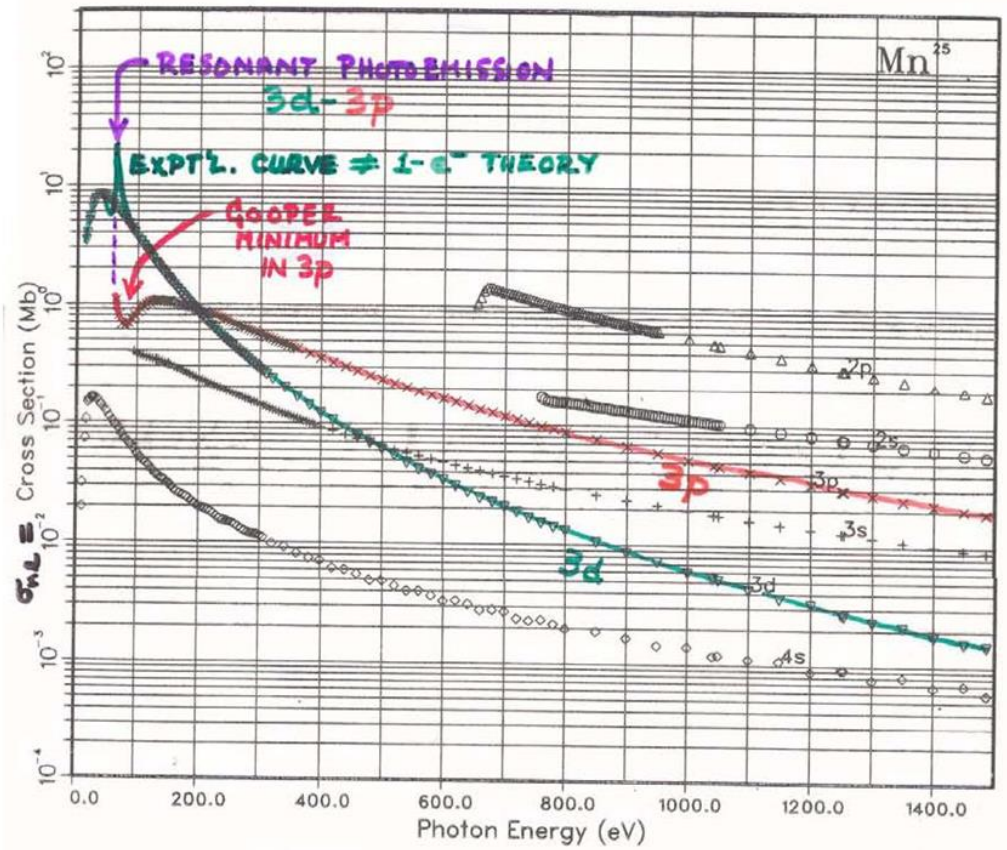

Mn binding energies(eV) are:

1s(2) 6455.26	2s(2) 755.155	2p(6) 653.681
3s(2) 90.8814	3p(6) 60.9150	4s(2) 7.14671
3d(5) 12.0486		

Single-atom resonant photoemission:

Ex. – Mn atom: Mn3d emission, resonance with Mn3p

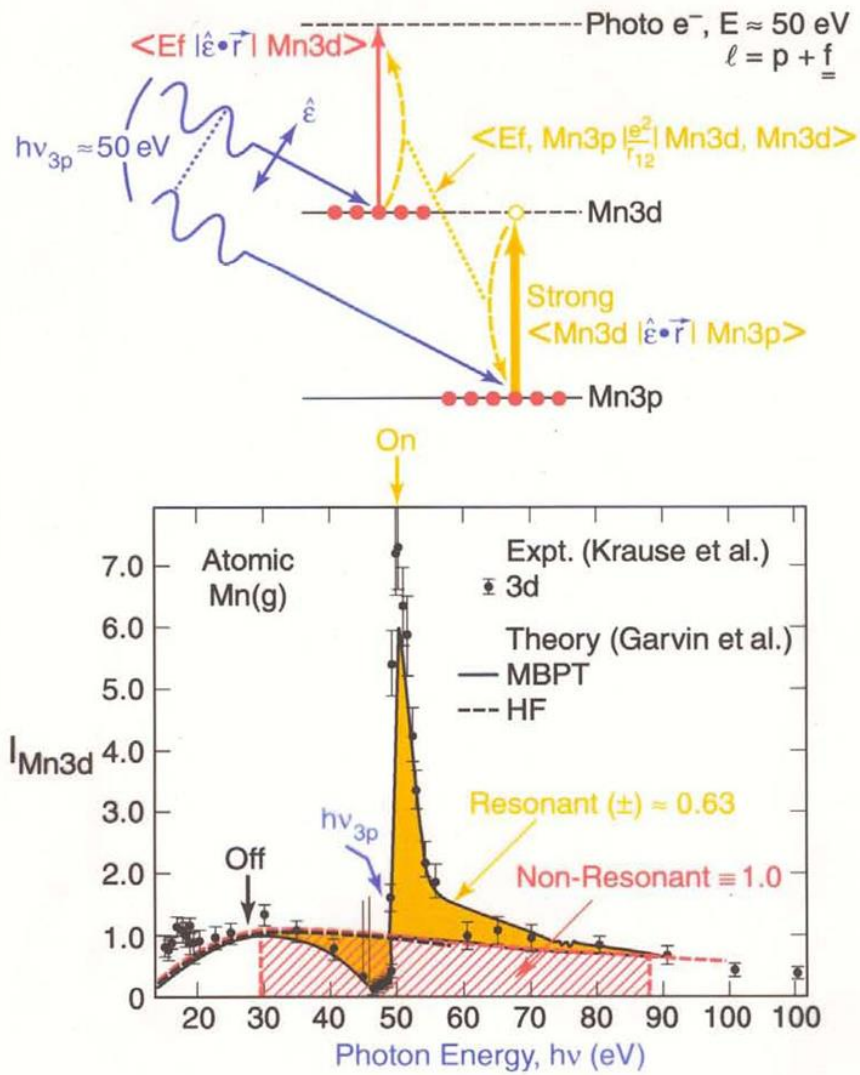

SINGLE-ATOM RESONANT PHOTOEMISSION:

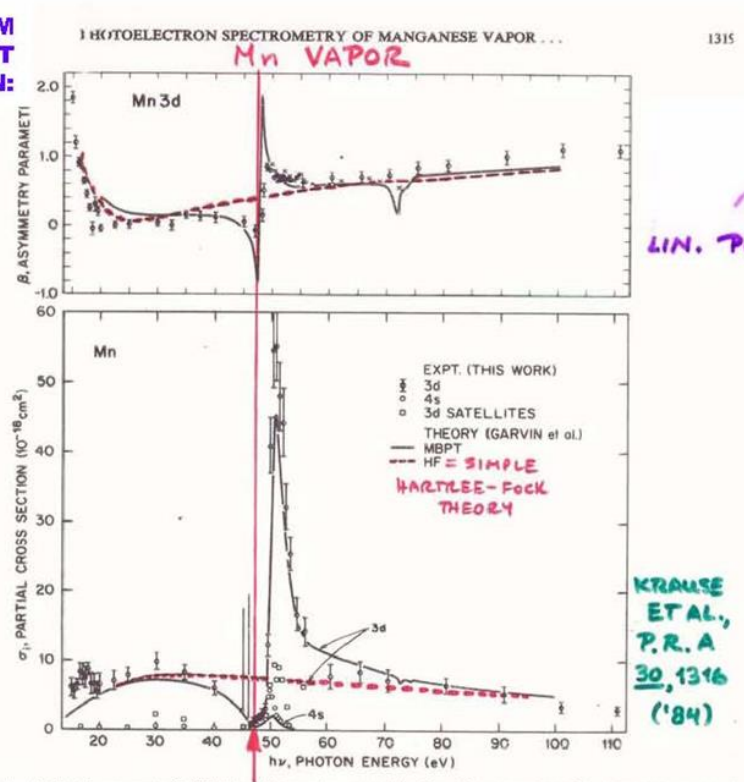

β_{3d}

σ_{3d}

KRAUSE ET AL., P.R.A 30, 1316 ('84)

FIG. 2. Angular distribution parameter β of $3d$ photoelectrons (upper panel) and partial cross sections of $4s$, $3d$ and satellite peaks (lower panel). Crosses (×) for β are from Ref. 3, theory from Ref. 6. The resonance near 50 eV is due to the $3p \rightarrow 3d$ excitation into the partially filled $3d$ subshell of Mn.

$h\nu = E_b^V(Mn\,3p)$

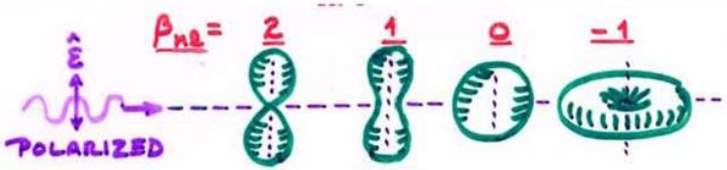

RESONANT PROCESS:

IF $h\nu \approx E_b$ OF $n\ell'$ SUBSHELL INSIDE OF $n\ell$ SUBSHELL OF INTEREST (E.G., 3p FOR 3d), TWO "CHANNELS" COUPLE-

USUAL 3d: $Mn^0 \ldots 3s^2 3p^6 3d^5 4s^2 \xrightarrow{h\nu} Mn^+ \ldots 3s^2 3p^6 3d^4 4s^2 + e^-$ (PHOTOELECTRON)

RESONANT 3p: $Mn^0 \ldots 3s^2 3p^6 3d^5 4s^2 \xrightarrow{h\nu} Mn^0 \ldots 3s^2 3p^5 3d^6 4s^2 e^-$

$\xrightarrow[\text{ZATION}]{\text{AUTOIONI-}} Mn^+ \ldots 3s^2 3p^6 3d^4 4s^2$ + ELECTRON @ SAME E_{KIN} AS PHOTOELECTRON

(≈ AUGER)

COUPLING MUCH ENHANCES CROSS SECTION

$SrTiO_3$ and $La_{0.67}Sr_{0.33}MnO_3$ band structures and DOS

$SrTiO_3$-band insulator

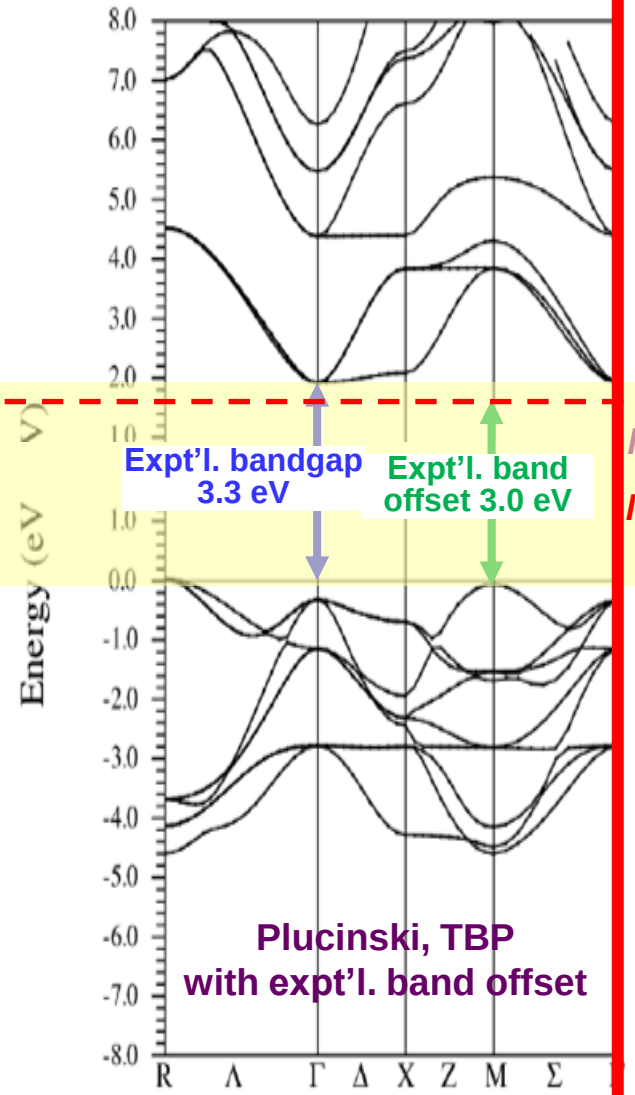

Plucinski, TBP
with expt'l. band offset

$La_{0.67}Sr_{0.33}MnO_3$- Half-Metallic Ferromagnet

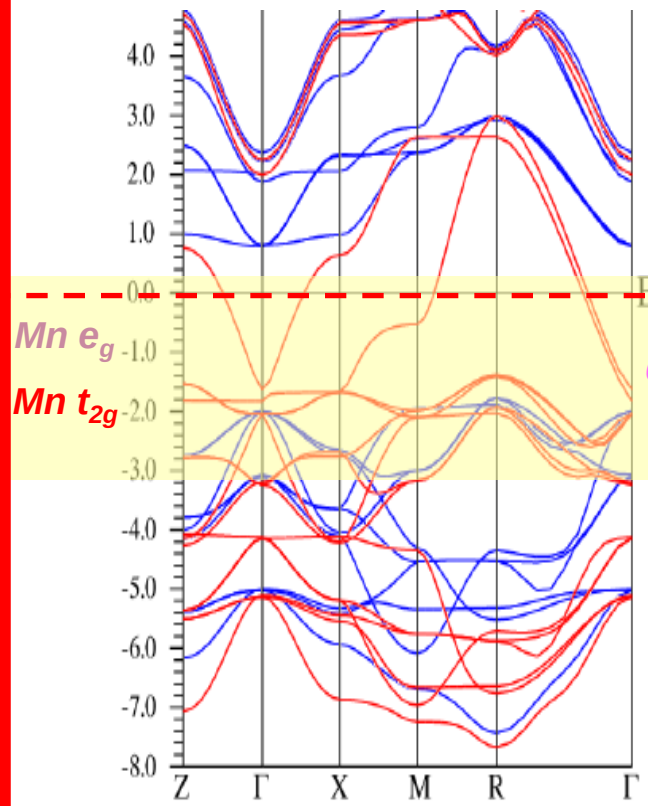

Spin-up
Spin-down
Chikamatsu et al., PRB 73, 195105 (2006); Plucinski, TBP

Projected DOSs

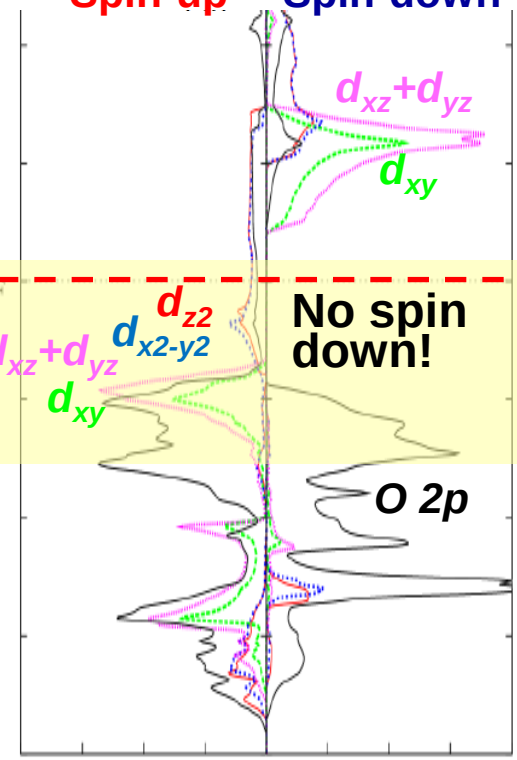

Zheng, Binggeli, J. Phys. Cond. Matt. 21, 115602 (2009)
Plucinski, TBP

Resonant Photoemission—$La_{0.6}Sr_{0.4}MnO_3$, Mn 3d with Mn 2p

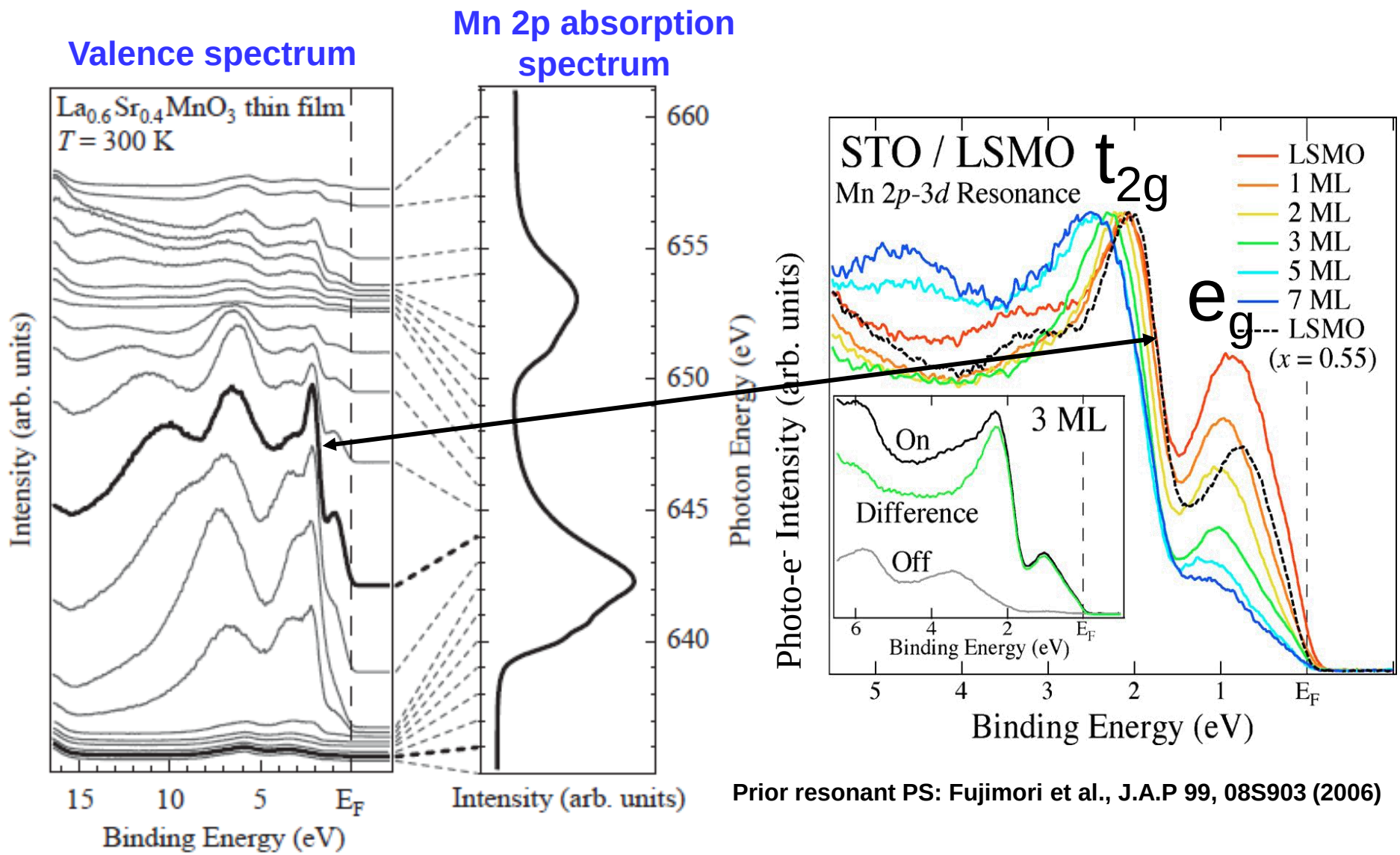

Prior resonant PS: Fujimori et al., J.A.P 99, 08S903 (2006)

K. Horiba et al. / Journal of Magnetism and Magnetic Materials 272–276 (2004) 436–437

MATRIX ELEMENTS IN THE SOFT X-RAY SPECTROSCOPIES: DIPOLE LIMIT

- ***Photoelectron spectroscopy/photoemission:***

$$I \propto \left|\hat{e} \bullet \langle \varphi_f(1) | \vec{r} | \varphi_i(1) \rangle\right|^2$$

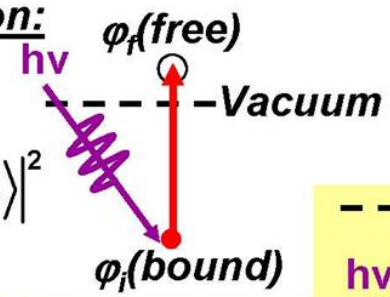

- ***Near-edge x-ray absorption:***

$$I \propto \left|\hat{e} \bullet \langle \varphi_f(1) | \vec{r} | \varphi_i(1) \rangle\right|^2$$

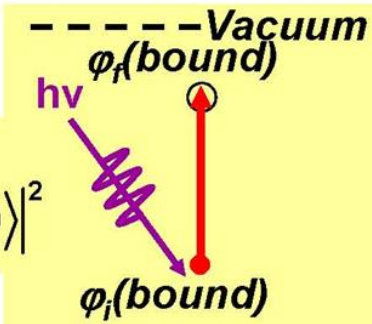

- ***Auger electron emission:***

$$I \propto \left| \langle \varphi_f(1)\varphi_1(2) | \frac{e^2}{r_{12}} | \varphi_3(1)\varphi_2(2) \rangle - \langle \varphi_1(1)\varphi_f(2) | \frac{e^2}{r_{12}} | \varphi_3(1)\varphi_2(2) \rangle \right|^2$$

Direct — Exchange

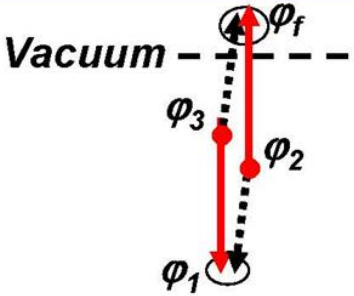

- ***X-ray emission:***

$$I \propto \left|\hat{e} \bullet \langle \varphi_f(1) | \vec{r} | \varphi_i(1) \rangle\right|^2$$

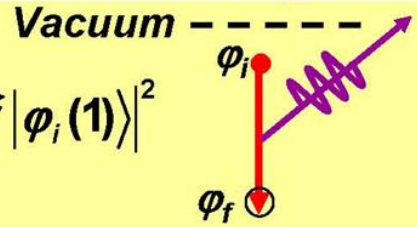

CALCULATION OF PHOTOELECTRON INTENSITIES—THE 3-STEP MODEL

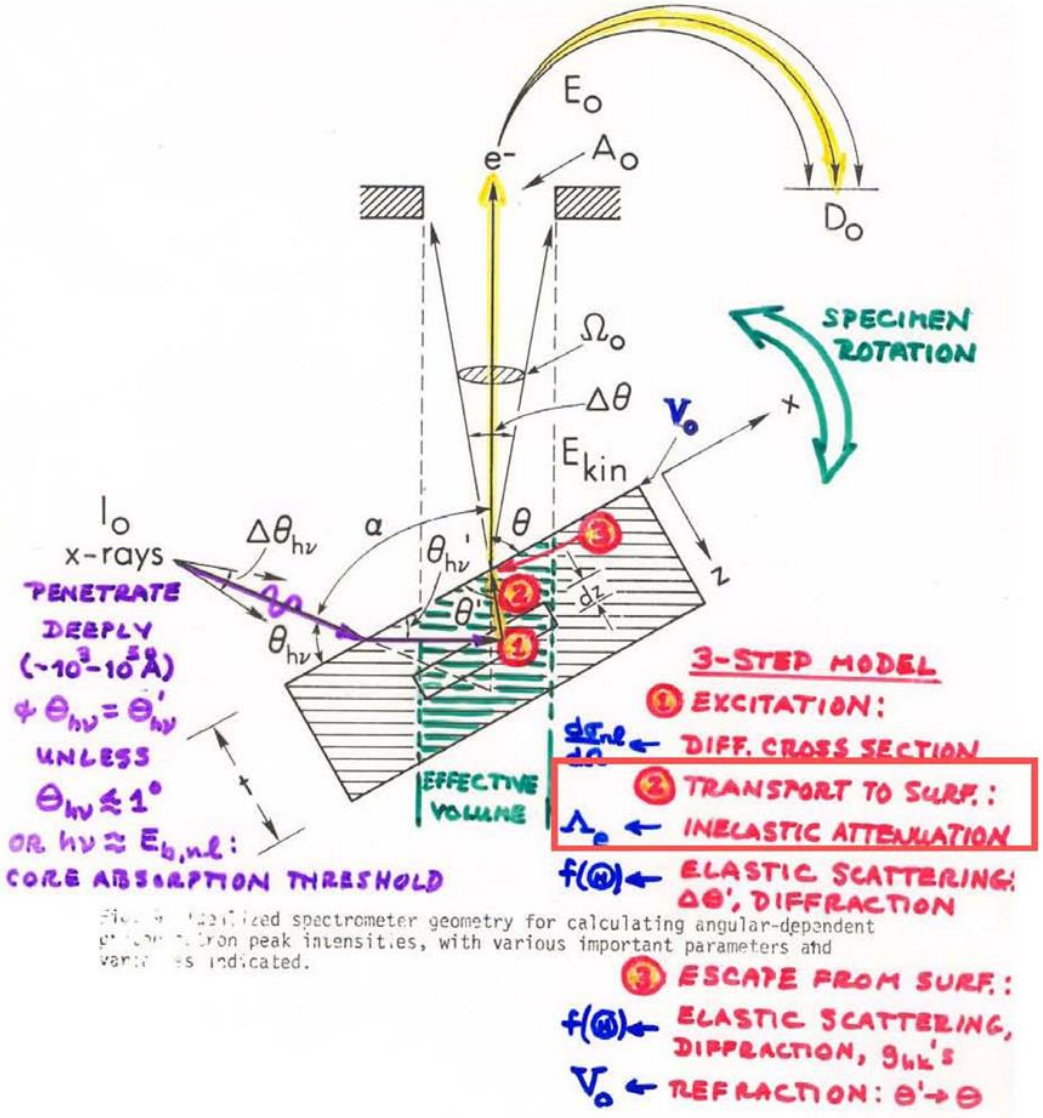

Fig. 4. Idealized spectrometer geometry for calculating angular-dependent photoelectron peak intensities, with various important parameters and variables indicated.

Electron inelastic mean free paths for 41 elements-theory

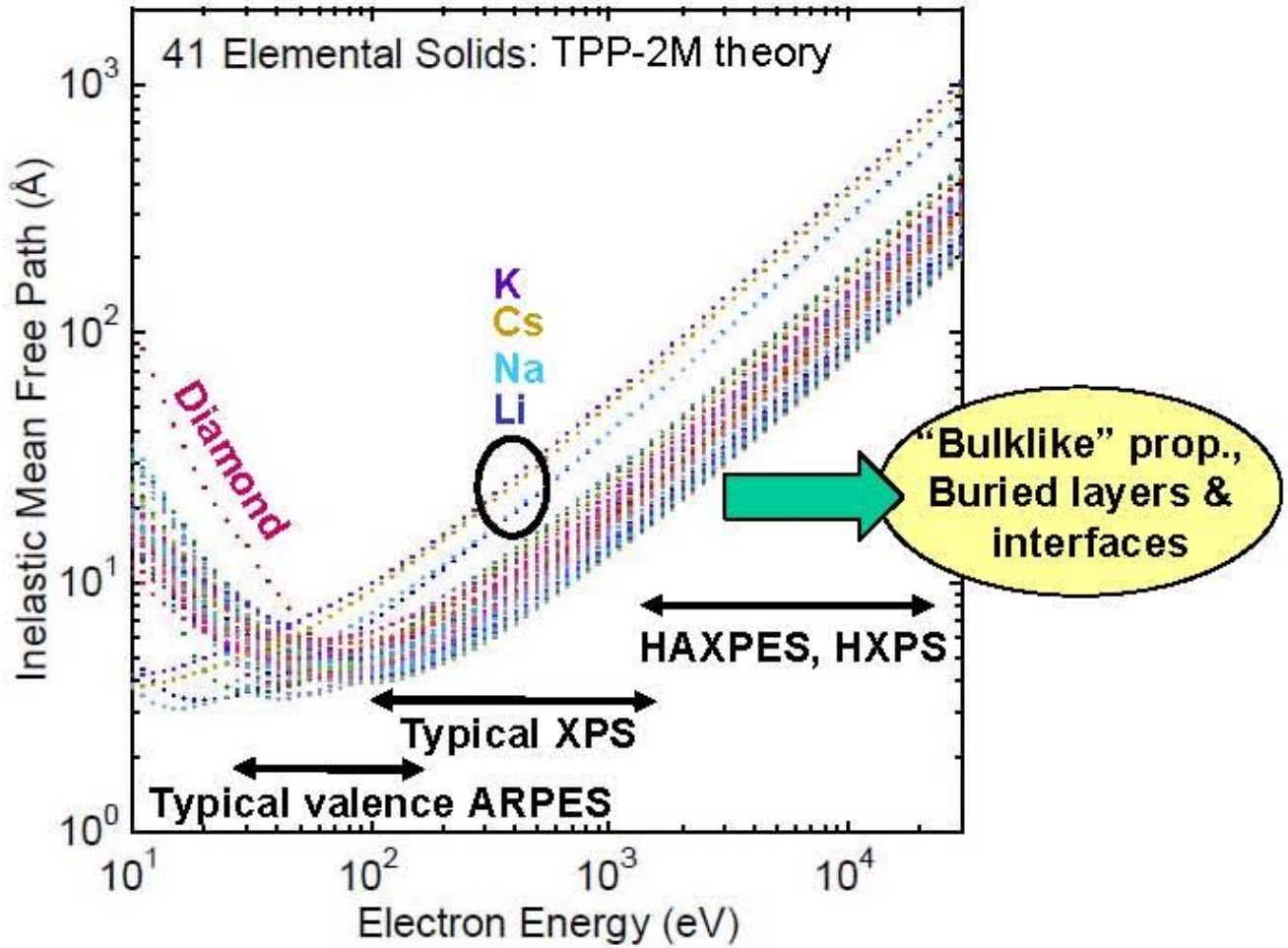

Tanuma, Powell, Penn, Surf. Interface Anal. 37, 1 (2005) and TBP

Inelastic mean free paths in solids

Estimation from the TPP-2M formula: any compound

$$\Lambda_e \approx \lambda = \frac{E}{E_p^2[\beta \ln(\gamma E) - (C/E) + (D/E^2)]}$$

where

$$\beta = -0.10 + 0.944/(E_p^2 + E_g^2)^{1/2} + 0.069\rho^{0.1}$$

$$\gamma = 0.191\rho^{-0.50}$$

$$C = 1.97 - 0.91U$$

$$D = 53.4 - 20.8U$$

$$U = N_v \rho / M = E_p^2 / 829.4$$

and $E_p = 28.8\ (N_v\rho/M)^{1/2}$ is the free-electron plasmon energy (in eV), ρ is the density (in g cm^{-3}), N_v is the number of valence electrons per atom (for an element) or molecule (for a compound), M is the atomic or molecular weight, and E_g is the bandgap energy (in eV). These equations are collectively known as the TPP-2M equation.

Tanuma, Powell, Penn, Surf. Interface Anal. 21, 165 (1994)

Inelastic mean free paths for many materials

Downloadable program:
http://www.quases.com/products/quases-imfp-tpp2m/

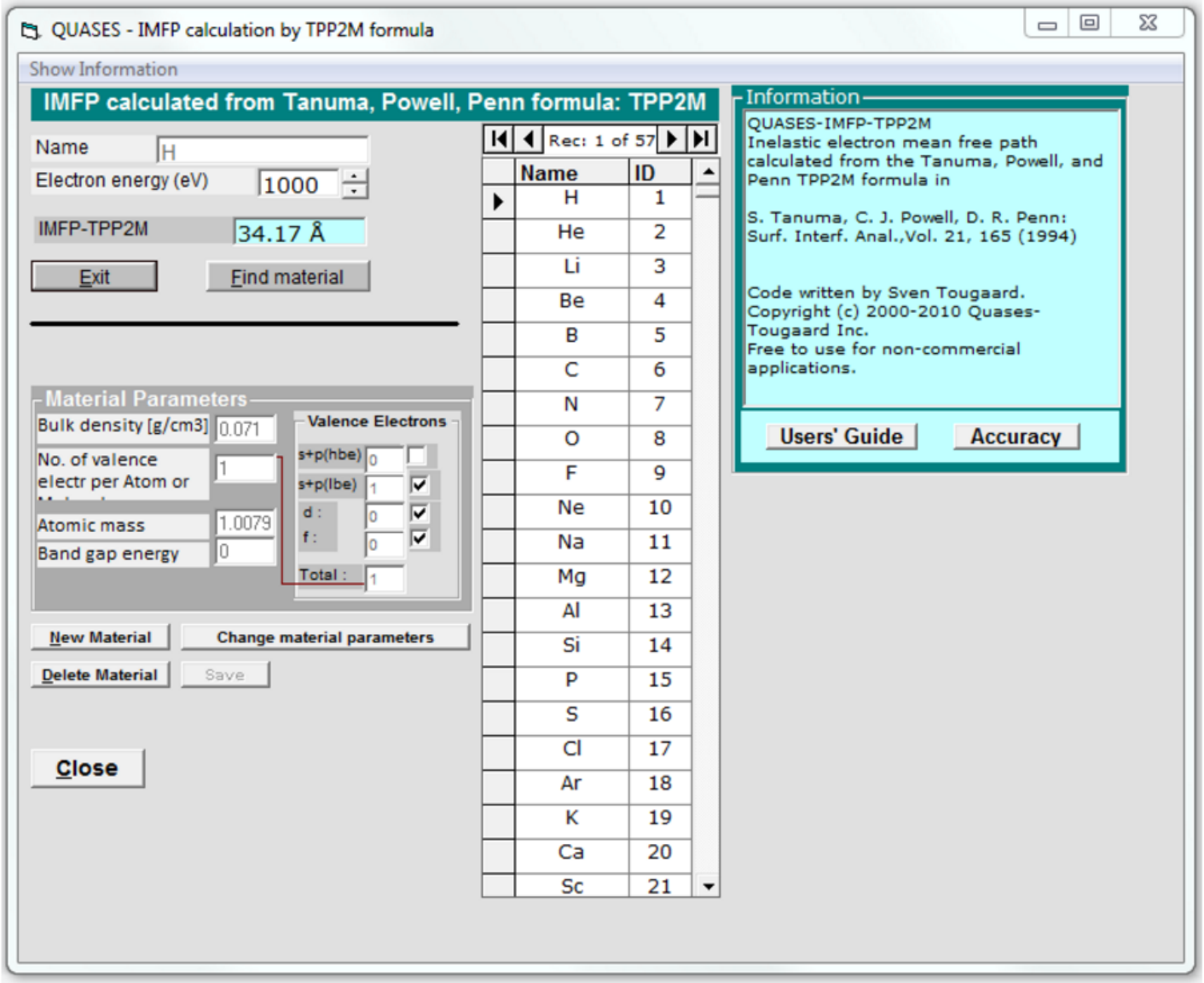

CALCULATION OF PHOTOELECTRON INTENSITIES—THE 3-STEP MODEL

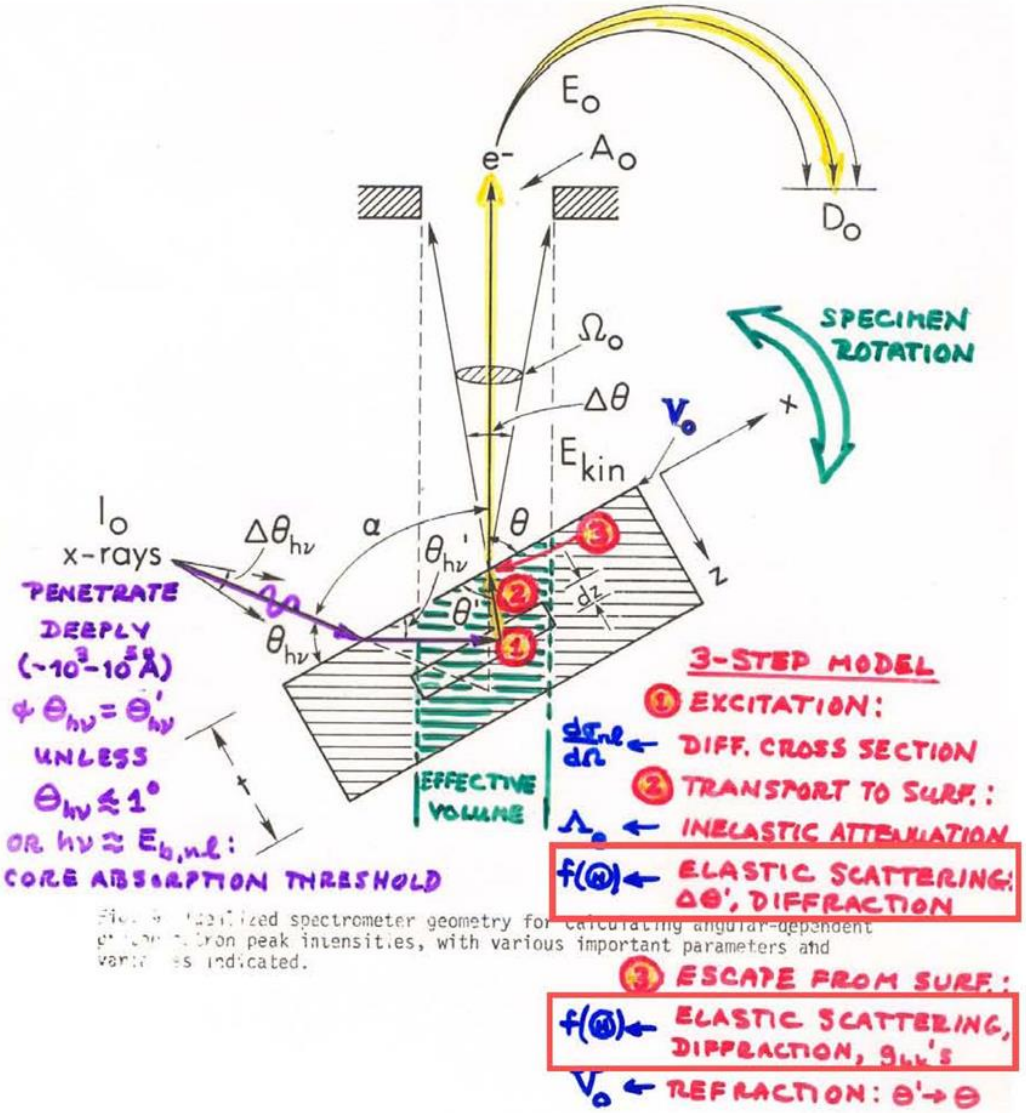

Fig. 4. Idealized spectrometer geometry for calculating angular-dependent photoelectron peak intensities, with various important parameters and variables indicated.

Switching from bulk to surface sensitivity for lower electron takeoff angles

Simplest interpretation:

Average emission depth = $\Lambda_{inelastic} \sin\theta_{takeoff}$

How valid?

$E_{kin} \approx$ 500-1000 eV

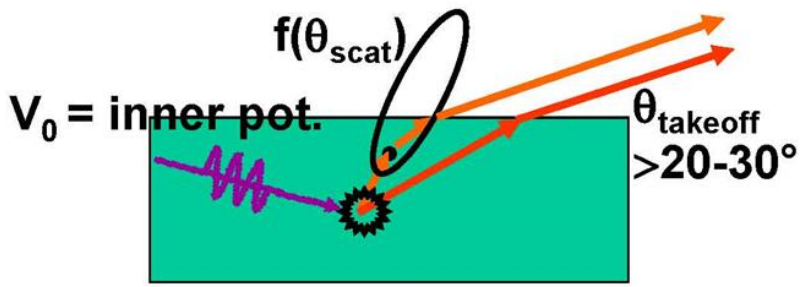

E.g.: A. Jablonski and C. J. Powell, J. Vac. Sci. Tech. A 21, 274 (2003), Plus a general program for modeling of arbitrary multilayer structures and concentration gradients (without V_0), but with Monte Carlo elastic scattering: Prof. Wolfgang Werner, TU Vienna, http://www.iap.tuwien.ac.at/~WERNER/SESSA.htmlx

EFFECTS OF ELASTIC SCATTERING ON ANGULAR DISTRIBUTIONS: POLYCRYSTALLINE OR AMORPHOUS SAMPLE

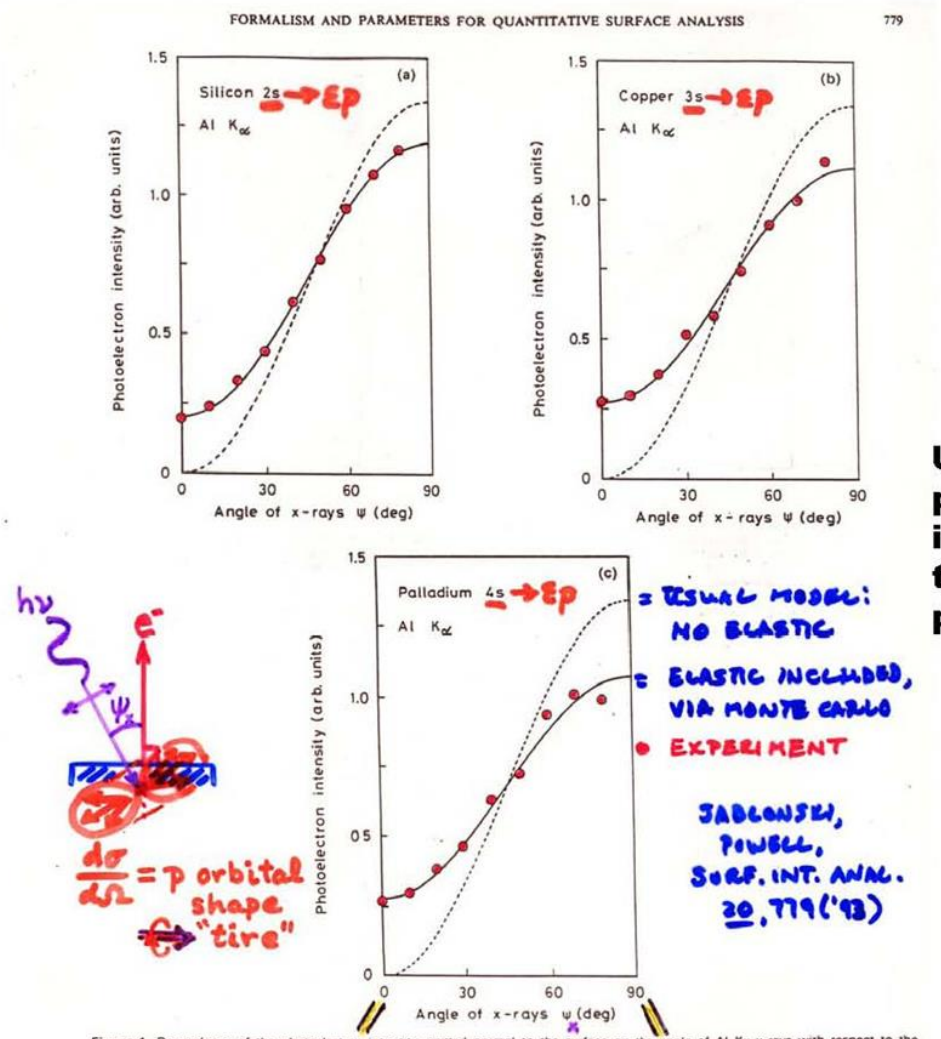

Up to this point, included in the SESSA program

Intensity increased by elastic scattering

Intensity decreased by elastic scatt.

Surface sensitivity enhancement for grazing exit angles

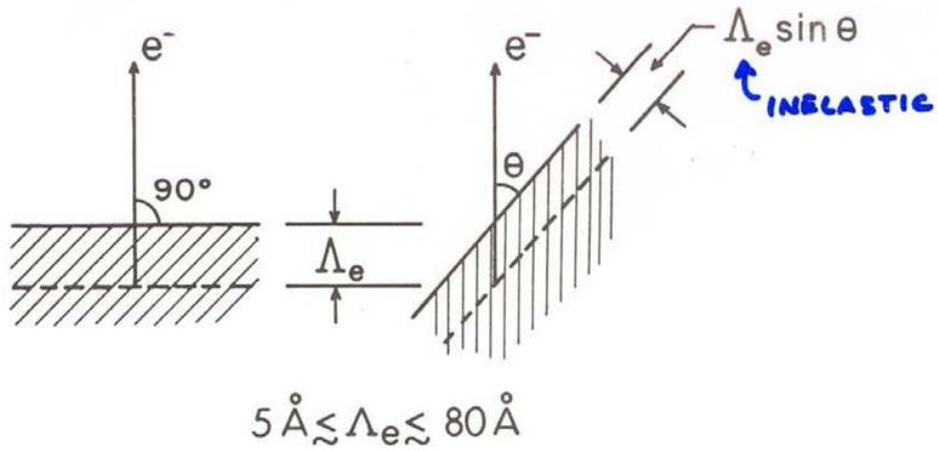

Fig. 5. Illustration of the basic mechanism producing surface sensitivity enhancement for low electron exit angles θ. The average depth for no-loss emission as measured perpendicular to the surface is $\Lambda_e \sin\theta$.

E.g.- Λ_e = 28 Å in Au(s) at 1400 eV

	θ	Mean Depth	No. layers
"BULK" →	90°	28 Å	~9
"SURFACE" →	10°	~4.4 Å	~1.5

... BUT REFRACTION AT SURFACE AND ELASTIC SCATTERING CAN REDUCE SURFACE ENHANCEMENT, ESP. AT LOW θ ≲ 30°

∴ **BEST QUANTITATIVE ANALYSIS FOR RANGE 20-30° ≤ θ ≤ 90°**

CALCULATION OF PHOTOELECTRON INTENSITIES—THE 3-STEP MODEL

→ **The SESSA program calculates this for arbitrary multilayer samples, but neglecting x-ray optics and electron refraction**

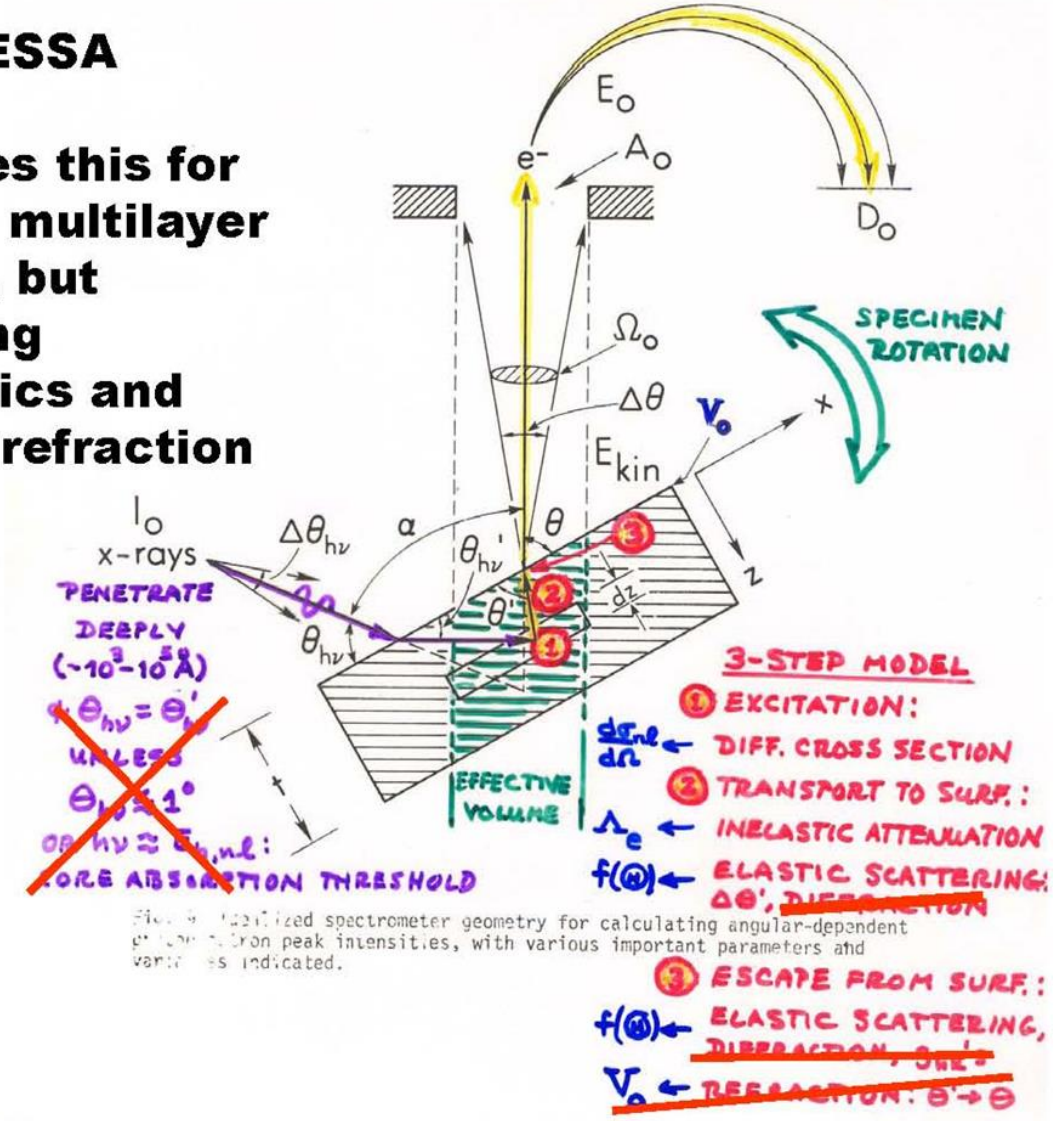

Fig. 4. Idealized spectrometer geometry for calculating angular-dependent photoelectron peak intensities, with various important parameters and variables indicated.

The SESSA program for XPS simulations

https://drive.google.com/drive/folders/0B-VeL-nROIxaME41T2dEb1d2MFk?usp=sharing

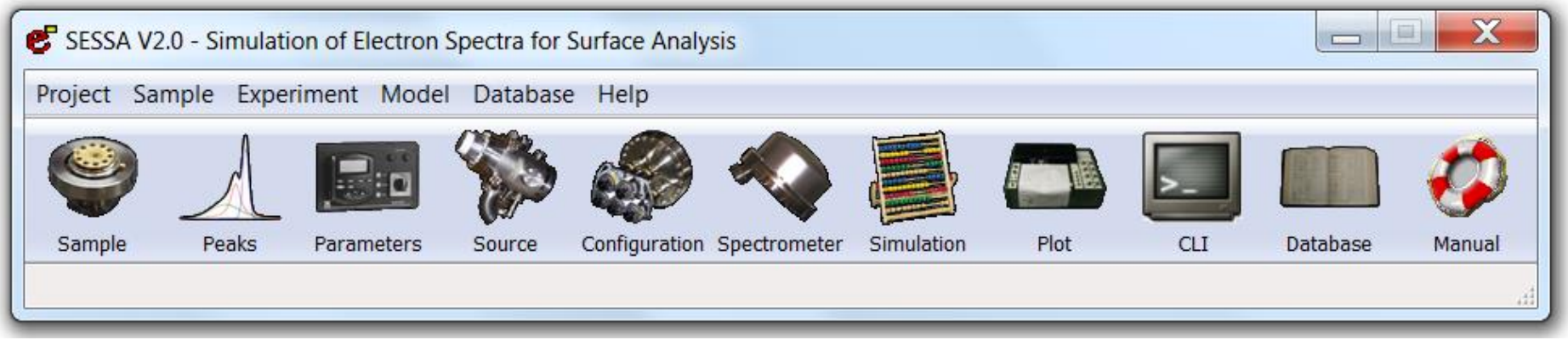

CALCULATION OF PHOTOELECTRON INTENSITIES—THE 3-STEP MODEL

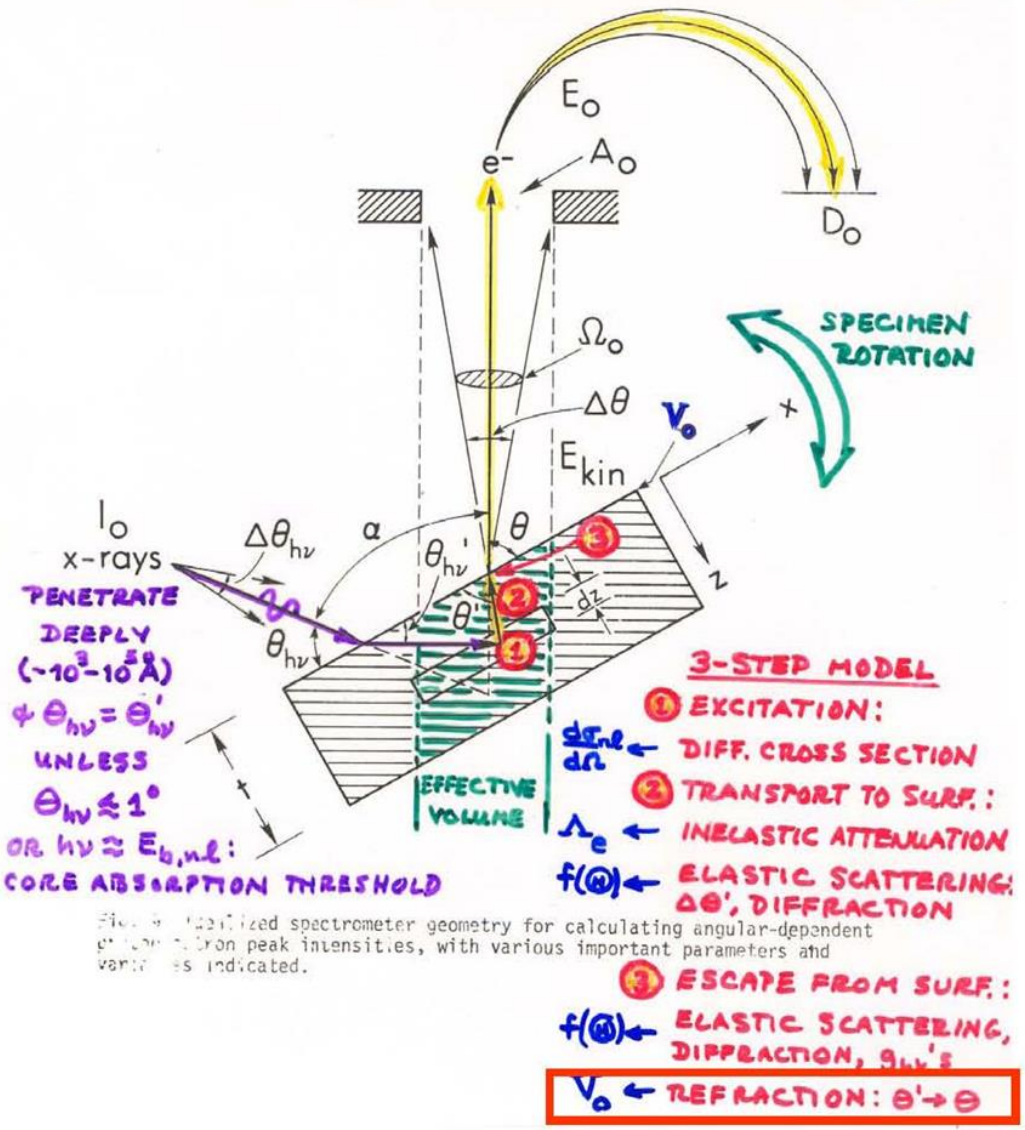

Fig. 4. Idealized spectrometer geometry for calculating angular-dependent photoelectron peak intensities, with various important parameters and variables indicated.

Electron Refraction at the Surface Due to the Inner Potential

$$\theta = \cos^{-1}\left[\left(1+\frac{V_0}{E'_{kin}}\right)^{1/2}\cos\theta'\right] \quad \text{or} \quad \theta = \tan^{-1}\left[\sqrt{\sin^2\theta' - \frac{V_o}{E_{kin}}} \Big/ \cos\theta'\right]$$

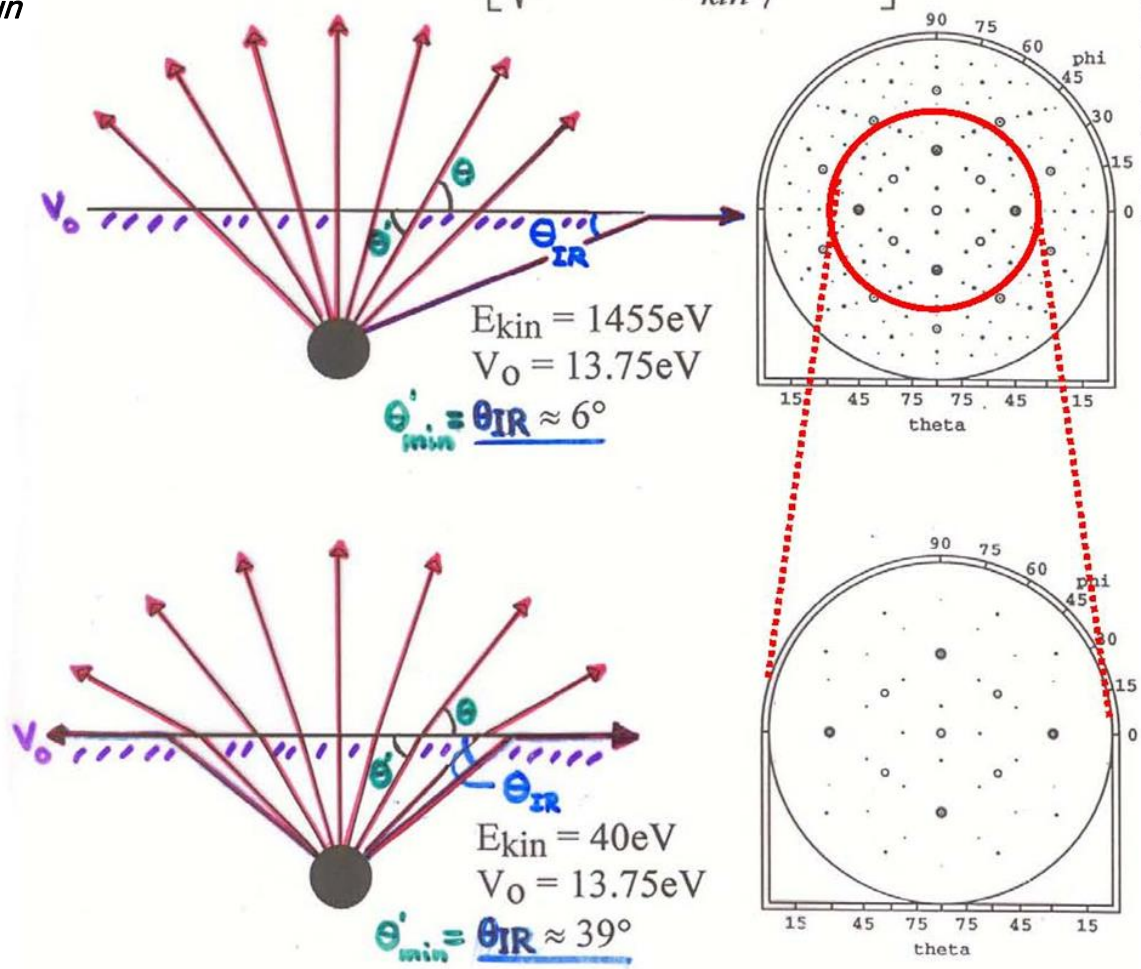

Observed Low-Index Directions Above W(110)

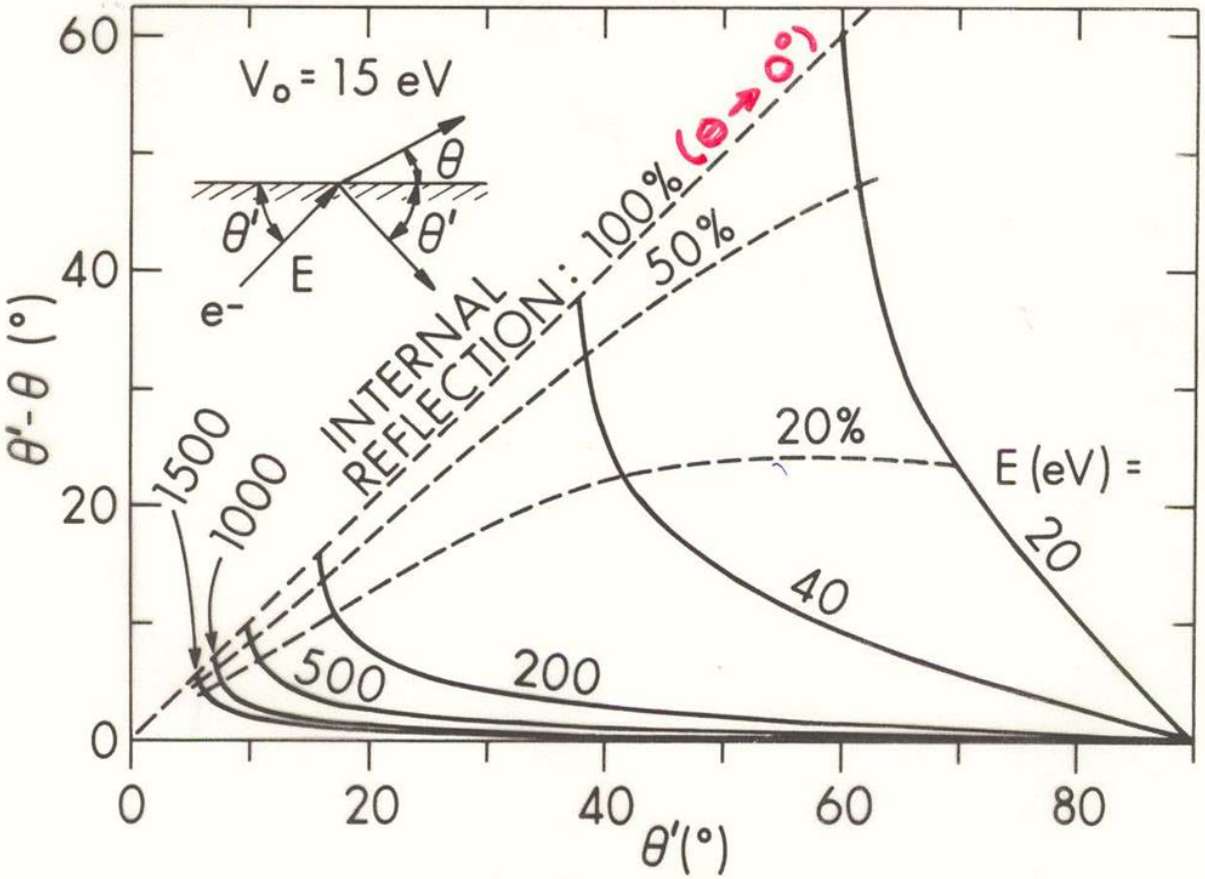

Fig. 14. Calculation of electron refraction effects for different electron kinetic energies and a typical V_0 value of 15eV. The degree of refraction is indicated by the difference θ' (internal) − θ (external) Contours of equal probablility of internal reflection are also shown. (From ref. (5).)

CALCULATION OF PHOTOELECTRON INTENSITIES—THE 3-STEP MODEL

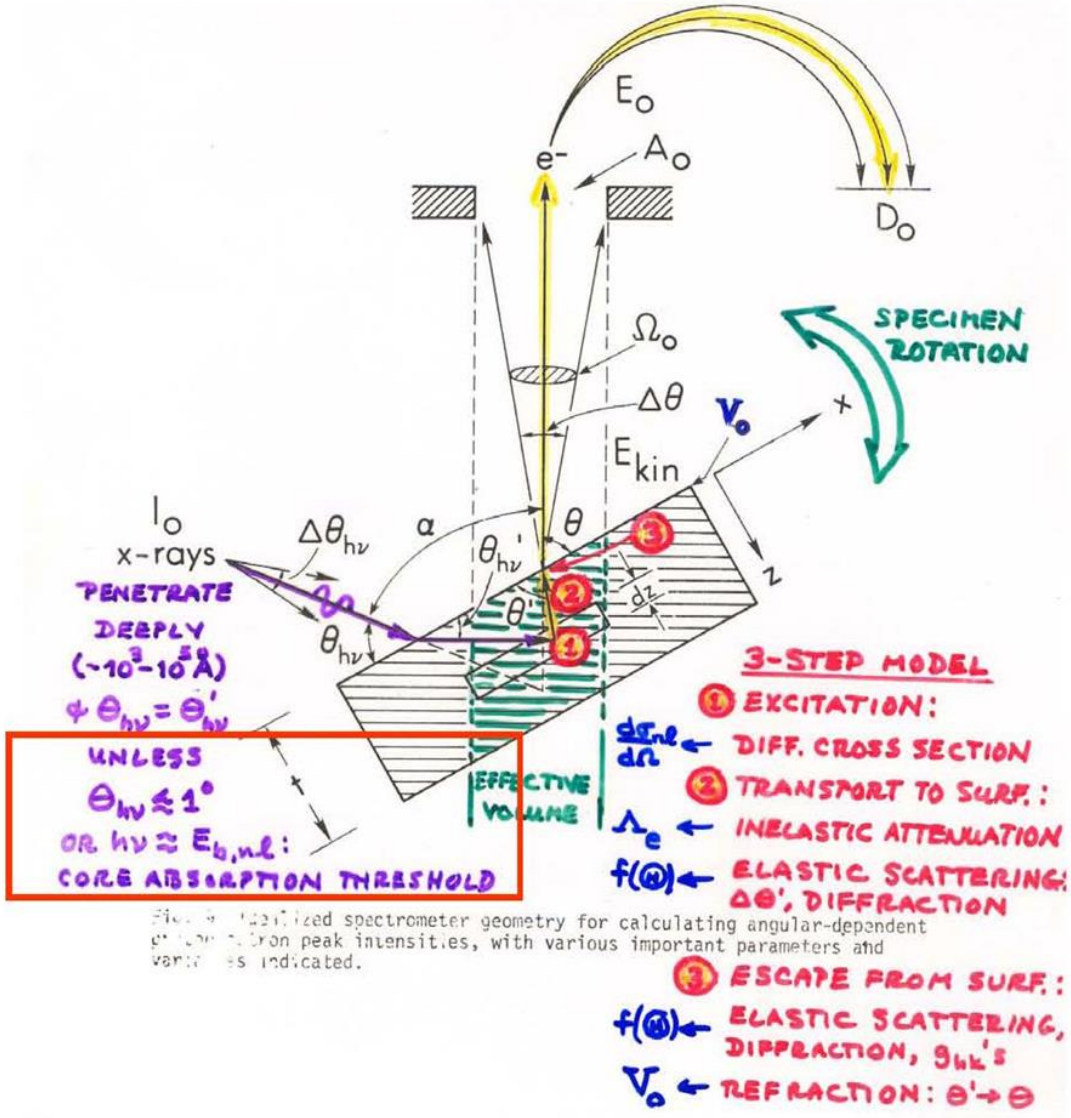

Fig. 4. Idealized spectrometer geometry for calculating angular-dependent photoelectron peak intensities, with various important parameters and variables indicated.

http://www-cxro.lbl.gov/optical_constants/

X-Ray Interactions with Matter

Website

Contents

These pages utilize *JavaScript*, but the decaffeinated versions are still available.

Reference

B.L. Henke, E.M. Gullikson, and J.C. Davis. *X-ray interactions: photoabsorption, scattering, transmission, and reflection at E=50-30000 eV, Z=1-92*, Atomic Data and Nuclear Data Tables Vol. **54** (no.2), 181-342 (July 1993).

By Eric Gullikson. Please direct any comments to EMGullikson@lbl.gov

SOME X-RAY OPTICAL EFFECTS: REDUCED PENETRATION DEPTHS AND INCREASED REFLECITIVITY AT GRAZING INCIDENCE ANGLES

θ_{CRIT} = Grazing angle at which reflectivity begins ($R \approx 0.20$)

$= [2\delta]^{0.5}$

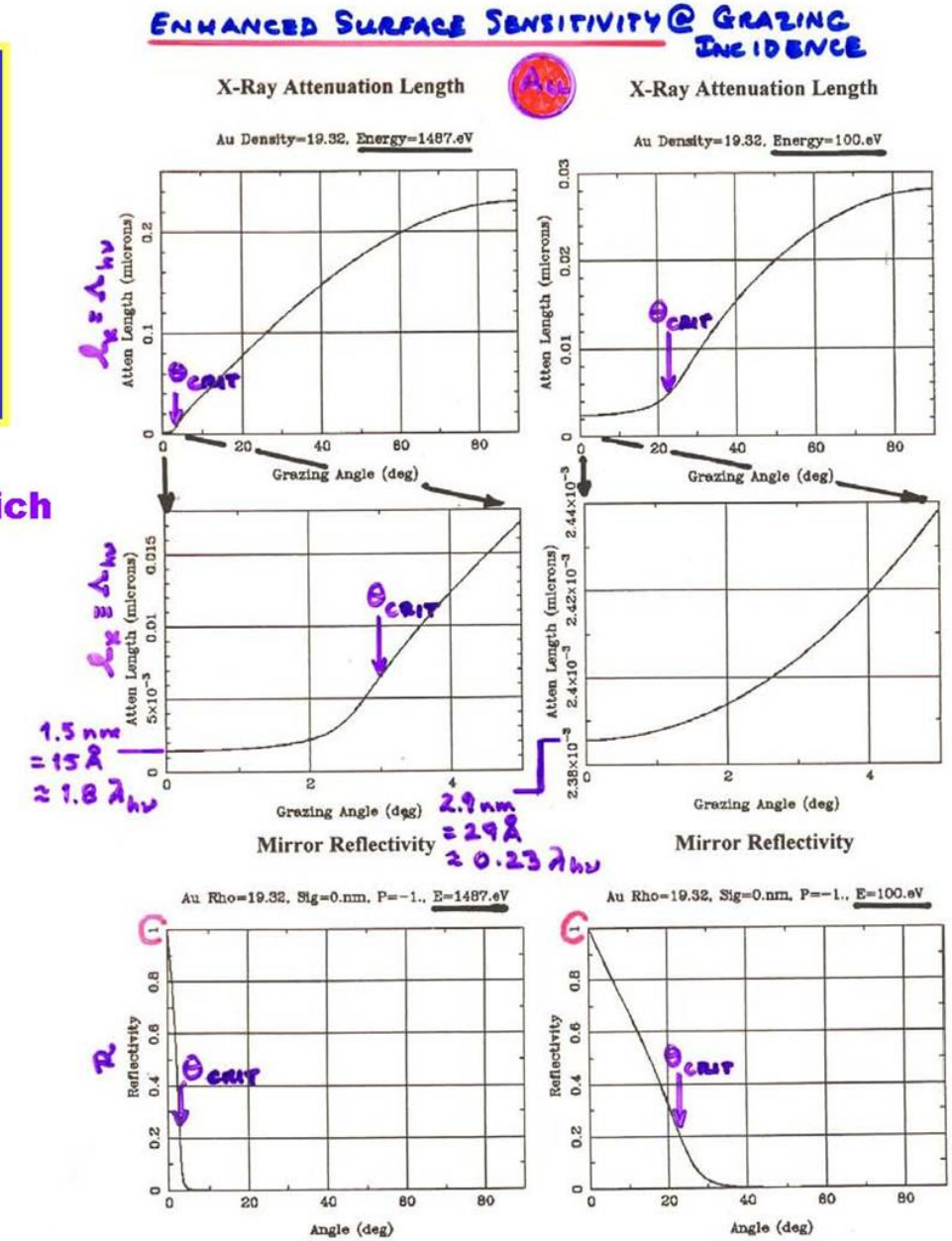

X-ray Optical Effects in Photoemission: The Beginning

B.L. Henke, Phys. Rev. A 6, 94 (1972)

- *Enhanced surface sensitivity as critical angle approached*
- *Effects on average depth and intensity in photoemission (x-ray emission also)*
- *Determination of optical constants from data*

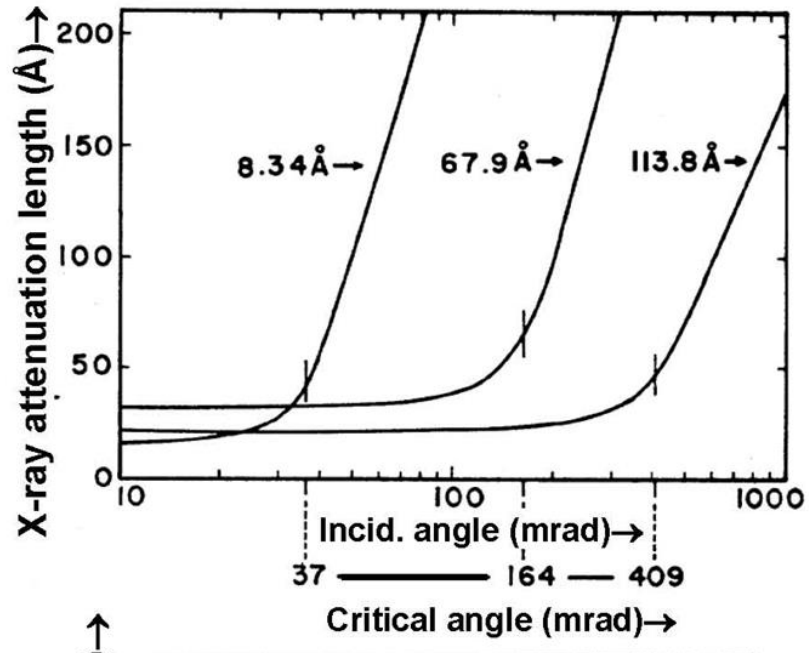

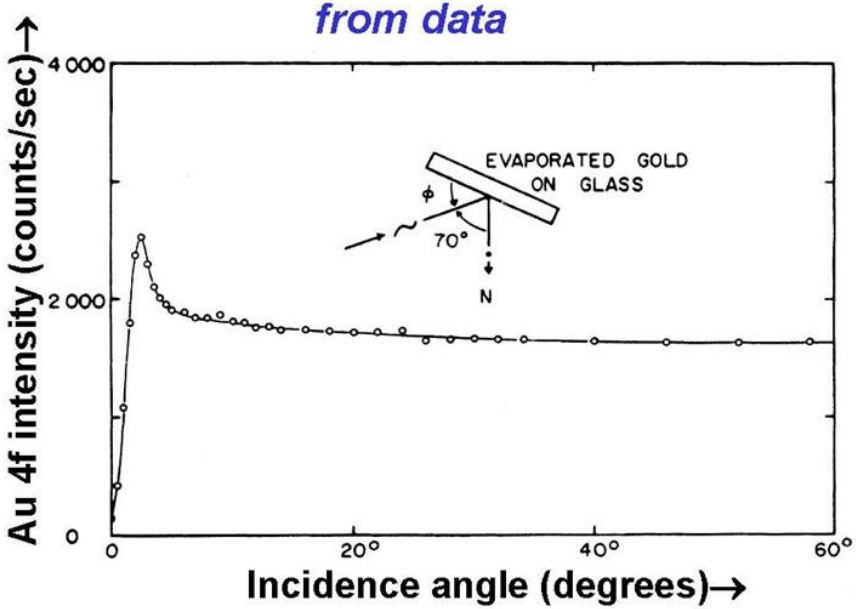

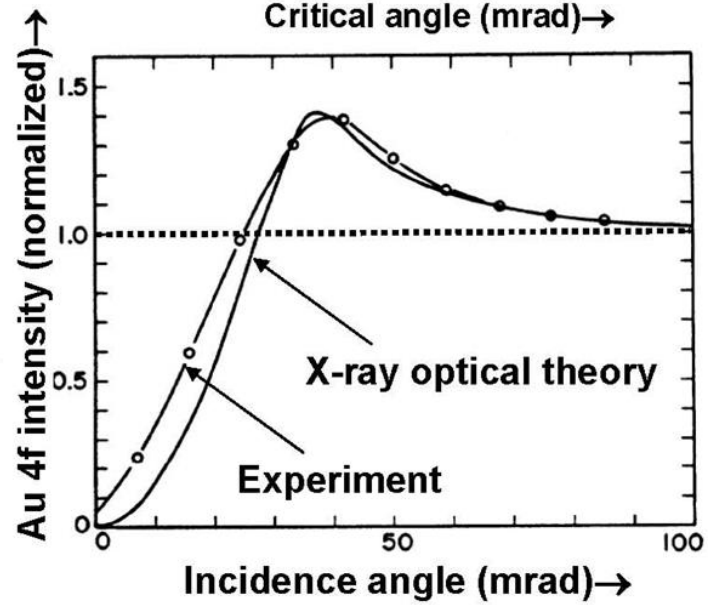

X-ray Optical Effects in Photoemission: Reduced inelastic backgrounds in total x-ray reflection

Kawai et al., Spectrochim. Acta B 47, 983 ('92)

Chester & Jach, Phys. Rev. B 4817262 ('93)

Jach & Landree, Surf. & Int. Anal. 31, 768 ('01)

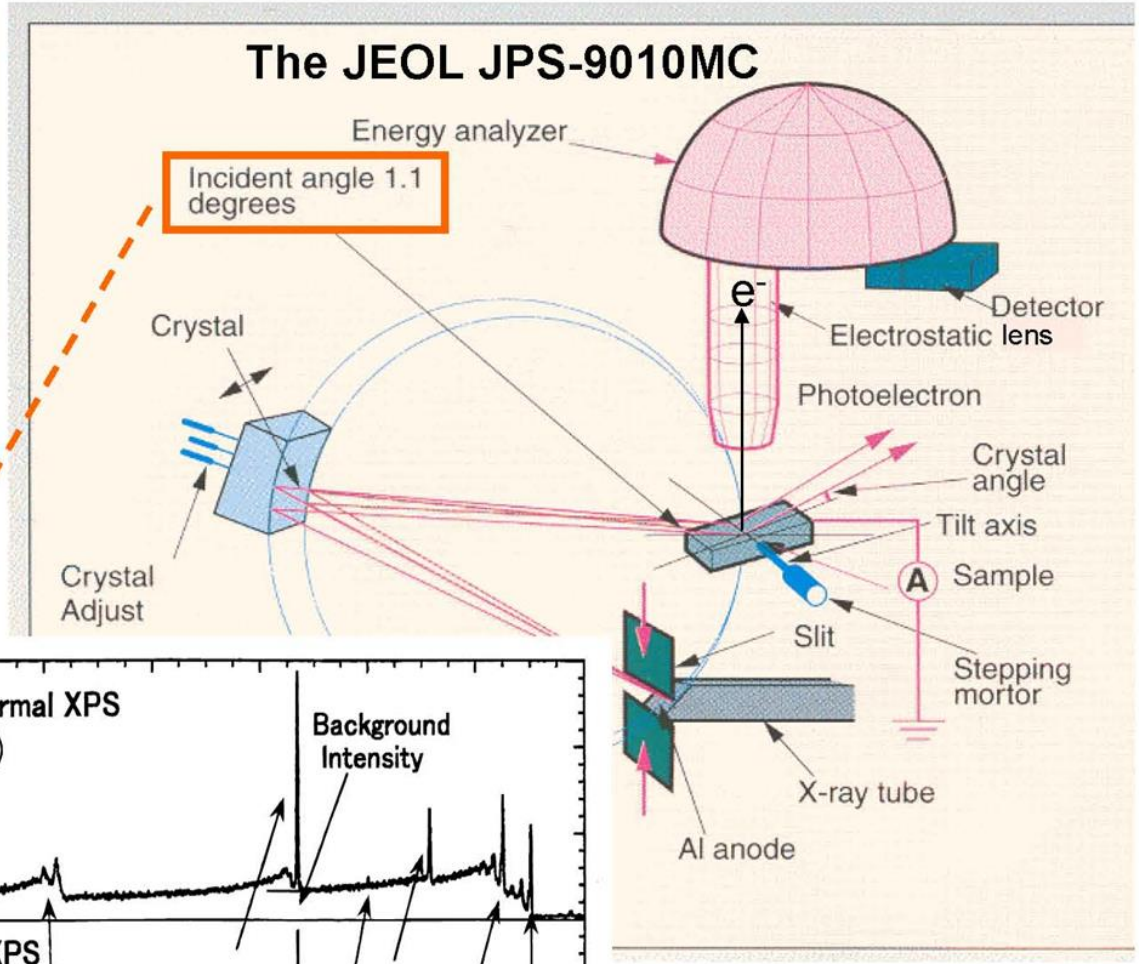

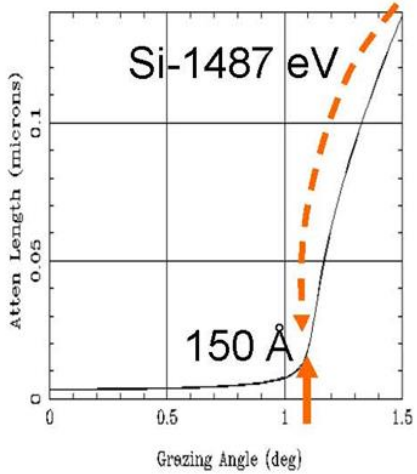

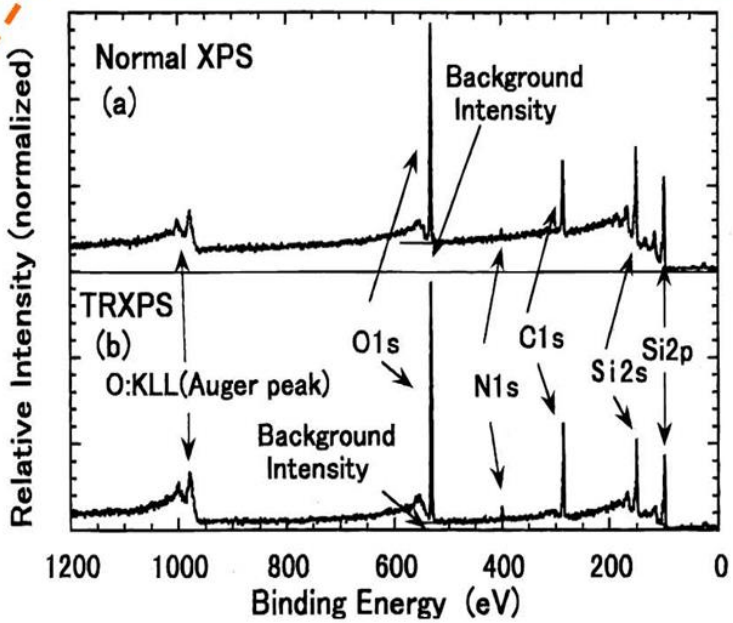

Y. Iijima, K. Miyoshi, S. Saito, Surf. Interf. Anal. 27(1999) 35E42.